THE STUDY ON OXYSTEROL-BINDING PROTEIN (OSBP) AND RELATED PROTEIN 9 (ORP9) LIGANDS: STEROLS AND PHOSPHATIDYLINOSITOL 4-PHOSPHATE

by

Xinwei Liu

Submitted in partial fulfilment of the requirements
for the degree of Master of Science

at

Dalhousie University
Halifax, Nova Scotia
August 2013

DEDICATION PAGE

I would like to dedicate this work to my patents, Jue Liu and Weilai Wang, for their unwavering support and encouragement. Especially, I would like to thank my mother for everything she has given me along the way because without her I would not have made it to where I am today.

TABLE OF CONTENTS

LIST OF FIGURES

ABSTRACT

The oxysterol-binding protein OSBP-gene family is composed of 12 members with a common C-terminal sterol-binding domain (SBD). OSBP and ORP9 are members of the family that are localized to the endoplasmic reticulum (ER) and Golgi apparatus by their FFAT (two phenylalanines in an acidic tract) motif and PH (pleckstrin homology) domain, respectively. These two proteins are implicated in sterol transfer between these organelles. Here we utilized Förster resonance energy transfer (FRET) between cholestatrienol (CTL), a fluorescent cholesterol analog, and dansyl-PE (DNS-PE) to demonstrate that both full-length ORP9L and truncated ORP9S rapidly extract sterols from liposomes. *In vitro,* OSBP, ORP9L and ORP9S specifically extracted phosphatidylinositol 4-phosphate (PI(4)P) from liposomes, suggesting PI(4)P is also a ligand for these proteins. Overexpression of ORP9L or ORP9S attenuated PI(4)P immunofluorescence detection in CHO cells. These results indicate that OSBP and ORP9 may transport sterol and PI(4)P in cells, possibly in opposite directions.

LIST OF ABBREVIATIONS USED

25-OH	25-hydroxycholesterol
ABC	Adenosine triphosphate (ATP)-binding cassette
ACAT	Acyl-CoA cholesterol acyltransferase
ADP	Adenosine diphosphate
ApoA-I	Apolipoprotein A-I
Arf1	Adenosine diphosphate (ADP)-ribosylation factor 1
ATP	Adenosine triphosphate
BSA	Bovine serum albumin
CD	Methyl-β-cyclodextrin
CE	Cholesteryl ester
CERT	Ceramide transfer protein
CHO	Chinese-hamster ovary
Chol	Cholesterol
CK1	Casein kinase 1
COPII	Coatomer II
CTL	Cholestatrienol
Dansyl-PE	Dansyl-phosphatidylethanolamine
DHE	Dehydroergosterol
DMEM	Dulbecco's modified Eagle medium
ERC	Endocytic recycling compartment
ERK	Extracellular-signal-regulated kinase
FBS	Fetal bovine serum

FFAT	Two phenylalanines in an acidic tract
FRET	Förster resonance energy transfer
GFP	Green fluorescent protein
GST	Glutathione S-transferase
HDL	High density lipoprotein
HEK	Human embryonic kidney
HePTP	Haematopoietic tyrosine phosphatase
HMG-CoA	3-hydroxy-3-methyl-glutaryl-CoA
HMG-CoAR	3-hydroxy-3-methyl-glutaryl-CoA reductase
INSIG	Insulin-induced gene
JAK2	Janus kinase 2
LCAT	Lecithin-cholesterol acyltransferase
LD	Lipid droplet
LDL	Low-density lipoproteins
LDLR	Low-density lipoproteins receptor
LE	Late endosome
Lectin	*R.Communis* agglutinin
LXR	Liver X receptor
MAPK	Mitogen-activated protein kinase
MLN64	Endosomal metastatic lymph node protein 64
MSP	Major sperm protein
NPC	Niemann-pick C
NVJ	Nuclear-vacuolar junction

Nvp1	Nuclear vacuolar protein 1
OH	OSBP homology
ORP	Oxysterol-binding protein-related protein
OSBP	Oxysterol-binding protein
OSH	Oxysterol-binding homology
PAGE	Polyacrylamide gel electrophoresis
PC	Phosphatidylcholine
PDK	Phosphoinositide-dependent kinase
PE	Phosphatidylethanolamine
PFN	Profilin
PH	Pleckstrin homology
PI	Phosphatidylinositol
PI(3)P	Phosphatidylinositol 3-phosphate
PI(4)P	Phosphatidylinositol 4-phosphate
$PI(4,5)P_2$	Phosphatidylinositol 4,5-bisphosphate
PI4K	PI4-kinases
PKD	Protein kinase D
PM	Plasma membrane
PP2A	Protein phosphatase type 2A
PP2Cε	Protein phosphatase 2Cε
PS	Phosphatidylserine
PX	Phox homology
RCT	Reverse cholesterol transport

RILP	Rab7-interacting lysosomal protein
S1P	Site-1 protease
S2P	Site-2 protease
Sar1	Secretion-associated RAS
SBD	Sterol-binding domain
SCAP	SREBP-cleavage activating protein
SCP	Sterol carrier protein
SDS	Sodium dodecyl sulfate
shRNA	Short hairpin RNA
SM	Sphingomyelin
SNARE	N-ethylmaleimide-sensitive factor attachment protein receptor
SRB1	Scavenger receptor B1
SRE	Sterol-regulatory element
SREBP	Sterol regulatory element binding protein
SSD	Sterol-sensing domain
START	Steroidogenic-acute regulatory (STAR)-regulated lipid transfer
STAT3	Signal transducer and activator of transcription 3
TG	Triglyceride
TGN	Trans-Golgi network
VAP	Vesicle-associated membrane protein (VAMP)-associated protein
α-TTP	α-Tocopherol transfer protein

ACKNOWLEDGEMENTS

I would like to acknowledge the individuals who have contributed to this research in various aspects over the last two years. Without their generous help, the work presented here would not be possible. I would first like to thank my supervisory committee members, Drs. Roy Duncan and Barbara Karten, for their valuable criticisms and suggestions on my research and willingness to share lab equipment. I am grateful to Robert Zwicker for his excellent and reliable technique assistance. I would like to thank the Ridgway group and the rest of the ARC for their valuable insights, sharing lab materials and equipments. Especially, I would like to thank Mark Charman, Dr. Asako Goto and Daniel Arsenault, for their patience and willingness to teach. I am also thankful to Steven Whitefield for his assistance with microscopy techniques.

The research was financially supported through the Canadian Institute for Health Research (CIHR).

Finally, I would like to thank my supervisor, Dr. Neale Ridgway, for providing me with an interesting project with continual support and constructive criticisms over the last two years. I am grateful for all of the input I have received and the challenges that I faced. They inspire me to better understand scientific research.

CHAPTER 1 INTRODUCTION

1.1 Cholesterol and fluorescent cholesterol analog

Cholesterol ((3β)-cholest-5-en-3-ol) is a 27-carbon amphipathic molecule with a 3-hydroxyl group and a 17-hydrocarbon fused ring structure composed of one 5-carbon and three 6-carbon rings. Cholesterol is an essential mammalian cell membrane component, serving structural and signalling functions, as well as a metabolic precursor for other important molecules, such as bile acids, steroid hormones, and vitamin D. The amphipathic property allows cholesterol to align with lipids in cell membranes, with the polar group (3-hydroxyl) facing the cytosol or organelle matrix. The unique fused four-ring structure and hydrocarbon chain interact with proximal lipid hydrocarbon chains, conferring biophysical interactions that enhance integral membrane cohesion and packing. Membranes with enhanced packing have reduced fluidity and permeability [1]. Due to its structure, cholesterol positions between lipids containing saturated hydrocarbon chains. Cholesterol also preferentially interacts with lipids providing additional shielding to the 3-hydroxyl group [2] or lipids such as sphingomyelin (SM), through hydrogen bonding [3]. Cholesterol and SM are also important for a controversial membrane moiety called lipid rafts, which are believed to provide a structural scaffold where related proteins gather and function for different biological processes such as signal transduction and membrane trafficking [4,5].

In addition, cholesterol also interacts with various proteins. Many of these proteins are involved in cholesterol homeostasis (such as sterol regulatory element binding protein cleavage activating protein (SCAP)) or trafficking (such as Niemann-

Pick C 1 and 2). This project focuses on oxysterol-binding protein (OSBP) and its related proteins (ORPs). Members from this protein family bind cholesterol and are implicated in cholesterol trafficking [6]. Despite its importance in cells, cholesterol is also related to some pathological conditions. For example, abnormal cholesterol homeostasis causing high cholesterol levels in the circulation may lead to atherosclerosis. Disrupted cholesterol trafficking, like that observed in NPC disease, causes cholesterol accumulation in lysosomes of various organs and eventually leads to death in childhood [7]. The disease is caused by recessive loss-of-function mutations in NPC1 or NPC2 proteins that are required in cholesterol egress from late endosomes (LE) and lysosomes [7].

Since cholesterol is an important biological molecule and has been implicated in human diseases, cholesterol homeostasis, organization and trafficking have been intensely studied. Recently, fluorescent cholesterol analogs have been used to study cholesterol functions both *in vivo* and *in vitro*. Most of the cholesterol analogs (such as BODIPY-cholesterol and 22-NBD-cholesterol) are conjugated with fluorescent groups to visualize cholesterol distribution in membranes (reviewed in [8]). Moreover, there is also a small group of distinct fluorescent analogs that have conjugated double bonds within the four-ring system of cholesterol that confer fluorescent properties. There are two typical members in this group: dehydroergosterol (DHE) and cholestatrienol (CTL) (Figure 1.1). These molecules are less perturbing than sterols conjugated with fluorescent probes since they do not have a bulky fluorescent group. Compared with cholesterol, DHE has three more double bonds, two in the 4-member ring and one in the hydrocarbon chain, and an extra methyl group in the hydrocarbon chain (Figure 1.1). The extra methyl

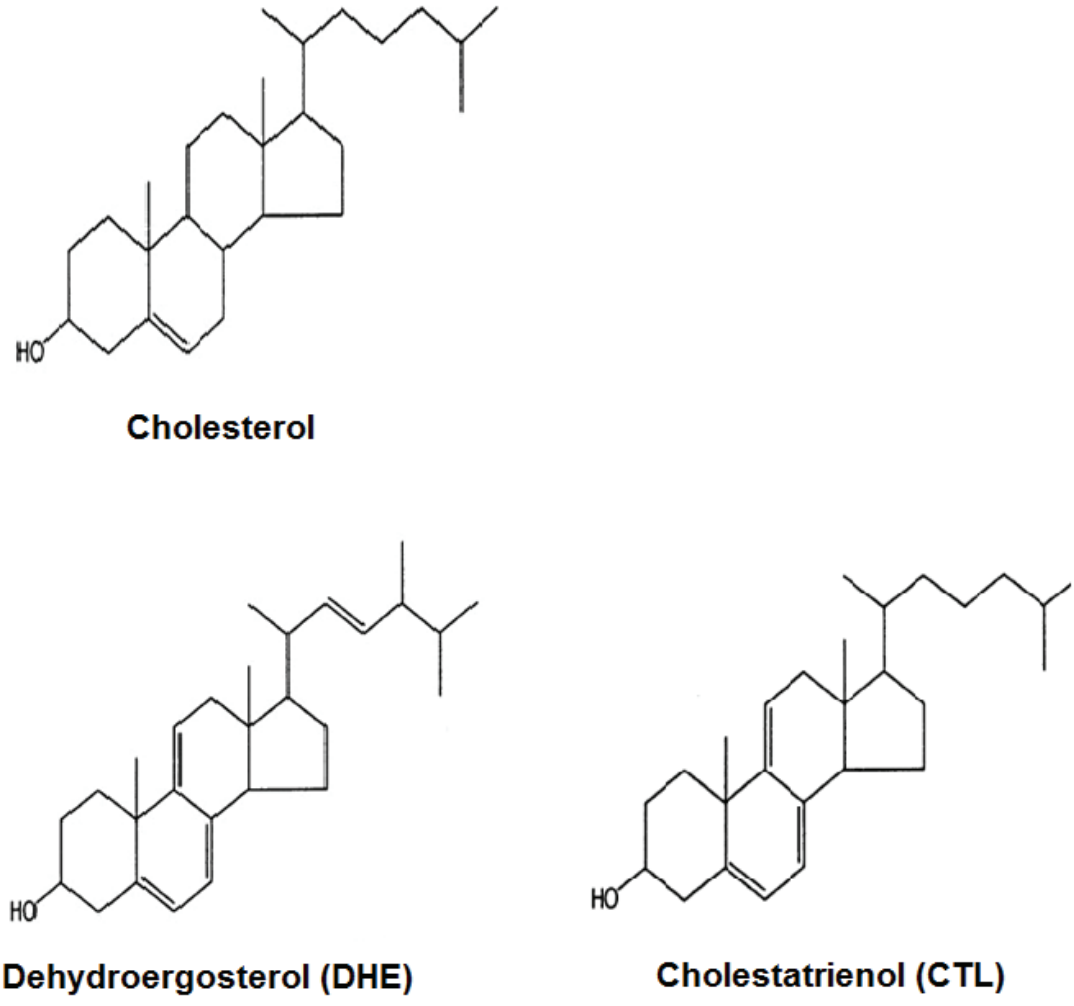

Figure 1.1 Structure of cholesterol and the two fluorescent analogs: dehydroergosterol (DHE) and cholestatrienol (CTL). Adapted from reference [9].

group at carbon 24 of DHE may affect the membrane and domain properties relative to cholesterol, suggested by the fact that campesterol, which also contains this methyl group, demonstrated poor interaction with membrane lipids as monitored by differential scanning calorimetry [10]. Despite the disturbance caused by the extra methyl group, DHE has been used to image cholesterol in cultured cells [8] and to study sterol transport between liposomes by cholesterol binding proteins such as oxysterol-binding protein (OSBP)-related protein 5 (ORP5) [11]. The other fluorescent cholesterol analog in this group, CTL, has two more double bonds in the fused ring structure compared with cholesterol (Figure 1.1; [12]). Relative to cholesterol, CTL demonstrates a similar membrane orientation, motion and lipid condensation with surrounding lipids examined by using electron paramagnetic resonance, nuclear magnetic resonance and fluorescent spectroscopy [13]. CTL is suitable for live-cell imaging to study cholesterol transport and was used to study cholesterol transport by NPC2 *in vitro* [14]. My project is to use one of the fluorescent cholesterol analogs to study cholesterol transport by OSBP and ORP9, based on Förster resonance energy transfer (FRET) between fluorescent probes. How DHE and CTL were used in the FRET-based assays will be described later in this chapter.

1.2 Cholesterol homeostasis

Cellular cholesterol levels are tightly regulated on several levels, including cholesterol synthesis, uptake, efflux and esterification. *De novo* synthesis and uptake are two ways a cell obtains cholesterol. *De novo* cholesterol synthesis produces 70% of the total body cholesterol [15]. Starting from acetyl-CoA, cholesterol is synthesized by a multi-step pathway in the ER, peroxisomes and cytosol. The pathway is regulated by the ER-anchored rate-limiting enzyme 3-hydroxy-3-methyl-glutaryl-CoA (HMG-CoA)

reductase (HMG-CoAR) [16]. The remainder of the cholesterol is obtained by endocytic uptake. Cholesterol and cholesteryl ester (CE) packed in low-density lipoproteins (LDL) is recognized by the LDL receptor (LDLR) on the plasma membrane, engulfed by cells, and CE is hydrolysed in the lysosomes. The levels of HMG-CoAR and LDLR are regulated by a transcriptional factor called sterol-regulatory element (SRE) binding protein (SREBP). SREBP resides in the ER where it associates with two other proteins, SREBP cleavage-activating protein (SCAP) and insulin-induced gene (INSIG). When cholesterol levels are low, SREBP associates with SCAP and translocates from the ER to Golgi apparatus in coatomer II (COPII) coated vesicles. At the Golgi apparatus, cleavage processes are carried out sequentially by site-1 protease (S1P) and site-2 protease (S2P) to release the N-terminal SREBP fragment. The released SREBP fragment translocates to the nucleus and activates transcription of the HMG-CoAR and LDLR genes to gain more cholesterol. In contrast, under cholesterol replete conditions, cholesterol and 25-hydroxycholesterol bind to SCAP and INSIG, respectively [17]. The bindings induce a conformational change in SCAP and INSIG and causes SREBP to be retained in the ER and unavailable for Golgi translocation [18]. Furthermore, HMG-CoAR is regulated on other levels. HMG-CoAR activity is inhibited via reversible phosphorylation by AMP-stimulated protein kinase [19]. Moreover, when sterol levels are high, proteasomal degradation of HMG-CoAR occurs [20].

Excess cellular cholesterol can be removed by reverse cholesterol transport (RCT) [21]. Adenosine triphosphate (ATP)-binding cassette (ABC) transporter ABCA1 is ubiquitous [22] and mediates cholesterol exit from a cell to lipid-poor apolipoprotein (Apo) A-I bound with ABCA1 to generate nascent high density lipoprotein (HDL).

Lecithin-cholesterol acyltransferase (LCAT) converts cholesterol in HDL into CE. A more spherical HDL particle generated from the esterification serves as a unidirectional cholesterol acceptor and uptakes more cholesterol from macrophage cells facilitated by ABCG1 [23]. Mature HDL enters the circulation and is absorbed by organs, such as the liver, where CE is selectively removed by the scavenger receptor B1 (SRB1) and further metabolized to bile acid for excretion. Expression of the proteins involved in RCT is regulated by the liver X receptor (LXR), which is activated by oxysterol binding [24]. Furthermore, excess cellular cholesterol can be reduced by esterification. Excess cholesterol in the ER is accessible to acyl-CoA cholesterol acyltransferase (ACAT), which esterifies cholesterol for storage in cytoplasmic lipid droplets [25].

1.3 Intracellular cholesterol transport

Although cholesterol is an essential molecule for the viability of mammalian cells and has various important functions, it is not evenly distributed within a cell. Cholesterol is enriched in the plasma membrane (PM) (65% to 80% of total cellular cholesterol), endocytic recycling compartment and trans-Golgi network (TGN). However, cholesterol is low (0.1-2% of total cell cholesterol) in the ER, where newly synthesized cholesterol is produced [26-28]. The uneven distribution of cholesterol indicates that there are various pathways responsible for cholesterol delivery between different cellular compartments. Since it is hydrophobic, cholesterol must be transported either by vesicle- or nonvesicle-mediated (protein-mediated) pathways, or more likely a combination of both. Vesicle-mediated cholesterol transport is generally ATP-dependent and includes four essential steps including vesicle budding, transport, tethering, and fusion (reviewed in [29]). Each step contains sequential and ordered reactions, mediated by specific

proteins. For example, vesicle budding requires coating proteins (such as COPI) that are mediated by small GTPases of the ADP (adenosine diphosphate)-ribosylation factor 1 (Arf1)/secretion-associated RAS superfamily (Sar1) family [30]; cytoskeleton and motor proteins (such as dynein-dynactin) are involved in vesicle transport [31-33]; tethering and fusion with target membrane is mediated by soluble N-ethylmaleimide-sensitive factor attachment protein receptor (SNARE) proteins [34]. In nonvesicle-mediated transport, soluble sterol transport proteins, which typically contain a hydrophobic pocket, can bind and transport cholesterol across the aqueous space. Nonvesicle-mediated transport can be facilitated by specialized proteins at sites of membrane contact, where membranes from different organelles closely oppose each other [35].

Cholesterol derived from LDL uptake in the endocytic pathway largely depends on vesicle-mediated transport. The LDL particles containing cholesterol and CE are recognized by LDL receptors (LDLR) at the PM and internalized into cells in clathrin coated vesicles. In early endosomes (or sorting endosomes), LDLRs dissociate from vesicles and recycle back to the PM through the endocytic recycling compartment (ERC). Meanwhile, through vesicular fusion, some cholesterol from LDL and the endocytosed PM is also delivered to the cholesterol-rich compartment ERC [36-38]. Along with the LDLR, cholesterol in the ERC can be delivered to the PM by vesicular transport [39], which is regulated by the GTPase Rab11 [40]. However, reverse transport from PM to ERC is thought to be non-vesicular, requiring an unknown lipid transfer protein [39]. As early endosomes mature into LEs, CE remaining in the endocytic pathway is hydrolyzed by acid lipase to release more cholesterol, which is further transported from late endosomes to other compartments, such as TGN, ER, and lysosomes. Little is known

about the cholesterol sorting processes in the LEs. The aforementioned NPC1 and NPC2 are a set of proteins found in LE and involved in cholesterol export. NPC2 is a highly glycosylated soluble protein, while NPC1 is a large transmembrane protein. *In vitro,* NPC1 cannot rapidly transport its bound cholesterol to liposomes. However, NPC1 can rapidly bind the cholesterol already bound to NPC2 [41]. Therefore, in cells, NPC2 can bind cholesterol in the lumen of the LE and transfer it to NPC1 for further delivery to other cellular compartments.

Newly synthesized cholesterol can be transported through the Golgi apparatus to the PM by vesicle-mediated transport, based on the fact that rapid cholesterol transport from ER to PM is inhibited under low temperature or ATP-depletion conditions [42,43]. However, a non-vesicular transport pathway is likely to be more important for most cholesterol transport from the ER to PM (reviewed in [35,44]). Mammalian cells treated with brefeldin A, which causes Golgi disassembly and blocks further anterograde vesicular transport, blocks >90% of protein secretion but newly synthesized cholesterol transport to the PM is only reduced by 20% [43,45]. Also, *S.cerevisiae* with conditional defects in vesicular proteins required for ER to PM trafficking do not have defective cholesterol delivery to the PM [46]. Furthermore, excess cholesterol in the ER triggers ACAT to esterify cholesterol to CE for storage in lipid droplets (LDs). The CE transport pathway from the ER to LDs remains to be elucidated, but it is possible that transport is achieved by diffusion, since the monolayer of some LDs remain connected with the ER outer leaflet [44,47,48]. Alternatively, the transport can be facilitated by specialized sterol transport proteins.

Although non-vesicular cholesterol transport between various cellular compartments is strongly implicated, proteins that are involved in cholesterol transport remain to be elucidated. Besides the aforementioned NPC proteins, which are involved in cholesterol exit from the LE, sterol carrier proteins (SCPs), caveolins, and steroidogenic-acute regulatory (StAR)-regulated lipid transfer (START) proteins are also possible sterol transporters (reviewed in [44]). StAR is involved in cholesterol transfer from the outer mitochondrial membrane to the inner membrane. There are at least 14 more proteins containing a START domain in humans [49]. One member of this group, known as endosomal metastatic lymph node protein 64 (MLN64), is implicated in cholesterol transport from LE to mitochondria, supported by the fact that depletion of MLN64 by siRNA in Chinese-hamster ovary (CHO) cells attenuated cholesterol transport to the mitochondrial inner membrane [50]. Furthermore, members of the oxysterol-binding protein (OSBP)/OSBP-related proteins (ORPs) are also candidates for cellular cholesterol transport. The OSBP/ORP family members will be discussed in more detail later in this chapter. Part of my project is to study the possible cholesterol transport function of OSBP and ORP9 using *in vitro* assays.

1.4 Phosphoinositides and phosphatidylinositol 4-phosphate

Phosphoinositides are phosphorylated products of phosphatidylinositol (PI) that contribute less than 1% of the total cellular lipid content. PI is primarily synthesized in the ER and consequently delivered to other cellular compartments via vesicle-mediated or protein mediated transport. PI is then subject to reversible phosphorylation at the 3, 4 and 5 positions of the inositol ring to produce seven different phosphoinositide species. Each of these phosphoinositides has a unique distribution pattern in cells. For

example, phosphatidylinositol 3-phosphate (PI(3)P) is mainly present in endosomes and phosphatidylinositol 4,5-bisphosphate ($PI(4,5)P_2$) is concentrated in PM [51].

Early studies on phosphoinositides focused on the intracellular messenger, called inositol (1,4,5)-trisphosphate, which is generated from $PI(4,5)P_2$ by phospholipase C [52]. Besides their role as a metabolic precursor, phosphoinositides also bind to proteins. Proteins bind phosphoinositides via their phosphoinositide binding modules, such as pleckstrin homology (PH) and phox homology (PX) domains (reviewed in [53]). Particular modules have specific phosphoinositide binding preference. For instance, PX domain specifically binds PI(3)P. PI(4)P and $PI(4,5)P_2$ show high binding affinity for the PH domain of OSBP/ORPs [54].

Due to their unique distribution patterns and binding preference to particular proteins, phosphoinositides are excellent mediators of biological functions in different cellular compartments [51]. For example, $PI(4,5)P_2$ in the PM is required for proper function of several ion channels (such as K^+ and Ca^+ channels). PI(4)P in the TGN regulates vesicular trafficking since limitation of PI(4)P levels in yeast showed disrupted anterograde trafficking [55]. OSBP and ORP9 target to the TGN via the interaction between their PH domains and PI(4)P [56,57]. Furthermore, recruitments can be generated by coincidence detection when a phosphoinositide molecule and one or more co-receptors in the membrane bind simultaneously to a protein. This dual (or multiple) recognition allows a more specific membrane-cytosol interaction [58]. For example, both clathrin adaptors AP-1 and AP-2 bind some of the same cargo proteins but are recruited to TGN and PM, respectively, partially due to the different phosphoinositide species within these membranes [59-62].

More importantly for my project, a recent study shows that PI(4)P is also a ligand for the sterol binding domain of the oxysterol-binding homology 4 (Osh4p), a yeast orthologue of OSBP [63]. PI(4)P is enriched in the TGN by the activity of PI4-kinases (PI4K), PI4KIIα and PI4KIIIβ [64]. In contrast, PI(4)P can be dephosphorylated by Sac1, a phosphatase that is located primarily in the ER and Golgi apparatus. Through the spatial separation of PI(4)P (TGN) and Sac1 (ER), dephosphorylation probably occurs after PI(4)P is transported back to the ER via vesicular or protein-mediated transport [65]. Osh4p is a good candidate for this transport, since it binds PI(4)P [63]. Besides being a precursor for $PI(4,5)P_2$ in the PM, PI(4)P has been implicated in other biological functions. PI(4)P is an important lipid component of the Golgi apparatus, since depletion of PI4KIIα and PI4KIIIβ disrupts Golgi integrity and function [60]. Furthermore, PI(4)P together with Arf1 recruits cytosolic proteins such as the clathrin adaptor AP-1. PI4KIIIβ, which catalyzes the phosphorylation of PI, is activated by Arf1. Therefore, Arf1 can regulate PI(4)P production to change the lipid environment of TGN and cooperate with PI(4)P to recruit proteins for specific biological functions. For example, some plus-strand RNA viruses utilize host Arf1 to stimulate PI(4)P production catalyzed by PI4KIIIβ, generating a PI(4)P-rich organelle for viral RNA replication [66].

1.5 Oxysterol-binding protein (OSBP) and OSBP-related proteins (ORPs)

OSBP, the founding member of a large family of lipid-binding proteins, was discovered in 1984 due to its high binding affinity for various oxysterols *in vitro* [67]. The protein was later purified from the cytosol of hamster livers [68]. The rabbit and human cDNAs encoding this protein were cloned [69,70]. Through genomic analysis, an additional eleven members and seven members were identified in human or yeast

S.cerevisiae genomes, respectively [71,72]. OSBP/ORPs are characterized by a C-terminal sterol-binding domain (SBD) or OH (OSBP homology) domain containing a signature sequence (EQVSHHPP), which is conserved in ORPs among species. Besides the SBD, which is responsible for sterol and oxysterol binding, many ORPs have additional functional domains, such as the two phenylalanines in an acidic tract (FFAT) motif and PH domain. Furthermore, ORPs have been identified in fruit flies (*Drosophila melanogaster*) [73], plants [74,75], worms (*Caenorhabditis elegans*) [76], slime mould (*Dictyostelium discoideum*) [77], and a parasitic protist (*Cryptosporidium parvum*) [78]. The phylogenetic tree constructed using ORP sequences from 120 unique taxa reveals that ORPs are classified based on type rather than taxonomy, indicating a set of common ancestors [78]. The presence of closely related human and yeast ORPs in each cluster suggest more recent gene duplication events [78].

1.5.1 The yeast OSH and human ORP families

The seven members of the yeast OSBP homologue (OSH1-7) family are classified into four subfamilies, based on amino acid sequence (Figure 1.2A). Subfamily I is composed of Osh1p and Osh2p; subfamily II is Osh3P; subfamily III is composed of Osh4p (also known as Kes1p) and Osh5p; subfamily IV is composed of Osh6p and Osh7p. Osh proteins from subfamily I & II are structurally more similar to OSBP, since these Osh proteins also contain a FFAT motif and PH domain (Figure 1.2A). However, proteins from subfamilies III & IV only contain the conserved SBD. The presence of the phosphoinositide binding PH domain confers specific targeting. For example, the PH domain of Osh1p binds to PI(4)P and PI(4,5)P_2 *in vitro* and targets Osh1p to Golgi [57,79]. In the yeast, it is known that Osh proteins have similar distribution patterns,

supported by the fact that most of the exogenous green fluorescent protein (GFP)-tagged Osh proteins are in the cytoplasm [80]. In addition, some Osh proteins are enriched in specific cellular compartments. For instance, Osh4p also localizes in the Golgi apparatus [81] and Osh2p is enriched in the PM [80]. Interestingly, the ubiquitous protein distribution partially explains the fact that deletion of all *Osh* genes is lethal, while expressing any one of the Osh proteins rescues the cells [72]. This also indicates that Osh proteins have functional overlap.

The twelve members of the human ORP family can be sorted into six subfamilies based on sequence similarity (Figure 1.2B). The human ORP family is sorted as, OSBP, ORP4L and ORP4S in subfamily I, ORP1L, ORP1S and ORP2 in subfamily II, ORP3, ORP6 and ORP7 in subfamily III, ORP5 and ORP8 in subfamily IV, ORP9L and ORP9S in subfamily V, ORP10 andORP11 in subfamily VI. For most members of the human ORP family, a typical set of structural components includes the PH domain, FFAT motif and SBD, with certain exceptions. The full version of ORP2 does not have the PH domain; members in subfamily IV and VI lack the FFAT motif. Instead, for proteins in subfamily IV, both ORP5 and ORP8 have a C-terminal transmembrane domain that substitutes the function of the FFAT motif in ER localization. A moiety with three ankyrins is identified in ORP1 (full-length) and also in yeast Osh1p and Osh2p. Corresponding functions of these ORP domains and their putative roles in biological processes will be discussed with more detail in the sections that follow. Furthermore, some ORPs have short isoforms that have lost some of their functional domains (PH domain and FFAT motif) compared with their full-length isoforms. For example, ORP1S and ORP9S lack a PH domain. Short isoforms expression is due to alternative gene

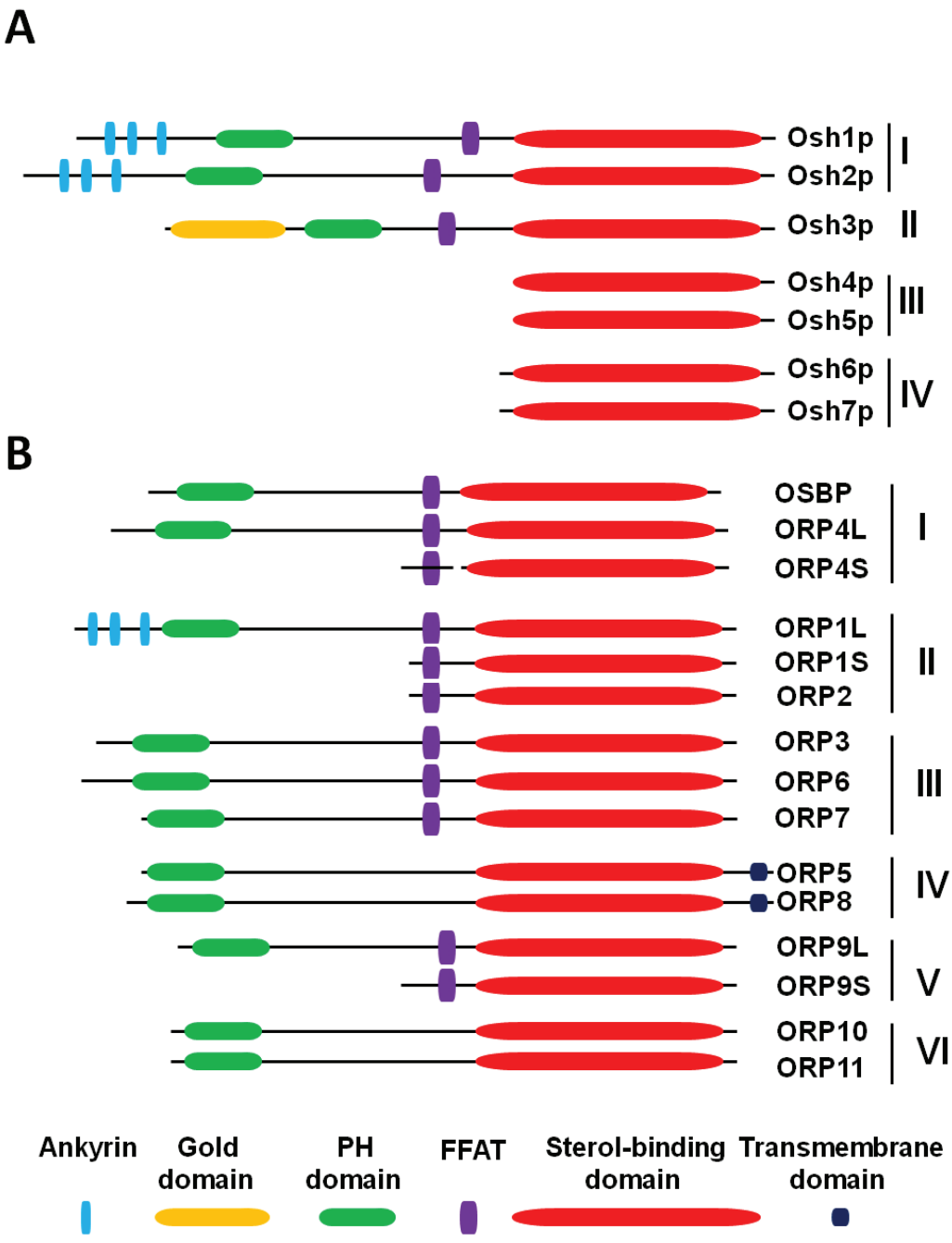

Figure 1.2 Structural organization of yeast and human ORP families. Yeast and human family members are classified into different subfamilies based on their sequence similarity. Some full-length or long (L) human ORPs have short (S) variants, which are also illustrated in the figure. Individual domains are color-coded: blue, ankyrin; yellow, gold domain; green, PH; purple, FFAT; red, sterol-binding (OH); dark blue, transmembrane. The disconnection in ORP4S indicates the alternative translation start site.

promoter (ORP1, ORP4 and ORP9) or alternative splicing (ORP3) [82-84].

Unlike yeast, the distribution of mammalian ORP is more complex and tissue-specific. Studies on human and mice ORP genes reveal that their mRNAs are ubiquitously expressed in most human tissues, but the transcript levels are significantly different from tissue to tissue [71,85-87]. OSBP is ubiquitous in all tissues but enriched in the brain, heart, kidney and liver [71]. Tissue-specific distribution also exists among ORPs within the same subfamily. For example, ORP3 is enriched in kidney, lymph nodes and thymus; ORP6 is identified in the brain and skeletal muscle; ORP7 is strictly found in gastrointestinal tract [88]. ORP9, like OSBP, is identified in various human tissues, such as heart and spleen [71,85]. At the cellular level, mammalian ORP distribution is regulated by the functional domains, like PH domain and FFAT motif. For instance, the PH domain of ORP9L is responsible for its TGN localization; the FFAT and SBD of ORP9L mediate its ER retention [56,84]. ORP1L targets to late endosomes, regulated by its PH domain and ankyrin repeat; ORP1S that lacks these domains is mainly cytosolic [83].

1.6 ORP function domains

The functional domains of ORPs including sterol-binding and PH domains, FFAT motif and ankyrin repeat have been mentioned in previous sections. In the coming sections, more detail for these domains and regions will be discussed.

1.6.1 Sterol-binding/OH domain

The structure of Osh4p with bound ergosterol was solved by X-ray crystallography at 1.5-1.9 Å resolution [89]. This structure provides an insight into how

the SBD of ORPs interacts with their sterol ligands. Generally speaking, Osh4p has two functional moieties, a hydrophobic pocket to accommodate the sterol and an α-helical lid that covers the entrance of the hydrophobic pocket. The unique hydrophobic pocket is composed of a 19-strand antiparallel β-sheet, forming a β-barrel with a hydrophobic core inside. The β-barrel is flanked by a two-stranded β-sheet and three α-helices structure connected with the N-terminal α-helix lid. The three α-helices also plug the other end of the β-barrel. Cholesterol, ergosterol, and oxysterols are accommodated in the sterol-binding pocket of Osh4p with the same alignment: the 3-hydroxyl group of the sterol is positioned at the bottom of the hydrophobic pocket and the hydrocarbon side chain interacts with the α-helical lid. The 3-hydroxyl group forms direct hydrogen-bond with Gln^{96} and indirect interactions with Trp^{46}, Tyr^{97}, Asn^{165} and Gln^{181} by hydrogen bonding with a water molecule. Surprisingly, hydroxyl groups in other oxysterols, except for 25-hydroxycholesterol (25-OH), do not show any ordered interactions with the α-helical lid. This observation partially explains why Osh4p can bind various oxysterols. Osh4p structure could only be solved with the N-terminal α-helix lid deleted due to its flexibility [89].

Although none of the mammalian ORP structures have been solved, the SBD of these proteins probably adopts a similar structure to bind sterols and oxysterols. A structure modeling study of ORP2 (similar in size compared with Osh4p) revealed that this protein has a similar binding pocket compared with Osh4p [90]. Sterol and oxysterol binding to mammalian ORPs has been identified using *in vitro* assays [91,92]. In specific, ORPs are incubated with radioactive labeled sterol and oxysterols dissolved in aqueous buffer with or without detergent, respectively. His-tagged ORPs bound with sterols are

sedimented after binding with Talon resin. For oxysterols, unbound oxysterols are removed by dextran/charcoal. Sterol and oxysterol bindings are determined by scintillation counting. OSBP binds cholesterol with a K_d=173 nM while it binds 25-OH with a higher affinity (K_d=10 nM) [69,82,91,93]. ORP4L binding to 25-OH (K_d= 10 nM) is inhibited by a mutations in the putative lid region, indicating the importance of the lid region in ligand binding [82]. Surprisingly, ORP9L does not bind cholesterol and 25-OH dispersed in aqueous solution [56]. More examples showing that mammalian ORPs bind cholesterol and oxysterols dispersed in solution are reviewed elsewhere [6]. As mentioned earlier, cholesterol can be dispersed in aqueous solution to test ORP binding activities, but cholesterol is present within membranes in cells. An assay testing whether ORPs extract cholesterol from liposomes is another method to study the cholesterol binding function. This assay better simulates the cholesterol environment in cells. In this assay, ORPs are incubated with liposomes incorporated with [^{3}H]cholesterol. ORPs with extracted [^{3}H]cholesterol are separated from liposomes by centrifugation to determine extraction activities. Results using this liposomal extraction assay show that OSBP removes cholesterol from membranes. Surprisingly, ORP9L that does not bind cholesterol dispersed in aqueous solution but extracts cholesterol from liposomes with comparable activity to OSBP [56]. Thus, cholesterol binding by the SBD of ORPs may be activated upon membrane contact. Furthermore, cholesterol and oxysterol binding by ORPs has also been shown in cultured cells using photoactivatable [^{3}H]cholesterol and [^{3}H]25-OH [90]. These analogs are photoactivatable due to their C-6 diazirine ring, which can be activated by ultraviolet light and detected by fluorography [94]. OSBP, ORP1-3, ORP5-11 and the SBD of ORP4 in COS cells demonstrated photo-25-OH

binding. All members of ORPs, except for ORP4 and ORP9, demonstrated photo-cholesterol binding.

A recent study revealed that PI(4)P is also a ligand for Osh4p [63]. Osh4p specifically extracts PI(4)P from liposomes. More importantly, the structure of Osh4p with bound PI(4)P has been solved by X-ray crystallography at 2.6 Å resolution [63]. Osh4p bound with PI(4)P demonstrates a highly similar overall structure compared with its ergosterol bound structure (Figure 1.3A). Specifically, the two acyl chains of PI(4)P are accommodated in the hydrophobic pocket while the phosphorylated inositol ring resides at the entrance of the pocket (Figure 1.3A). The N-terminal lid of Osh4p adopts a different conformation to accommodate the phosphorylated inositol ring. The two acyl chains probably form weak Van Der Waal's interactions with the inner side of the pocket. In contrast, the phosphorylated inositol ring forms various direct and water mediated interactions with the protein (Figure 1.3B). Interactions formed with the 4-phosphate group include direct hydrogen-bonds with His^{143}, His^{144} and Arg^{344} and a water mediated interaction with Ser^{25} in the lid. The phosphodiester group connecting the inositol ring and the glycerol backbone is hydrogen-bonded with Lys^{109}, Lys^{336} and the amide group of Ala^{29} (Figure 1.3B). Moreover, interactions are also identified between the hydroxyl groups of the inositol ring and Ser^{25}, Leu^{27} and Glu^{340} through direct or indirect interactions. Supported by results from molecular modeling and *in vitro* assays, Osh4p specifically recognizes PI(4)P but not other phosphoinositides such as $PI(4,5)P_2$ [63].

Several residues of Osh4p that interact with the inositol 4-phosphate group are highly conserved in yeast and mammalian ORPs. Recombinant Osh4p with mutations in these residues (Lys^{109}, His^{143}, His^{144}, Glu^{340}, Arg^{344} and Lys^{336}) demonstrates normal

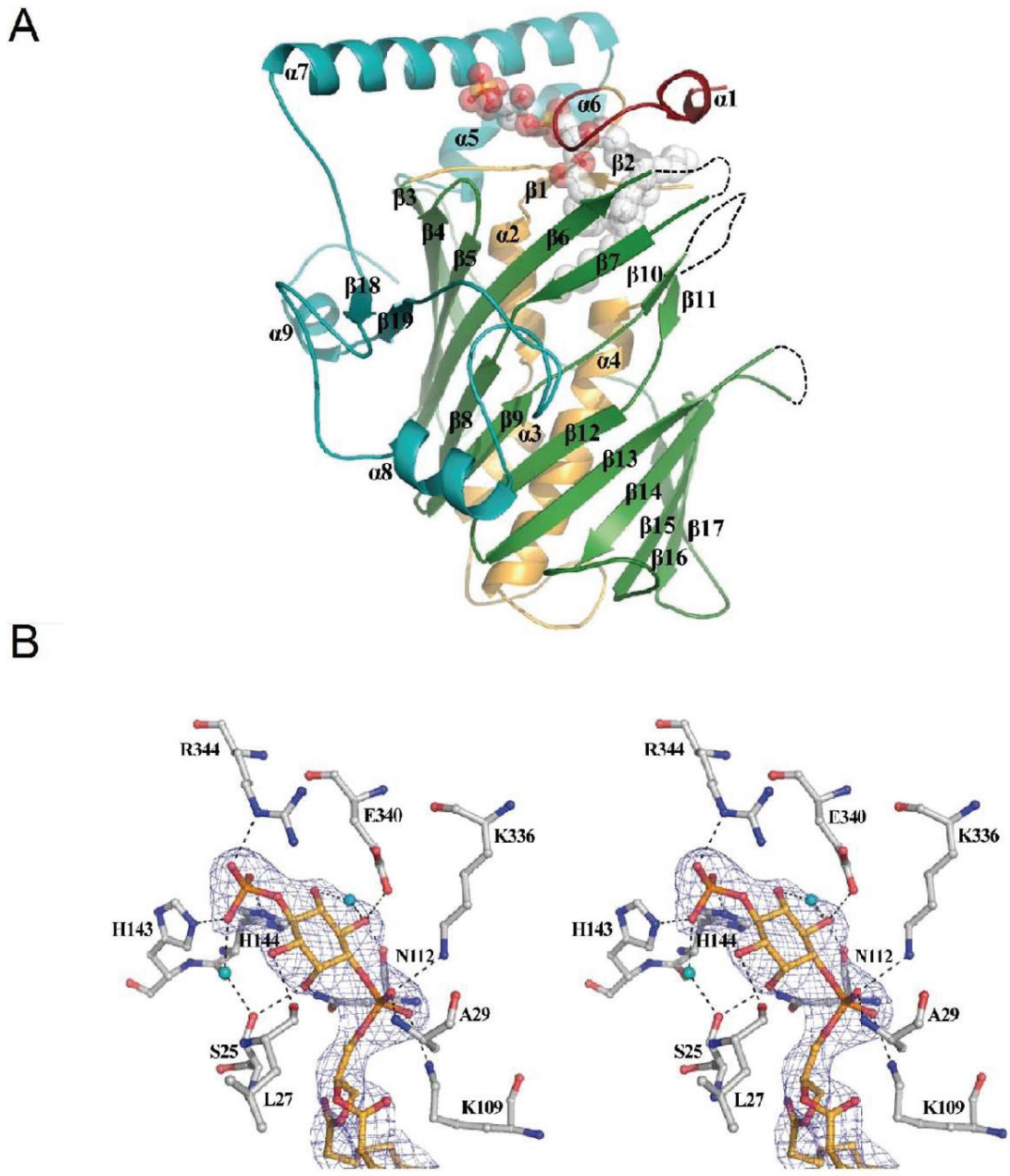

Figure 1.3 Structure of Osh4p bound with PI(4)P. (A) Overall structure of Osh4p bound with PI(4)P. Different structural moieties of Osh4p are color-coded: lid, red; N-terminal domain, orange; β-barrel, green; C-terminal domain, cyan. PI(4)P is presented as spheres and also color-codes: carbon, white; oxygen, red; phosphorus, orange. (B) Interactions formed by the inositol 4-phosphate group of PI(4)P and involved Osh4p residues. Nitrogen, oxygen, phosphorus are coded as blue, red, and orange. Carbon atoms from residues and PI(4)P are shown in white and yellow, respectively. Water molecules involved in the interactions are show as cyan spheres. Adapted from reference [63].

DHE extraction that is not suppressed by the presence of PI(4)P in liposomes, indicating these residues are essential in PI(4)P rather than sterol binding [63]. Collectively, these results prompt us to think that the PI(4)P binding activity to the SBD is a common function of ORPs. Therefore, one aim of my project is to investigate whether PI(4)P is also a ligand for OSBP and ORP9.

1.6.2 PH domain and phosphoinositide binding

PH domains are composed of 100-120 amino acids with limited primary sequence similarity, but form a conserved tertiary structure [95]. The PH domain consists a seven stranded β-sandwich, capped by an α-helix. Conserved basic residues in loops opposite to the α-helix cap are responsible for phosphoinositide binding. The well-known function of the PH domain is its ability to bind phosphoinositides. The binding between the PH domains and phosphoinositides has been identified in some yeast and human ORPs. For instance, the PH domain of OSBP and Osh1p specifically binds PI(4)P in the Golgi apparatus of cultured cells [57,79]. Since different phosphoinositide species are enriched in particular cellular compartments, these interactions can mediate the localization of some ORPs to specific membranes.

The PH domains of OSBP and ORP9L were extensively studied in recent years. *In vitro* assays reveal that PI(4)P or PI(4,5)P_2 is required for OSBP PH domain binding to purified Golgi membranes [57]. Another assay using full-length OSBP and ORP9L or their PH domains fused with glutathione S-transferase (GST) tested the interaction between the PH domains and phosphoinositides immobilized on nitrocellulose membrane. For full-length OSBP and ORP9L and their PH domains, binding was

identified for PI(3)P, PI(4)P, but not PI(4,5)P_2 [56]. In cultured cells, OSBP translocation to the Golgi is promoted by 25-OH treatment and requires the PH domain interaction with PI(4)P [57,79,91]. Moreover, this translocation is negatively regulated by protein kinase D (PKD), supported by the fact that phosphorylation by PKD decreased OSBP Golgi localization in CHO cells upon 25-OH treatment [96]. In contrast, ORP9L localizes to the Golgi apparatus independent of 25-OH treatment via its PH domain [56,84]. PI(4)P binding to the PH domain of OSBP and ORP9L requires some conserved basic residues, like Arg^{109} and Arg^{110} in OSBP and Arg^{22} in ORP9L. Mutations of these residues cause a PI(4)P binding defect. For example, ORP9L R22E barely demonstrates any binding activity toward PI(4)P [56]. OSBP targeting to the Golgi apparatus is also mediated by Arf1, which is involved in phosphoinositide coincidence detection [97]. A histidine residue (His^{79}) essential for the interaction with Arf1 is conserved in both OSBP and ORP9L [56,91]. Coincidence detection mediated by phosphoinositides and co-receptors may exist in other ORPs, as well. The putative dual interactions may confer stronger interaction and specificity for the PH domain targeting process.

Surprisingly, Osh4p and Osh6p do not have a PH domain but have a region that serves a similar phosphoinositide binding function [81,98]. Osh4p specifically binds PI(4,5)P_2 or PI(4)P with similar affinity. The region responsible for the phosphoinositide binding is identified to be residue 205-314, corresponding to β-strand 9-17 of Osh4p (Figure 1.3A). Also, mutations in this region (such as Glu^{312}) cause a phosphoinositide binding defect and disrupt Osh4p Golgi localization in yeast cells [81]. It is important to note that the PI(4,5)P_2 binding region of Osh4p is opposite the mouth of the sterol/PI(4)P binding pocket (Figure 1.3A). Therefore, two regions of ORPs may be involved in

phosphoinositide binding, the SBD and PH domain (or a region that serves a similar function). Moreover, the polar head group of phosphoinositide binds with some basic residues of the PH domain. In contrast, the entire PI(4)P molecule is accommodated in the SBD, based on the solved Osh4p structure.

1.6.3 FFAT motif

The FFAT motif (E-F/Y-F/Y-DAxE), as its name indicates, has two conversed phenylalanine residues embedded in an acid region and binds vesicle-associated membrane protein (VAMP)-associated protein (VAP) A and VAP B in mammalian cells [82,84,99]. The yeast VAPs are SCS2 (suppressor of choline sensitivity) and SCS22 [100]. VAP is an ER tail-anchored protein with a C-terminal transmembrane domain. A major sperm protein (MSP) homology domain is at the N-terminus followed by a coiled-coiled domain, which is responsible for the dimerization of VAPs [101]. The FFAT motif is accommodated in a hydrophobic pocket formed by several residues of VAP, such as Lys^{45}, Thr^{47}, Lys^{87}, and Lys^{118} for VAP-A [102].

Human ORP members of subfamily I, II, III and V contain a FFAT motif (Figure 1.2B), except for the ORP4S variant. The interaction between VAP and FFAT motif causes ER localization of several ORPs. OSBP is cytosolic and localizes in the ER through the interaction between VAP and its FFAT motif [99,103,104]. The ER localization of OSBP via the FFAT motif is regulated by phosphorylation at two phosphorylation sites, Thr^{379} and the following five serines (site 1) and Ser^{192} and the following two serines (site 2) [105]. In CHO cells, an OSBP mutant mimicking phosphorylation at site 2 and dephosphorylation at site 1 constitutively localized with

VAP [105]. Although endogenous ORP9L is mainly identified in the Golgi apparatus, over-expressed ORP9L co-localizes with VAP in a FFAT motif-dependent manner [56,84]. Overexpressed ORP9S is cytosolic and ER localized through VAP protein binding, verified by a FFAT motif defective mutant [56]. As mentioned earlier, ORP1L localizes to the LE, regulated by its ankyrin repeats and PH domain [83]. The FFAT motif is not responsible for this localization. However, under low cholesterol conditions, ORP1L undergoes a conformational change and exposes its FFAT motif, examined by a FRET-based assay with the two termini of ORP1L fused with fluorescent tags [106]. The exposed FFAT motif induces the formation of ER-LE membrane contact sites observed by electron microscopy [106].

1.6.4 Ankyrin domain

Ankyrin repeats containing 33 residues, forming two-antiparallel α-helices connected with a β-hairpin loop, are widely identified in proteins. A general function shared by the ankyrin repeat is to facilitate specific protein-protein interactions (reviewed in [107]). Human ORP1 and yeast Osh1p and Oshp2p contain three ankyrin repeats that are important for localization and function. For instance, the interaction between ankyrin repeats and nuclear vacuolar protein 1 (Nvp1) is required for Osh1p localization to the nuclear-vacuolar junction (NVJ) [108]. Moreover, the ankyrin repeats in ORP1L directly interact with Rab7 and Rab7-interacting lysosomal protein (RILP) facilitating microtubule-based LE/lysosome transport [109,110].

1.7 Sterol/lipid transport by ORPs

All ORPs have a sterol-binding domain and many of these have been shown to bind sterols and oxysterols. Additional functional domains, such as the PH domain and FFAT motif, specifically bind with phosphoinositides and VAP, respectively, conferring specific localization of ORPs between organelles. Collectively, these properties have inspired researchers to speculate that ORPs have a sterol transfer function or are associated with signalling events. Furthermore, the new finding of Osh4p binding with PI(4)P is strong evidence showing that ORP function is not limited to sterols and oxysterols.

1.7.1 Sterol/lipid transfer in yeast

Direct and indirect evidence has accumulated in recent years indicating a sterol transport function for Osh proteins. Essentially, the structure of Osh4p bound with ergosterol and other sterols was resolved, implying the SBD of ORP is capable of accommodating sterols and transporting the bound sterols across an aqueous space [89]. Furthermore, Osh4p transfers cholesterol and ergosterol between liposomes *in vitro*, a process stimulated by $PI(4,5)P_2$ present in donor and/or acceptor liposomes [111]. $PI(4,5)P_2$ does so by binding to the β-strand 9-17 of Osh4p (Section 1.6.2). Indeed, all Osh proteins can transfer cholesterol *in vitro* and are stimulated by anionic phospholipids, such as phosphatidylserine (PS) [112]. In cultured cells, sterol transfer by Osh proteins is implicated by an esterification-based assay, which measures the esterification of exogenous radiolabeled cholesterol and ergosterol by the ER-localized enzyme ACAT, reflecting sterol transport from the PM to the ER [111]. The attenuated esterification in

the Osh-depleted and membrane permeable strains implies that Osh4p and other Osh proteins are responsible for sterol transfer from the PM to the ER.

The discovery that PI(4)P is also a ligand for Osh4p has prompted authors to hypothesize a different sterol transfer model, in which Osh4p exchanges PI(4)P and ergosterol between membranes [63]. Osh4p binds PI(4)P using a different set of residues compared with its sterol binding. Recombinant Osh4p (such as Osh4p-H143A/H144A) with mutations that are essential for PI(4)P binding demonstrated normal DHE extraction but showed an attenuated DHE transfer rate in FRET-based transfer assays, suggesting that the sterol transfer process is coupled with PI(4)P binding. Furthermore, it was shown that Osh4p counter-exchanges PI(4)P and DHE between liposomes.

1.7.2 Mammalian ORPs implicated in sterol transport

There is also evidence that some mammalian ORPs can function as sterol transport proteins. Knockdown of OSBP in CHO cells using short hairpin RNA (shRNA) altered the normal cellular cholesterol distribution, with a reduction of cholesterol content in the Golgi apparatus and endosomal membranes [113]. *In vitro* experiments showed that OSBP transfers cholesterol between liposomes when acceptor liposomes contained 2 mol% of PI(4)P [105]. The stimulated cholesterol transfer requires PI(4)P binding to the PH domain of OSBP, since the PH defective mutant (OSBP-R109E/R110E) demonstrated 3 fold less transfer activity [105]. Together with the fact that OSBP translocates between the ER and Golgi apparatus, it has been speculated to transport cholesterol from the ER to Golgi apparatus [57,84,114]. This possible cholesterol transport function for OSBP provides an explanation for the fact that OSBP is

required to activate SM synthesis [115,116]. Cholesterol transported by OSBP from the ER to the Golgi apparatus alters the Golgi apparatus membrane lipid environment, favoring the recruitment of ceramide transfer protein (CERT) that transfers ceramide to the Golgi apparatus for SM synthesis [6]. OSBP also affects cholesterol homeostasis beyond the ER and Golgi apparatus. OSBP depletion causes 3-fold more cholesterol egress from the PM mediated by ABCA1 in CHO cells; overexpression of sterol-binding defective OSBP prevents ABCA1 down-regulation but ER and Golgi localization defective OSBP does not [117]. These results imply that OSBP also regulates cholesterol distribution in post-Golgi compartments.

ORP9L is also implicated in cholesterol transport. Similar *in vitro* experiment as used for OSBP demonstrated the cholesterol transfer activity of ORP9L between liposomes [56]. ORP9L is mainly localized in the TGN but may translocate to the ER mediated by its FFAT motif [56,84]. Therefore, ORP9L may also be involved in the cholesterol transport process between the ER and Golgi apparatus. Depletion of ORP9L in CHO cells causes cholesterol to accumulate in LEs, indicating that disruption of cholesterol transport in the ER and Golgi apparatus affects downstream cholesterol containing compartments [56]. ORP9L depletion also resulted in Golgi fragmentation, probably due to cholesterol content changes in the Golgi apparatus. Interestingly, overexpressed ORP9S is mainly cytosolic with some localization in the ER and results in Golgi fragmentation and cell growth cessation [56]. However, the cholesterol extraction and transfer activities by ORP9S between liposomes have not been reported.

As stated above, some ORPs have been shown to have sterol transfer activity. More specifically, OSBP and ORP9 have been implicated in cholesterol transport

between ER and Golgi. Important questions remaining to be elucidated are how cholesterol is delivered by ORPs from one membrane to another and how ORPs achieve unidirectional transport. Cholesterol transfer can be achieved via two possible mechanisms (reviewed in [6]). In the first mechanism, ORPs may extract sterols from a membrane and consequently translocate and release the bound sterol molecule to another membrane that is physically separated from the first one. Sterol transfer based on this mechanism exists but is relatively slow, supported by the fact that Osh4p extracts cholesterol from a donor liposome and diffuses through a barrier to reach an acceptor liposome, at which the bound cholesterol is delivered [112]. However, Osh4p incubated with both donor and acceptor liposomes together demonstrates a more potent and rapid cholesterol transfer, indicating close membrane contact (the second possible mechanism) is required [112]. The membrane contact is probably achieved by Osh4p binding to anionic lipids using its second lipid binding site distal to the SBD (section 1.6.2). Indeed, many yeast ORPs are identified in regions where membrane contact may occur. Osh1p is identified in NVJ, where the nucleus and the vacuole membranes are oppositely apposed [80]. Osh2p, Osh3p, Osh6p and Osh7p locate at closely opposed cortical ER and PM membrane contact sites [112]. However, mammalian ORPs (except for ORP1L) have not been reported to be involved in any membrane contact.

The directionality of sterol transfer between compartments is important for any specific transfer processes. OSBP and ORP9 are hypothesized to transfer nascent cholesterol from ER to the Golgi apparatus, therefore regulating Golgi cholesterol content. The directionality may be achieved by an ER and Golgi phosphorylation cycle. CERT, like OSBP and ORP9, contains a PH domain and FFAT motif and transports

ceramide from ER to the Golgi apparatus for SM synthesis. A phosphorylation cycle that regulates this transport was reported [118]. Phosphorylation by PKD at Ser^{132} of CERT attenuates its Golgi localization and ceramide transfer activities [119]. Moreover, phosphorylation at nine adjacent serine residues by casein kinase 1 (CK1) γ2 further reduces ceramide transfer and SM synthesis [120]. In contrast, protein phosphatase 2Cε (PP2Cε) interacts with VAP and dephosphorylates CERT, causing increased Golgi localization and SM synthesis [121]. Although the complete phosphorylation cycle that regulates OSBP and ORP9 cholesterol transport has not been fully characterized, some results have showed consistency with this speculation. For example, OSBP phosphorylation by PKD attenuates its Golgi localization [96]. The new discovery that PI(4)P is also a ligand for Osh4p provides a new possible explanation for the directionality of sterol transfer. Osh4p delivers its bound DHE to liposomes containing anionic lipids. PI(4)P is different from other anionic lipids since it can be extracted to the sterol-binding pocket of Osh4p, filling the pocket once DHE is released [63]. This ligand exchange process blocks the re-extraction of DHE. *In vivo,* PI(4)P molecules enriched in the TGN may compete for binding to the sterol-binding pocket of Osh4p, leaving the newly transferred ergosterol molecule in the TGN. This sterol/PI(4)P transport mechanism has been proposed by De Saint-Jean and co-workers and is also illustrated in figure 4.1. However, PI(4)P binding to the sterol-binding pocket of mammalian ORPs remained to be elucidated.

1.8 Other ORP related functions

In addition to the possible function in sterol transport, ORPs have been implicated in other functions either related with or even beyond their sterol transfer

functions. Since these functions are not the main focus of this project, some of them will be discussed for a complete introduction of the ORP functions.

First, ORPs are involved in sterol-dependent cell signalling processes. OSBP has been shown to deactivate extracellular-signal-regulated kinase (ERK) by dephosphorylation in a sterol-dependent manner [122]. ERK is a component of the mitogen-activated protein kinase (MAPK) pathway, an important signal transduction pathway in most eukaryotic cells [123]. OSBP bound with cholesterol provides a scaffold that is favored for the recruitment of serine/threonine phosphatase PP2A (protein phosphatase type 2A) and haematopoietic tyrosine phosphatase (HePTP), which dephosphorylate and consequently inactivate ERK [122]. Cholesterol absence or replacement by 25-OH disrupts the recruitment and results in activation of ERK. Moreover, OSBP overexpression in mouse liver achieved by adenovirus demonstrates increased very low-density lipoprotein (VLDL), triglyceride (TG) and mRNA for INSIG-1 and SREBP-1c, indicating that OSBP plays a role in the insulin signalling pathway by regulating ERK activity [124]. OSBP is also involved in a signalling pathway that eventually activates pro-atherogenic profilin (PFN)-1 expression. The binding of 7-ketocholesterol to OSBP presumably induces a conformational change that in turn favors its interaction with Janus kinase 2 (JAK2) [125]. OSBP phosphorylated at Tyr^{394} by this kinase further recruits signal transducer and activator of transcription 3 (STAT3) for phosphorylation, and the phosphorylated STAT3 is required for the transcription of *Pfn* [125].

Protein kinase B, also known as Akt, is a member of the AGC-type kinase family (protein kinase A/ protein kinase G/ protein kinase-family kinases) and controls glucose

metabolism, apoptosis, and cell proliferation [126]. A hydrophobic motif (VPEFS^{287}Y) that serves as a target site for phosphoinositide-dependent kinase 2 (PDK-2) was identified in ORP9 by cross-reacting with a monoclonal antibody for phospho-Ser^{473} Akt, which is the phosphorylated product of PDK2 [127]. Therefore, ORP9 may also be a substrate for PDK-2. Indeed, ORP9S and Akt are coordinately phosphorylated by PDK-2 in bone derived marrow mast cells; knockdown of ORP9L resulted in a 3-fold increase in Akt phosphorylation in human embryonic kidney (HEK)-293 cells [127]. These results indicate that ORP9 can negatively regulate Akt and therefore affect this important signalling pathway.

There are also studies showing that some ORP functions are coupled with the cytoskeleton. As mentioned in Section 1.6.4, ORP1L utilizes its three ankyrin repeats to directly interact with RILP, which is recruited by the GTP-bound form of Rab7 at LE/lysosome membranes [110]. The resulting complex is composed of a RILP flanked by two ORP1L proteins and further recruits the p150^{Glued}with dynein-dynactin motor for LE transport toward the minus-end of the microtubule. Despite its crucial role in motor complex formation, ORP1L also senses the cholesterol content of the endosomal outer membrane to promote the transport process [106]. ORP10 localizes on microtubules, supported by its co-localization with β-tubulin in fluorescent images and dispersed pattern upon treatment with the depolymerising agent demecolcine [128]. In CHO cells, overexpressed ORP4 localizes with the intermediate filament protein vimentin and causes a disruption of vimentin network, along with a decrease in LDL-cholesterol esterification [82]. Since ORP4 is implicated in sterol transport, vimentin may interact with ORP4 and consequently mediate the cholesterol transport to the ER [129]. Although

ORPs directly or indirectly interact with the cytoskeleton, detailed functions of these interactions remained to be elucidated. The interaction may provide a structural platform for sterol transport or lead to further signalling events in a sterol-dependent manner.

1.9 Förster resonance energy transfer (FRET)-based assays in the study of sterol transport by OSBP and ORP9

In this project, we used fluorescent cholesterol analogs, DHE or CTL (Section 1.1), to study cholesterol transfer between liposomes by OSBP and ORP9. Different from experiments based on tracking radioactive sterols, the aforementioned fluorescent analogs allow us to use Förster resonance energy transfer (FRET) to monitor sterol movement. FRET is a distance dependent (1-10 nm) energy transfer process where one excited fluorophore (donor) transfers energy to another (acceptor) without emission of a photon [130]. For energy transfer to occur, the emission spectrum of a donor should have spectral overlap with the excitation spectrum of an acceptor. Both DHE and CTL can be excited near 320 nm, with their emission spectrum spanning from 370 to 400 nm [12,131-133]. The dansyl group of dansyl-phosphatidylethanolamine (PE) has an excitation spectrum spanning from 300 to 400 nm with its peak at 336 nm [130]. The spectral overlap between DHE or CTL and dansyl-PE makes the energy transfer possible from fluorescent cholesterol analog to dansyl-PE. FRET emission change caused by DHE/CTL extraction from liposomes containing both fluorescent sterol and dansyl-PE or by DHE/CTL transfer to liposomes containing only dansyl-PE can be measured to reflect the extraction and transfer activity by ORPs. Detailed descriptions of these FRET-based experiments using OSBP and ORP9 are described in Section 2.6 and 2.7.

We hypothesize that OSBP and ORP9 transfer cholesterol from the ER to the Golgi apparatus. Using the FRET-based assays, we attempted to study the extraction and transfer process *in vitro.* PI(4)P is shown to be a ligand for Osh4p. Osh4p residues involved in PI(4)P binding are conserved in mammalian ORPs. We attempt to show that PI(4)P is a also a ligand for OSBP and ORP9. The PI(4)P binding function may be required to regulate PI(4)P distribution and homeostasis and coupled with the cholesterol transport process.

CHAPTER 2 MATERIALS AND METHODS

2.1 Materials

Phospholipids, porcine brain PI(4)P and DHE were purchased from Avanti Polar lipids (Alabaster, AL). Cholesterol was from Steraloids (New Port, RI). CTL was generously provided by Peter Slotte (Åbo Akademi University, Turku, Finland). Dipalmitoyl PI, PI(4)P, PI(4,5)P_2 and anti-PI(4)P antibody mouse monoclonal IgM were obtained from Echelon Biosciences (Salt Lake City, UT). [^{3}H]Cholesterol, [^{3}H]PI, [^{14}C]PC, and [^{32}P] H_3PO_4 were purchased from Perkin-Elmer (Waltham, MA). Fetal bovine serum (FBS), bovine serum albumin (BSA), *Ricinus Communis* (*R.Communis*) agglutinin RCA_{120}, methyl-β-cyclodextrin (CD) and anti-β-actin monoclonal mouse antibody were purchased from Sigma-Aldrich (St. Louis, MO). ON-TARGETplus Human OSBPL9 siRNAs were purchased from Dharmacon (Lafayette, CO). The QuikChange™ II XL Site-Direct Mutagenesis Kit was purchased from Agilent Stratagene (Santa Clara, CA). Protease inhibitor cocktail tablet was from Roche Diagnostics (Mannheim, Germany). Talon® Superflow™ Metal Affinity Resin was obtained from Clontech (Mountainview, CA). GelCode Blue® stain reagent, Surfact-Amps® X-100 and albumin standard (2mg/mL) were purchased from Thermo Scientific (Rockford, IL). Liposofast liposome extrusion system and polycarbonate membranes (400 nm) were obtained from Avestin (Ottawa, ON). Thin-layer chromatography silica gel 60 Å plates were purchased from Whatman (Kent, UK). UltraCruz™ autoradiography film was from Santa Cruz Biotechnology (Santa Cruz, CA). Glycine, 40% acrylamide, Tween-20, nitrocellulose membrane were from Bio-Rad (Hercules, CA). Alexa-Fluor® 594 goat anti-mouse IgM and Alexa-Fluor® 488 goat anti-rabbit IgG, G

418, Benchmark™ Protein ladder (both pre-stained and not), Dulbecco's modified Eagle medium (DMEM) Baculovirus Direct Linear DNA kit, pENTR/D-TOPO cloning kit, Cellfectin reagent, ganciclovir, and SF900-II serum-free medium were purchased from Invitrogen (Burlongton, ON). Odyssey blocking buffer was obtained from LI-COR Biosciences (Lincoln, NE). A polyclonal ORP9 antibody was previously prepared in our lab [84]. Digitonin was purchased from Calbiochem™ (Darmstadt, Germany).

2.2 Cell culture and transfections

HeLa cells were cultured in monolayers in DMEM containing 10% (v/v) FBS (medium A) at 37 °C with 5% CO_2. For transfections, HeLa cells were sub-cultured onto 35 mm dishes in 2 mL of medium A with glass coverslips for fluorescence microscopy experiments or without coverslips for immunoblot experiments. The next day, 7 μL of Trans-IT TKO transfection reagent (Mirus, Madison, WI) with a pool of three ORP9L siRNA duplexes (a total concentration of 100 nM) or a non-targeting (NT) siRNA (100 nM) was incubated in 250 μL of DMEM for 20 min at room temperature. HeLa cells at 70% confluency were then incubated with the siRNA mixture in 1.25 mL of medium A for 48 h to knock down ORP9L expression.

CHO Tet-on cells were cultured in DMEM containing 5% FBS and 34 μg proline/ml (medium B). Expression of ORP9L and ORP9S were induced by the presence of doxycycline (1 μg/mL) in medium B for 24 h. SF21 cells were cultured in SF900-II medium containing 5% (v/v) FBS, 10 μg/mL G418 and 0.25 μg/mL fungizone (SF21 medium) in monolayers flask at 27 °C. SF21 cells were split when fully confluent (approximately every four days) at a 1/5 dilution. For protein purification, SF21 cells were cultured at 27 °C and split every second day in glass flasks on a shaker (150 rpm).

2.3 Baculovirus expression and purification of OSBP and ORP9

Baculoviruses encoding OSBP, OSBP R109E/R110E (OSBP-RR/EE), OSBP-H524A/H525A (OSBP-HH/AA), ORP9L and ORP9S were previously made in our lab. The cDNA ORP9L-H488A/H489A (ORP9L-HH/AA) was made by mutagenesis of the ORP9L cDNA cloned into pENTR/D-Topo using the QuikChange^{TM} II XL site-direct mutagenesis kit (Stratagene-Agilent). The forward and reverse primers for the mutagenesis were 5'-GCT GAG CAG GTT TCC GCT GCT CCA CCC ATT TCA GCC-3' and 5'-GGC TGA AAT GGG TGG AGC AGC GGA AAC CTG CTC AGC-3', respectively (Integrated DNA Technologies, Coralville, IA). The mutated cDNA was verified by sequencing and inserted into Baculodirect linear DNA containing a C-terminal V5-His-tag by recombination. The recombined Baculodirect DNA was transfected into SF21 cells using Cellfectin reagent. Cell supernatant (P1 stock) was collected after 5 days and used to transduce more SF21 cells. This transduction was repeated until recombined ORP9L-HH/AA was well expressed, as determined by immunoblotting. After determining the titer of the baculovirus P5/P6 stocks, a large scale SF21 cells (200 mL) infection was undertaken. In 20 mL of SF21 medium, $3.6x10^8$ SF21 cells were infected with baculovirus at a multiplicity of infection (MOI) of 0.1-0.2 for 1 h at room temperature, protected from light with constant shaking. Infected cells were then transferred into a 1 L glass flask to a final volume of 200 mL with SF21 medium incubated for 72 h at 27 °C.

Infected SF21 cells were collected by centrifugation at 300xg for 10 min and re-suspended in 20 mL of 50 mM phosphate buffer (pH 7.0) containing 300 mM NaCl, 30 mM imidazole (talon buffer) with protease inhibitors. The purification process was

conducted at 4 °C or on ice. Re-suspended cells were pushed through a 18 gauge needle twice and a 25 gauge needle once and lysed by sonication using a Fisher sonic dismembrator. The sonication was conducted three times (10 sec each time) with a setting of 40. Lysed cells were centrifuged at 35,000xg for 1 h. The supernatant was then mixed with Talon resin (equilibrated in Talon buffer) for 2 h. Talon resin was washed twice with Talon buffer to remove unbound proteins. OSBP, ORP9L or ORP9S were eluted from Talon resin with 5 mL of 50 mM phosphate buffer containing 300 mM NaCl and 150 mM imidazole. Proteins eluted from the column were collected in an Amicon Ultra-15 centrifugal filter unit (100,000 M.W. cutoff for OSBP or 30,000 M.W. cutoff for ORP9L and ORP9S) and concentrated by centrifugation to about 1 mL. Then, 10 mL of 20 mM Tris-HCl (pH7.4) and 250 mM NaCl was added into Amicon units. Proteins were concentrated again to approximately 1 mL and store at -80 °C. Protein purity was verified by SDS (sodium dodecyl sulfate)-8% PAGE (polyacrylamide gel electrophoresis) stained with GelCode Blue reagent. Protein concentration was determined by a μLowry assay [134].

2.4 Competitive sterol binding assay

Purified OSBP (20 pmol) was incubated for 2 h at room temperature with 100 nM of [^{3}H]cholesterol along with different concentrations of unlabeled DHE and CTL in 10mM HEPES (pH 7.4), 300 mM KCL, 2% (w/v) PVA and 0.05% Triton-X 100 (final concentrations) to disperse sterols. [^{3}H]Cholesterol, DHE and CTL stocks were prepared in ethanol. During incubation, Talon resin slurry was pre-washed 3 times with 10 mM HEPES (pH 7.4) and 100 mM KCL (binding assay buffer). Each assay received 25 μL of Talon resin slurry (1:1, v/v (bed volume/binding assay buffer)) and was vortexed for 25

min. After brief centrifugation, unbound sterols were removed by aspiration, leaving Talon resin and bound OSBP and sterols in the pellet. Talon resin was washed 3 times using 300 μL of binding assay buffer at 4 °C. Unbound sterols were removed by aspiration during washes. After the second wash, samples were transferred into new tubes to reduce background caused by [^{3}H]cholesterol binding to tube walls. OSBP bound to Talon resin was eluted with 100 μL of binding assay buffer with 150 mM imidazole. After brief centrifugation, eluted [^{3}H]cholesterol in the supernatant was measured by liquid scintillation counting. An experiment with 2 μM unlabeled cholesterol (20X of [^{3}H] cholesterol) was used to determine background non-specific binding. The result obtained from this experiment was subtracted from each assay.

2.5 Liposome preparation

Liposomes were used to examine ORP binding to lipids, and extraction and transfer of cholesterol or CTL, in the case of FRET-based assays. To prepare liposomes, lipids dissolved in chloroform were added into a glass tube and dried under nitrogen. Lipid film was hydrated in liposome buffer (25 mM HEPES, pH 7.4, 150 mM NaCl, 1 mM EDTA or 20 mM HEPES (pH 7.4) 100 mM NaCl, 1 mM EDTA) to a final concentration of 0.5 mM. Hydrated lipids was vigorously vortexed every 5-10 min for 1 h at room temperature. Liposomes were made by extrusion through a 400 nm diameter polycarbonate membrane using the Liposofast system. Liposomes were stored at 4 °C and used within 2 days. Before each experiment, liposomes were centrifugated at 15,000xg for 5 min to remove aggregates. Liposomes used in FRET-based assays were protected from light as much as possible.

2.6 Förster resonance energy transfer (FRET)-based extraction assay

FRET-based experiments were conducted using a Cary Eclipse fluorescence spectrophotometer with a single cell peltier accessory to maintain temperature at 30 °C. Measurements were taken in a 2x2 mm sub-micro fluorometer quartz cuvette (40 μL). The fluorescent cholesterol analog CTL (324/370 nm, excitation/emission) and dansyl-PE (370/520 nm, excitation/emission) were used as a FRET-pair. First, the emission change upon CTL extraction was validated by addition of methyl-β-cyclodextrin (CD). Liposomes containing 0 mol% CTL were measured to demonstrate the background emission; the relationship between CTL content and FRET emission was determined by measuring liposomes containing different CTL contents.

For a FRET-based extraction assay (Figure 2.1A), liposomes containing 2.5% dansyl-PE and 0% CTL or 2.5% CTL were prepared for background correction and extraction measurement, respectively. In each assay, 0.05 mM liposomes were excited at 324 nm (5 nm slit width) and measured at 520 nm (10 nm slit width) every 0.5 min over 5 min without (no-addition) or with 2.5 μM (150 pmol) of protein. Proteins were added after the first reading was taken. The detector was set to be 900 V. FRET emission values from each experiment were corrected by subtracting background emission at each corresponding time point and presented as a percent of time zero. Liposomes containing additional PI(4)P and cholesterol were assayed as described above. Extraction curves were fit using a one-phase exponential decay model (GraphPad Prism 5 Software).

2.7 FRET-based transfer assay

In the FRET-based transfer assay (Figure 2.1B), donor and acceptor liposomes were composed of PC/PE/PS/CTL (67.5:20:10:2.5:2.5, mol/mol) and

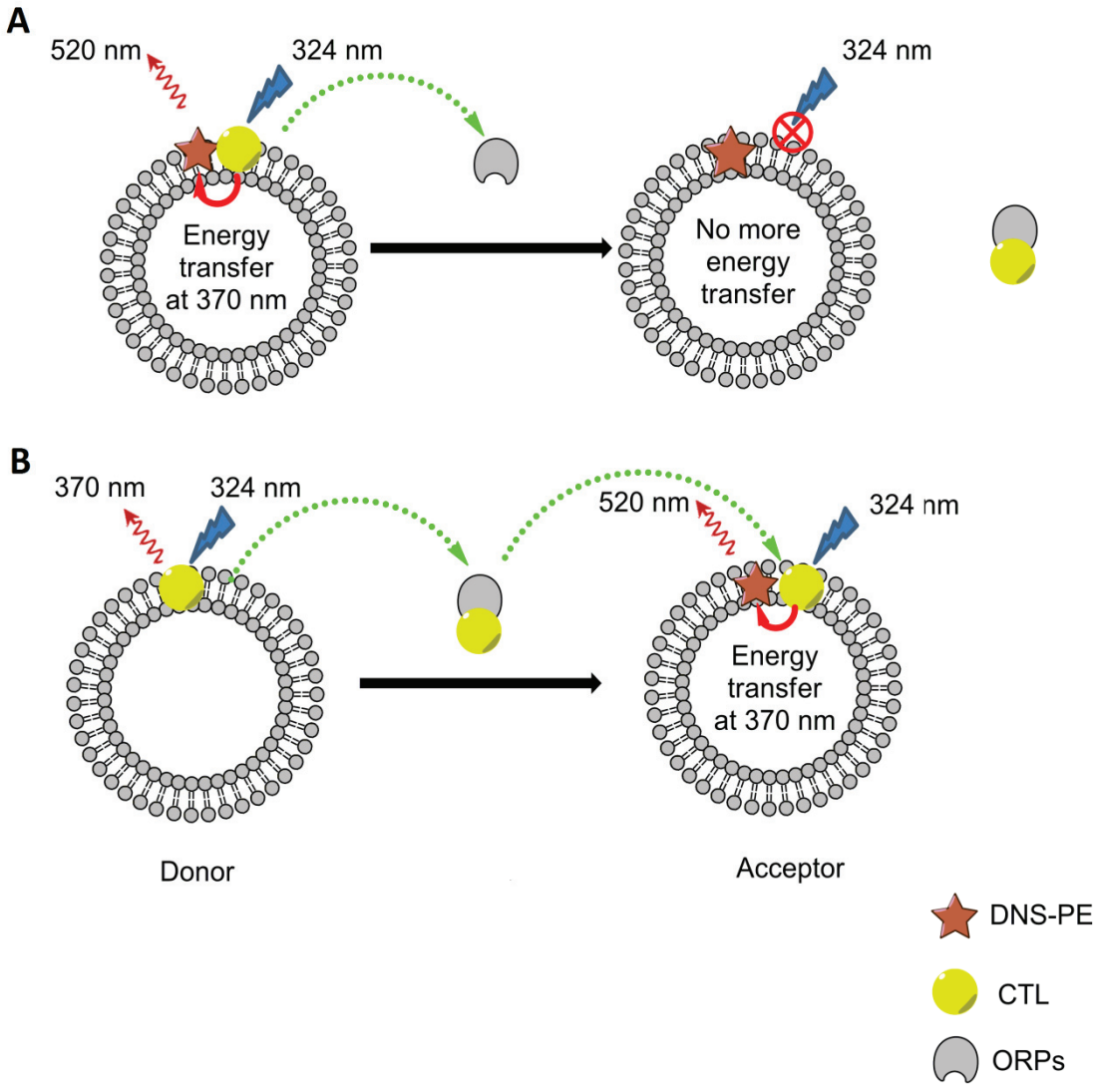

Figure 2.1. FRET-based extraction and transfer assay design. In both assays, liposomes were excited at 324 nm (5 nm slit width) and emission was measured at 520nm (10 nm slit width) every 0.5 min for 5 min without (no-addtion) or with 2.5 μM of OSBP or ORP9. OSBP or ORP9 were added immediately after first reading was taken. (A) For the extraction assay, liposomes contained both CTL and dansyl-PE. Since CTL and dansyl-PE were proximal to each other in one liposome, light emitted from CTL would be absorbed by dansyl-PE. Upon CTL extraction by OSBP or ORP9, the change in FRET emission was recorded. (B) For the transfer assay, donor liposomes contained CTL and acceptor liposomes contained dansyl-PE. The liposomes were incubated with ORP9 and the change in FRET emission resulting from CTL transfer to acceptor liposomes was measured by fluorometer.

PC/PE/PS/dansyl-PE (70:17.5:10:2.5, mol/mol), respectively. In liposome buffer, 0.1 mM donor and 0.05 mM acceptor liposomes were incubated without or with ORP9L or ORP9S added after the first reading was taken. The CTL transfer assay was measured in the same way as for a FRET-based CTL extraction assay (Section 2.6).

2.8 Purification of [^{32}P]PI(4)P from HeLa cells

Hela cells at 70% confluency on two 60 mm dishes were incubated with 2 mL of phosphate free DMEM containing 2% FBS (v/v) for 1 h. Cells then received 0.5 mCi of [^{32}P] H_3PO_4 and were incubated for approximately 16 h. Cells were washed once with phosphate-buffered saline (PBS) (10 mM sodium phosphate buffer, pH 7.4, 150 mM NaCl), scraped from dishes in 1 mL of PBS and transferred into a 13 mL screw cap glass tube. Lipids were extracted with 3.8 mL of $CHCl_3$/MeOH/12N HCl (2:4:0.1, v/v), 1.2 mL of $CHCl_3$, and 1.2 mL of water, with vortexing after each addition. The aqueous phase was separated by centrifugation at 1000 rpm (Allegra™ 6 Centrifuge) for 5 min and removed by pipetting. The organic phase was dried under nitrogen gas in a 40 °C water bath. Lipids were dissolved in 100 µL (50 µl each time) of $CHCl_3$/MeOH (2:1, v/v) and spotted on a TLC silica 60 Å plate along with an authentic PI(4)P standard. The TLC plate was developed in $CHCl_3$/MeOH/ 4M NH_4OH (9:7:2, v/v) for 1 h and dried for 20 min. The TLC plate was wrapped in saran wrap and exposed to UltraCruz™ autoradiography film for 20 min at room temperature. Using the developed film and the PI(4)P standard, the locations of PI(4)P and PI(4,5)P_2 were identified. [^{32}P]PI(4)P was then scraped from the TLC plate and extracted twice with 2 mL of $CHCl_3$/MeOH/12 M HCl (2:4:0.1, v/v) in 13 mL screw cap glass tubes. [^{32}P]PI(4)P was then mixed with 3.8 mL of $CHCl_3$/MeOH/12N HCl (2:4:0.1, v/v), 1.2 mL of $CHCl_3$, and 1.2 mL of water.

The lipids were resolved by TLC as described above. [^{32}P]PI(4)P extracted from the second TLC plate was dried under nitrogen gas in a 40 °C water bath and stored in 1 mL of $CHCl_3$/MeOH (2:1, v/v). A 5 µL of [^{32}P]PI(4)P sample was dissolved in scintillation cocktail to measure radioactivity.

2.9 Extraction assays using radioactive cholesterol and PI(4)P

A general outline of the radioactive based-extraction assay is illustrated in Figure 2.2. Liposomes (prepared as stated in Section 2.5.) were composed of PC/PE/PS/lactosyl-PE/[^{3}H]cholesterol (59:20:10:10:1, mol/mol) or PC/PE/PS/lactosyl-PE/[^{32}P]PI(4)P (or [^{3}H]PI) (59.5:20:10:10:0.5, mol/mol). For all extraction assays, OSBP or ORP9 and 0.03 µg/µL fatty acid-free BSA were incubated with 0.1 mM liposomes in liposome buffer (25 mM HEPES, pH 7.4, 150 mM NaCl, 1 mM EDTA) in a 25 °C water bath. After 20 min, liposomes were incubated with 10 µg of *R.Communis* agglutinin (lectin) on ice for 15 min and precipitated by centrifugation at 15,000 x g for 5 min. Radioactivity was measured in the supernatant to determine [^{3}H]cholesterol, [^{32}P]PI(4)P, or [^{3}H]PI extraction by OSBP or ORP9. A negative control experiment was conducted without proteins and used to correct for background. Percent extraction was calculated by setting total radioactivity input in each assay as 100%.

To determine whether inclusion of phosphoinositides would suppress [^{3}H]cholesterol extraction, liposomes containing 1 mol% [^{3}H]cholesterol and additional 0.5, 1, and 2 mol% of PI, PI(4)P or PI(4,5)P_2 were incubated with 50 pmol OSBP. A trace amount of [^{14}C]PC was incorporated into liposomes to correct for background caused by non-precipitated liposomes by subtracting supernatant [^{14}C]PC levels from supernatant [^{3}H]cholesterol levels. A fraction of the supernatant and pellet (dissolved in

1% SDS (w/v) solution) was assayed by SDS-8%PAGE and stained with GelCode Blue to examine the distribution of OSBP.

For direct phosphoinositide extraction assays, liposomes containing 0.5 mol% [^{32}P]PI(4)P or [^{3}H]PI were incubated with OSBP or ORP9 to directly measure extraction. The same procedures were followed as described above, but a trace amount of [^{14}C]PC was not applied for [^{32}P]PI(4)P extraction, due to the signal overlap between ^{14}C and ^{32}P.

2.10 Immunoblotting

After siRNA knockdown, HeLa cells were lysed in 2x SDS-lysis buffer (0.8% SDS (w/v), 25 mM Tris-HCl pH 6.8, 4% glycerol (v/v), 2% β-mercaptoethanol (v/v), and 0.02% bromophenol blue (w/v)). After heating at 95°C for 5 min, cell lysates were resolved by SDS-8% PAGE and transferred onto nitrocellulose membrane. Nitrocellulose membranes were blocked using Odyssey blocking buffer and Tris-buffered saline (TBS) (20 mM Tris-HCl pH 7.4 and 150 mM NaCl) (1:1, v/v) for 1 h. Antibodies were incubated in Odyssey blocking buffer and TBS (1:5, v/v) containing 0.01% Tween-20 (blocking buffer). ORP9L and actin were probed with a polyclonal (1/4000) and monoclonal (1/5000) primary antibodies, respectively, in blocking buffer. ORP9L and actin primary antibodies were then detected with goat anti-rabbit IRDye 680- (1/15000) and goat anti-mouse 800-conjugated (1/15000) secondary antibodies in blocking buffer, respectively. Bands were visualized and quantified using an Odyssey Infrared Imaging system (LI-COR Biosciences, Lincoln, NE).

2.11 Fluorescence Microscopy

After siRNA knockdown, HeLa cells cultured on coverslips were washed once

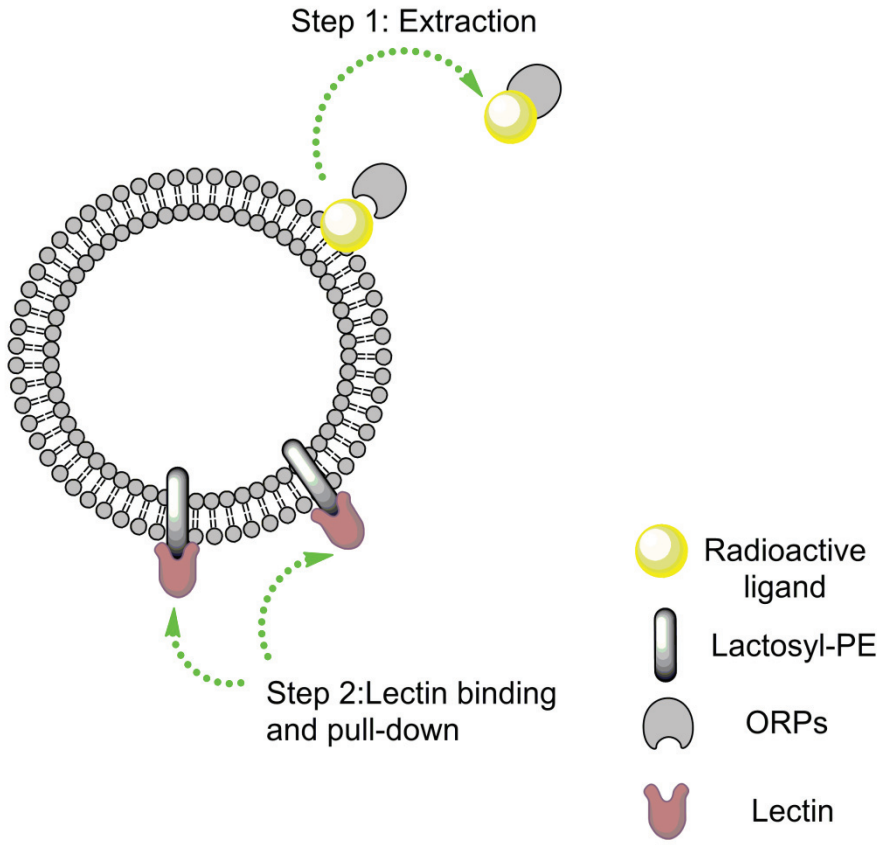

Figure 2.2. Mechanism of an extraction assay using radioactive ligand. Generally, in each extraction assay, liposomes contained radioactive ligands and 10% lactosyl-PE. Ligands were extracted by OSBP or ORP9; lactosyl-PE was bound to *R.Communis* agglutinin (lectin), and causing liposomes to be precipitated after centrifugation. Specifically, radioactive ligand could be either [^{3}H]cholesterol or [^{32}P]PI(4)P. In the first case, additional unlabeled PI, PI(4)P, or PI(4,5)P_2 were incorporated into liposomes to show competition with [^{3}H]cholesterol. Trace amount of [^{14}C]PC was added into liposomes to track liposome distribution and correct [^{3}H]cholesterol extraction. In the second case, liposome containing [^{32}P]PI(4)P was used to study direct PI(4)P extraction. Radioactivity was determined by scintillation counting.

with PBS, fixed in PBS containing 2% formaldehyde (w/v) for 10 min and permeabilized and quenched in 2 mL of PBS containing 20 μg/mL digitonin and 100 mM glycine for 20 min at room temperature. Coverslips were then blocked in PBS containing 1% BSA (w/v) for 1 h and probed with an anti-PI(4)P antibody (1/400) in 1% BSA overnight. The PI(4)P antibody was detected by a goat anti-mouse IgM-594 secondary antibody (1/2000) in 1% BSA. ORP9L was probed with ORP9 polyclonal primary antibody (1/2000) and a goat anti-rabbit IgG 488 secondary antibody (1/5000) in 1% BSA. Coverslips were then washed three times with 1% BSA and one time with distilled water before mounting on slides using Mowiol 4-88. Images were captured using a Zeiss Axiovert 200M inverted microscope using a 63X oil emersion objective and Hamamatsu Orca R2 Camera.

After 24 h of induction with 1 μg/ml doxycycline, CHO cells grown on coverslips were prepared the same as described above for fluorescence imaging. Images were captured using a Zeiss LSM 510 Meta laser scanning confocal microscope (0.8 μm sections) equipped with 63X oil emersion objective.

2.12 Statistical analysis

A two-tailed student t-test was used to determine statistical significance between corresponding samples (GraphPad Prism 5 Software).

CHAPTER 3 RESULTS

3.1 The fluorescent cholesterol analog CTL inhibits cholesterol binding to OSBP

OSBP and ORP9 were previously shown to extract and transfer [^{3}H]cholesterol between liposomes *in vitro* [56,105]. These radioactive-based assays showed extraction and transfer of cholesterol at one time point but failed to provide any kinetic information for the extraction process. Furthermore, some systematic errors can be associated with radioactive-based extraction and transfer assays. For example, cholesterol extraction may be underestimated since extraction may occur but the ORP could still associate with the liposome. Instead of using [^{3}H]cholesterol, we attempted to use a fluorescent cholesterol analog to study sterol extraction and transfer by OSBP and ORP9. CTL and DHE are two possible fluorescent analogs to use in this assay. CTL is a cholesterol analog that mimics the membrane behavior of cholesterol [12,13] and has been used to study cholesterol transfer between membranes by NPC2 [14]. DHE has been applied to study cholesterol and ergosterol transfer between membranes by ORP5 and Osh4p [11,63]. The emission spectra of both fluorescent analogs have spectral overlap with the excitation spectrum of dansyl-PE.

In order to determine which analog should be used in our FRET-based assays, competition for [^{3}H]cholesterol binding to OSBP was conducted in the presence of DHE or CTL in aqueous buffer with detergent (Figure 3.1). Cholesterol is a well-known ligand for OSBP [69,93]. If CTL or DHE also binds to OSBP, we would see suppression of [^{3}H]cholesterol binding in a competition assay. His-tagged OSBP used in these competitive binding assays was purified from SF21 cells transduced with baculovirus.

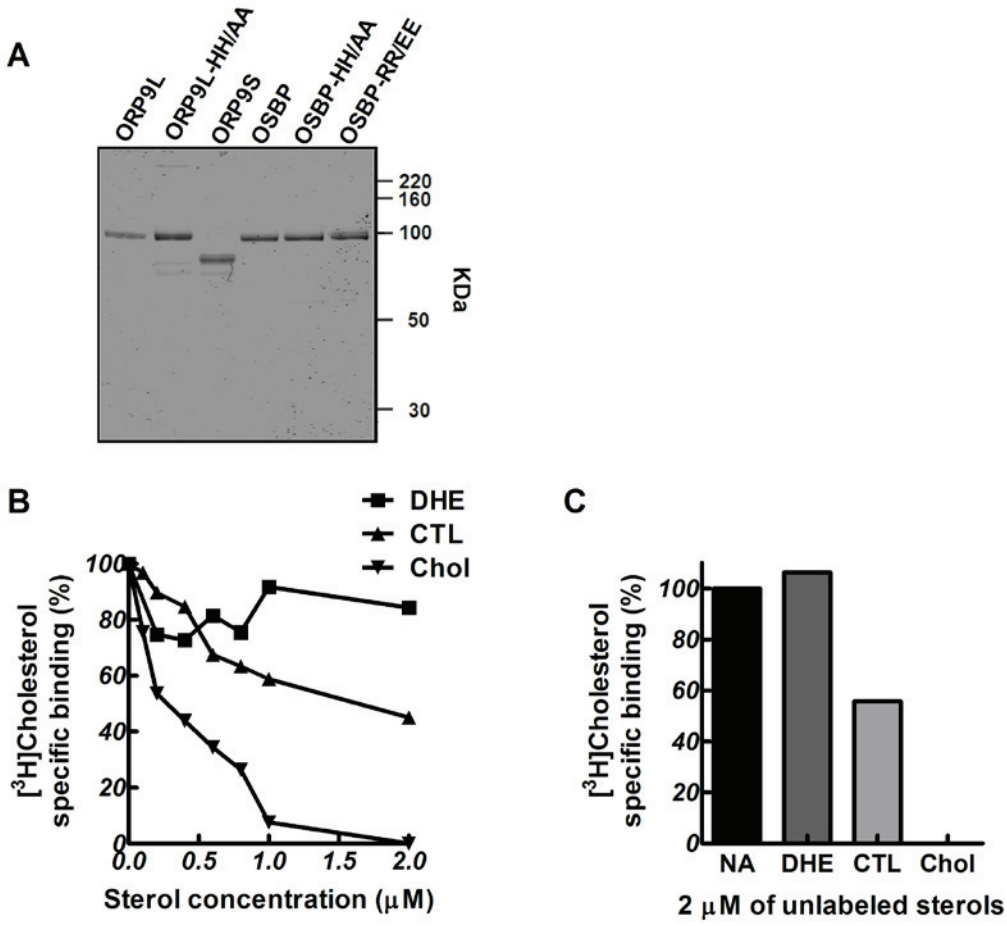

Figure 3.1. CTL competes with [^{3}H]cholesterol for binding to OSBP. (A) ORP9L, ORP9S, OSBP and their mutants (0.8 μg each) purified from SF21 cells infected by baculoviruses were resolved by SDS-8% PAGE and stained with Coomassie Blue. (B) OSBP (50 pmol) was incubated with 100 nM [^{3}H]cholesterol and increasing amount of unlabeled CTL or DHE (from 0 to 2 μM). (C) The [^{3}H]cholesterol binding assay was conducted with 2 μM of unlabeled sterols (20 fold excess of unlabelled sterols) again to verify inhibitory effect. In both (B) and (C), [^{3}H]cholesterol binding without unlabeled sterols is set as 100%. Specific binding is determined by subtracting the [^{3}H]cholesterol binding activity when 20 fold excess of unlabeled cholesterol is present. Results shown are from representative experiments.

The purity of OSBP was examined using SDS-8% PAGE and Coomassie Blue staining and was the only band identified in the gel (Figure 3.1A). For the competitive binding assay, specific binding was determined by subtracting non-specific binding (20X unlabeled cholesterol) from [^{3}H]cholesterol binding activity. The specific binding activity of OSBP with no unlabeled sterol was set as 100%. As expected, unlabelled cholesterol competed for [^{3}H]cholesterol binding to OSBP. A clear suppression for [^{3}H]cholesterol binding was observed when unlabeled CTL was added, reaching a maximum of 50% at 2 μM CTL. Interestingly, no such trend was identified when unlabeled DHE was present (Figure 3.1B). This experiment was repeated using 2 μM of CTL (20 fold of [^{3}H]cholesterol) and again showed about 50% inhibition of cholesterol binding; using 2 μM of DHE did not inhibit cholesterol binding (Figure 3.1C). These results indicated that CTL competitively bound to OSBP, but DHE did not. This is probably due to the structural difference between DHE and CTL (Figure 1.1). Therefore, CTL and dansyl-PE were selected for FRET-based assays.

3.2 Corrected FRET emission is proportional to CTL content

CTL can be excited at 324 nm and emits at 370 nm. This emission can be absorbed by proximal dansyl-PE, which eventually emits at 520 nm. This energy transfer mechanism allows us to design a FRET-based extraction assay to study CTL extraction. To demonstrate this, 0.1 mM liposomes containing both 5 mol% CTL and 2.5 mol% dansyl-PE prepared in liposome buffer were excited at 324 nm (5 nm slit width) and scanned from 350 nm to 600 nm (5 nm slit width). A peak was identified at round 520 nm that represented a typical dansyl-PE emission. Meanwhile, CTL emission at 370 nm was hard to observe in the curve (Figure 3.2A) since its energy was transferred to dansyl-

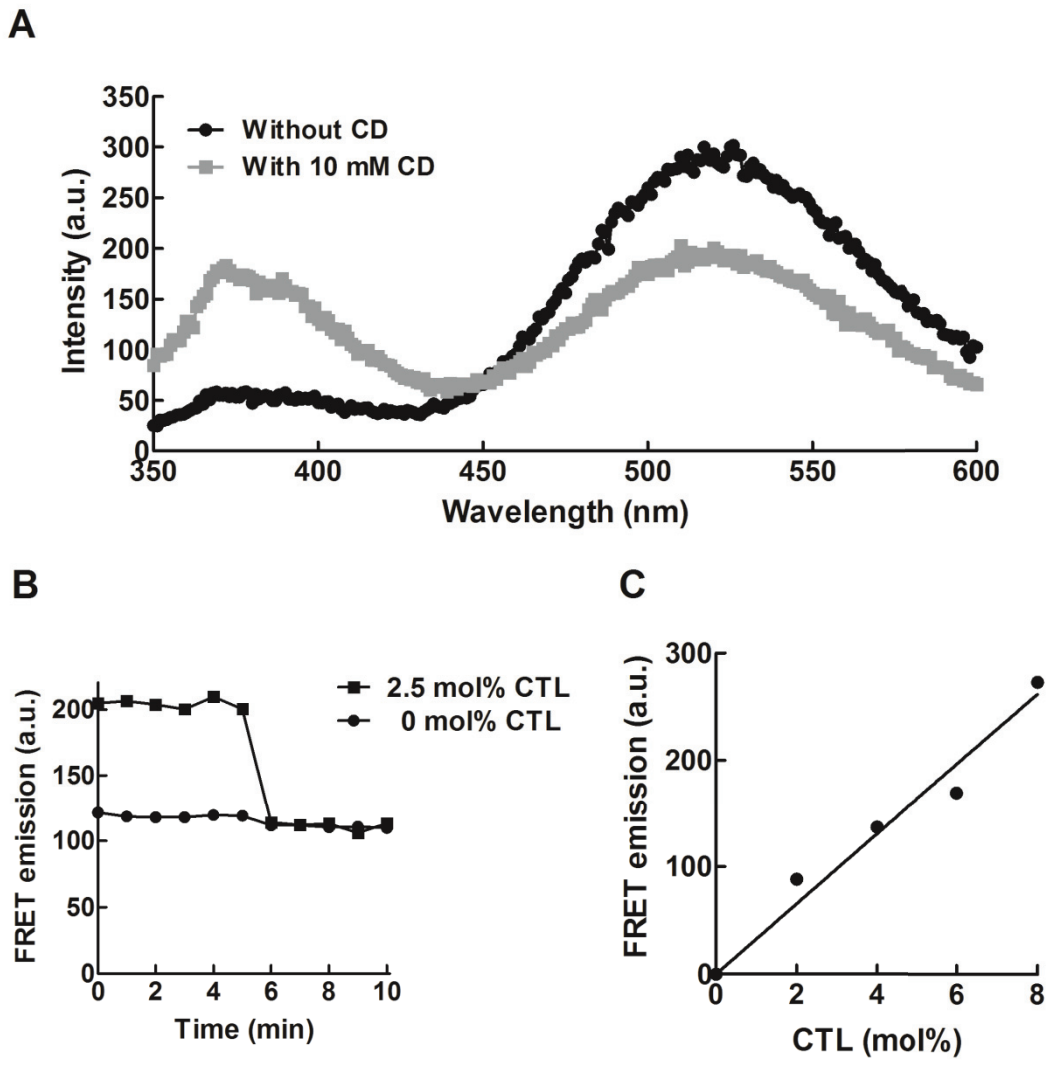

Figure 3.2. The FRET emission spectra and response to CTL content. Liposomes in liposome buffer were excited at 324 nm. (A) For the black curve, 0.1 mM liposomes containing 5 mol% CTL and 2.5 mol% dansyl-PE were scanned from 350 nm to 600 nm. Liposomes were scanned again after 10 mM of CD was added (grey curve). (B) Over 10 min, FRET emission of 0.05 mM liposomes containing 0 mol% or 2.5 mol% CTL with 2.5 mol% dansyl-PE was measured. For liposomes containing 2.5 mol% CTL, 2 mM of CD was added at 5 min. (C) A series of 0.05 mM liposomes containing 0, 2, 4, 6, or 8 mol% of CTL with 2.5 mol% dansyl-PE was measured. Results are plotted along with liposome CTL content and fit by linear regression. FRET emission in (B) and (C) was measured at 520 nm.

PE. It has been shown that CD sufficiently removes cholesterol from membranes [135,136] but does not extract dansyl-PE [137]. Therefore, after the addition of CD, CTL would be extracted leaving dansyl-PE in the liposome. In terms of the FRET-based extraction assay, we would expect to observe a FRET emission decrease and a CTL emission increase. To test this, 10 mM of CD (2000-fold excess compared with CTL content) was added to the assay. Indeed, it was evident that emission at 520 nm decreased and emission at 370 nm increased upon CD addition (Figure 3.2A). This CD extraction experiment also indicated that the FRET emission change is a good indicator of CTL extraction.

Since we would like to use FRET emission change to measure CTL extraction, it is important to understand the property of the emission. Also, understanding its properties would be crucial for us to interpret an extraction result. To verify the background emission, liposomes containing 0 mol% and 2.5 mol% of CTL, with 2.5 mol% dansyl-PE in both liposomes, were prepared and measured for 10 min. In 0 mol% CTL liposomes, more than 100 a.u. of emission was identified that was not caused by CTL energy transfer (Figrue 3.2B). Thus, 0% CTL liposome have a background emission at 520 nm. Emission measured using 2.5% CTL liposome had about 80 a.u. more than that from 0% CTL liposome. Adding 2 mM of CD (large excess compared with CTL content in liposome) caused the emission to decrease to background emission level (Figure 3.2B) similar to liposomes with 0 mol% CTL. This indicates that the emission difference (at 520 nm) between 0 mol% and 2.5 mol% CTL liposomes is the actual FRET emission. Therefore, all FRET-based extraction assays required 0 mol% CTL liposomes to correct for background emission. Next, the relationship between FRET emission and CTL

content in liposomes was investigated. Liposomes containing different amount of CTL (0, 2, 4, 6, and 8 mol%) with 2.5 mol% dansyl-PE were prepared and measured. Emissions at 520 nm were corrected using results with 0 mol% CTL liposomes and plotted with liposome CTL content (%). The plot showed that FRET emission was proportional to CTL content in liposomes (Figure 3.2C). Thus, FRET emission change within this range (from 0 to 8 mol%) could directly reflect CTL content change in liposomes. In our FRET-based assays, 2.5 mol% CTL was used.

3.3 ORP9L and ORP9S rapidly extract CTL from liposomes

OSBP and ORP9L extract cholesterol from liposomes [56,105] and therefore should extract the fluorescent cholesterol analog CTL. To test this, OSBP and ORP9 purified from SF21 cells were used in the newly developed FRET-based extraction assay. Purity of these proteins was assayed using SDS-8% PAGE and stained with Coomassie Blue (Figure 3.1A). In each extraction assay, 150 pmol (except for no addition) of protein was incubated with 0.05 mM liposomes containing 2.5 mol% CTL and 2.5 mol% dansyl-PE. True FRET emission was corrected by subtracting background emission (from 0 mol% CTL liposome). FRET emission at time 0 was set as 100%. When no protein was added (no-addition), FRET emission did not change over time. This result indicated that photo bleaching was negligible during the extraction assay. Surprisingly, when OSBP was added to the assay, there was no evidence of FRET emission change and therefore no CTL extraction (Figure 3.3). However, when ORP9L and ORP9S were added to the assay, FRET emission at 520 nm rapidly decreased by approximately 30% and 40%, respectively, and stabilized at round 1 min (Figure 3.3), indicating that ORP9L and ORP9S extracted CTL from liposomes. Furthermore, the FRET-based extraction

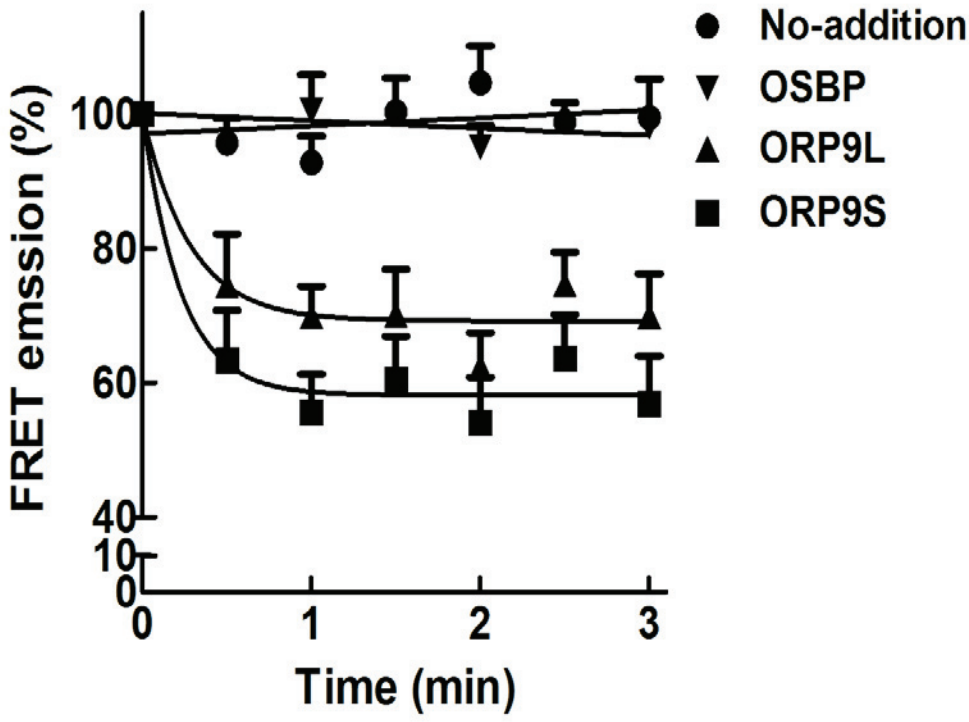

Figure 3.3. ORP9L and ORP9S extract CTL from liposomes. In each extraction assay, 0.05 mM liposomes containing 2.5 mol% CTL and 2.5 mol% dansyl-PE was incubated with 150 pmol OSBP, ORP9L or ORP9S at 30 °C. FRET emission was measured at 520 nm every 0.5 min for 5 min, corrected for background emission, and converted to percent using time 0 as 100%. OSBP results were from three repeats of one experiment. No-addition, ORP9L and ORP9S results shown are mean and standard errors from at least three different experiments. Each experiment has at least one repeat. Results are fitted by using linear regression (No-addition and OSBP) or one-phase exponential decay (ORP9L and ORP9S).

assay indicates that ORP9L and ORP9S rapidly extract CTL from liposomes, probably within 1 min under our experimental conditions (Figure 3.1). Previous [^{3}H]cholesterol based extraction assay failed to show this. Extraction occurred in a short time period. Therefore, to determine the extraction rate, more data points are required prior to 1 min.

3.4 Effect of cholesterol on CTL extraction by ORP9

The newly developed FRET-based extraction assay provided a way to investigate cholesterol transport by ORP9 *in vitro.* To verify the FRET emission changes we observed were due to CTL extraction, a competitive extraction assay with additional cholesterol was conducted. Liposomes containing 2.5 mol% CTL along with 2.5 mol% cholesterol were prepared and incubated with 150 pmol of ORP9L and ORP9S. Compared with previous results (Figure 3.3), ORP9L and ORP9S had similar extraction from 2.5 mol% CTL liposomes (Figure 3.4). As expected, addition of 2.5 mol% of cholesterol competed for CTL extraction by ORP9L and ORP9S. Moreover, in both cases, the extraction took longer to reach equilibrium compared with the experiments where no cholesterol was included. Therefore, the CTL extraction rates in both cases were suppressed. Together, these data are good evidence that the FRET emission change we observed for ORP9L and ORP9S are due to CTL extraction.

3.5 ORP9S and ORP9L do not transfer CTL

ORP9 not only extracts cholesterol from a liposome but also transfers it to acceptor liposomes [56]. Therefore, we attempted to set up a FRET-based transfer assay to determine whether ORP9 could also transfer its extracted CTL to an acceptor liposome. To this end, two different liposomes (donor and acceptor) were prepared;

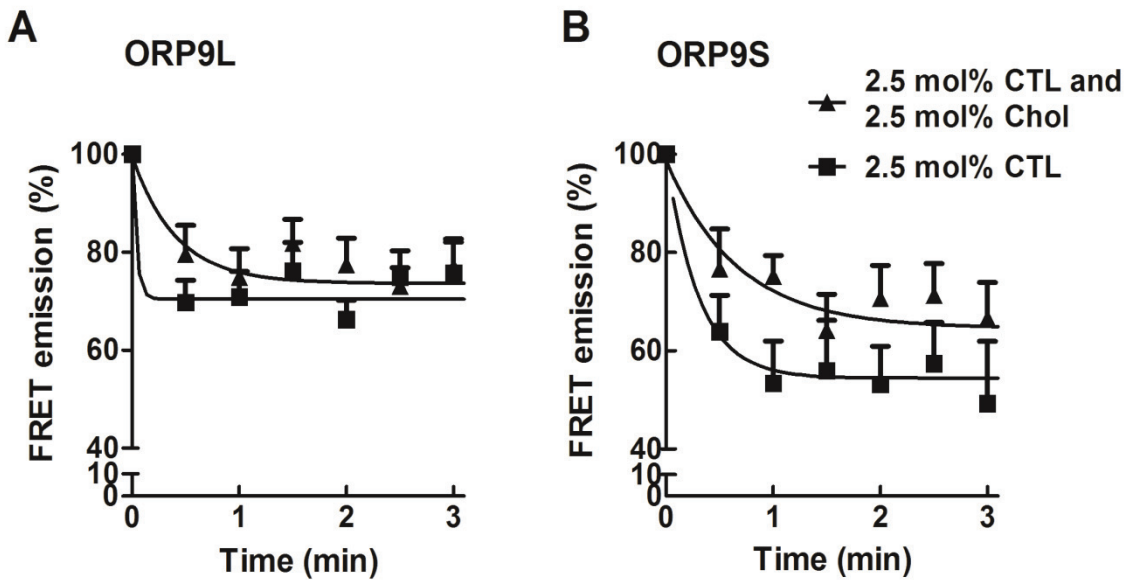

Figure 3.4. Additional cholesterol in liposomes inhibited CTL extraction. In each FRET-based competitive extraction assay, 150 pmol of ORP9 was incubated with 0.05 mM liposomes containing 2.5 mol% CTL only or liposome containing 2.5 mol% CTL with 2.5 mol% cholesterol at 30 °C. FRET emission measurement and calculation was conducted as described in the legend to Figure 3.3. Results are mean and standard errors from two different experiments. Each experiment had at least three repeats. Results are fitted by using one-phase exponential decay.

donor liposome contained 2.5 mol% CTL and acceptor liposome contained 2.5 mol% dansyl-PE. It is previously shown (section 3.2) that CTL and dansyl-PE together in one liposome can generate a FRET emission. If ORP9L or ORP9S transfers their bound CTL to a liposome containing 2.5% dansyl-PE, we would see a FRET emission increase (Figure 2.1B).

In the CTL transfer assay, 0.1 mM donor liposomes containing 2.5 mol% CTL and 0.05 mM acceptor liposomes containing 2.5 mol% dansyl-PE were incubated with 150 pmol of ORP9L or ORP9S. FRET emission was measured at 520 nm after excitation at 324 nm. The donor was twice as concentrated as the acceptor. Therefore, there would be more CTL molecules available in each assay for the possible CTL and energy transfer. No additional experiments were conducted to illustrate that there was no spontaneous CTL transfer, as indicated by lack of FRET emission increase. ORP9L or ORP9S were added after the first reading was measured. There was no noticeable FRET emission increase identified over 10 min after ORP9L or ORP9S were added (Figure 3.5A). The FRET emissions (approximately 140 a.u.) identified in all cases were probably due to background emission from dansyl-PE (Figure 3.5). Therefore, no CTL transfer occurred under these experimental conditions. Addition of PI(4)P to both donor and acceptor liposomes stimulates [^{3}H]cholesterol transfer between liposomes [56]. Thus, we attempted to examine if additional PI4P in donor and acceptor liposomes could stimulate CTL transfer. To test this, donor and acceptor liposomes with 1% of PI(4)P were incubated with ORP9L or ORP9S. Surprisingly, no evident FRET emission increase was identified in these experiments (Figure 3.5D). Furthermore, ORP9L and ORP9S were

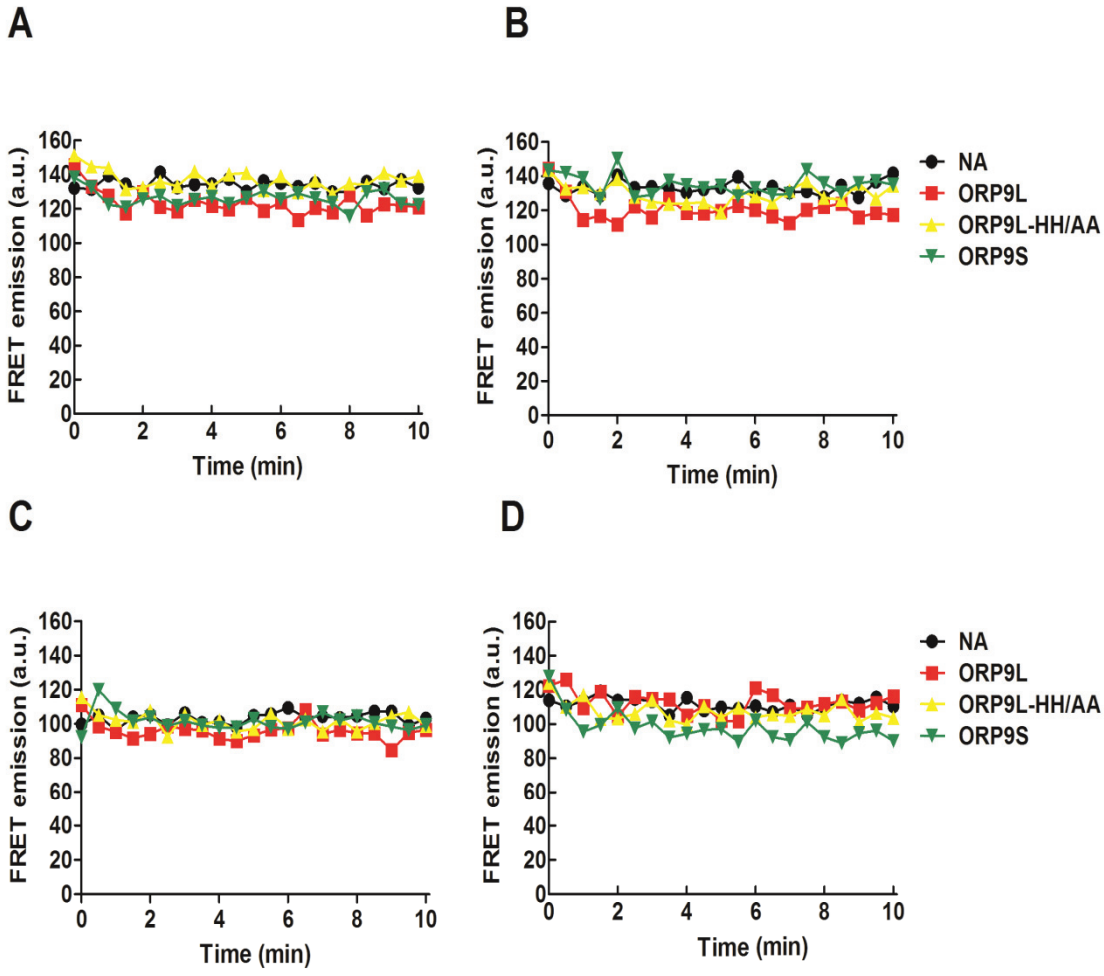

Figure 3.5. ORP9L and ORP9S do not transfer CTL between liposomes. ORP9L, ORP9L-HH/AA, and ORP9S (150 pmol) were incubated with 0.1 mM donor liposomes containing 2.5 mol% CTL and 0.05 mM acceptor liposome containing 2.5 mol% dansyl-PE for 10 min at 30 °C. FRET emission was measured every 0.5 min by excitation at 324 nm. Proteins were incubated with donor and acceptor liposomes without PI(4)P (A), donor liposomes with 1 mol% PI(4)P (B), acceptor liposomes with 1 mol% PI(4)P (C), both liposomes with 1mol% PI(4)P (D). Results are a representative from two repeat experiments.

incubated with donor and acceptor liposomes where only one contained 1% PI(4)P. Again, FRET emissions measured from these experiments showed no evident increase over 10 min (Figure 3.5B&C). Collectively, the FRET-based transfer assay under these experimental conditions failed to show any CTL transfer by ORP9L and ORP9S.

3.6 PI(4)P is a novel ligand for OSBP

It was recently shown that Osh4p (yeast orthologue of OSBP) specifically extracts PI(4)P from liposomes using its sterol binding pocket [63]. A phylogenetically conversed histidine pair directly interacts with the 4-phosphate group of PI(4)P [63]. These findings imply that PI(4)P may also be a ligand for members of the human ORP family. To test this, a OSBP [^{3}H]cholesterol extraction assay was used to determine whether addition of PI(4)P could suppress cholesterol extraction. In this competitive extraction assay, 50 pmol of OSBP was incubated with 0.1 mM of liposome containing 1% [^{3}H]cholesterol and increasing amounts of PI, PI(4)P, or PI(4,5)P_2 (0, 0.5, 1, and 2 mol%) at 25°C. Then, lectin was added to bind and pull-down the lactosyl-PE containing liposomes by centrifugation. An extraction assay where no phosphoinositides were added was set as 100%. If PI(4)P is also a ligand for the sterol binding domain (SBD) of OSBP, suppression of [^{3}H]cholesterol extraction should be observed. As expected, the presence of PI(4)P had an evident suppressive effect on [^{3}H]cholesterol extraction (Figure 3.6A); approximately 75% inhibition was reached when 2% PI(4)P was present. In contrast, PI or PI(4,5)P_2 in liposomes showed no inhibitory effect (Figure 3.6A). The PH domain of OSBP binds PI(4)P [57]. Moreover, at high PI(4)P content the interaction between the PH domain and PI4P causes OSBP to be retained on liposomes [56]. The retention causes OSBP to be sedimented in the pellet and unavailable for extraction

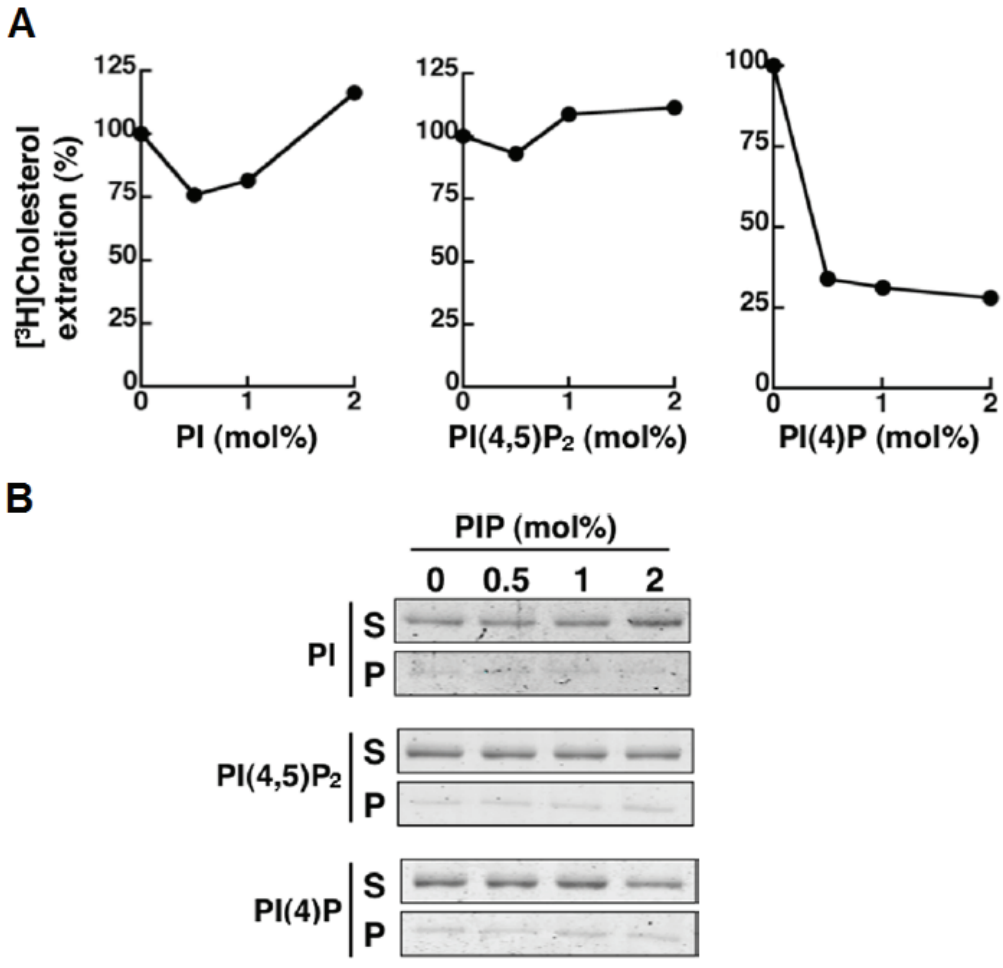

Figure 3.6. PI(4)P in liposomes inhibits [^{3}H]cholesterol extraction. (A) OSBP (50 pmol) was incubated with liposomes containing 1% [^{3}H]cholesterol with additional PI, PI(4)P or PI(4,5)P_2 (0, 0.5, 1, and 2 mol%) at 25 °C. [^{3}H]cholesterol extraction in the absence of phosphoinositides is set as 100% extraction. Results are from a representative experiment. (B) A fraction of the supernatant (S) and pellet (P) (dissolved in 1% SDS) from (A) was resolved in SDS-8% PAGE and stained with Coomassie Blue to illustrate the distribution of OSBP. Results are a representative from two repeat experiments.

determination. To verify that the results for the competitive extraction assays were not due to OSBP lost in the pellet, a fraction of the supernatant and pellet (dissolved in 1% SDS) from the competitive [^{3}H]cholesterol extraction was resolved in SDS-8% PAGE and stained with Coomassie Blue. Inclusion of up to 2% PI(4)P did not cause OSBP to be retained on liposomes (Figure 3.6B). The majority of the OSBP was observed in the supernatant. Therefore, the inhibition of [^{3}H]cholesterol extraction by PI(4)P is due to competition between these two OSBP ligands.

To verify that OSBP extracts PI(4)P from liposomes, assays using [^{32}P]PI(4)P were conducted. [^{32}P]PI(4)P was purified by TLC from HeLa cells labeled with [^{32}P]PO_4^{3-}, and verified by a porcine brain PI(4)P standard. For the [^{32}P]PI(4)P or [^{3}H]PI extraction assay, OSBP was incubated at 25°C with 0.1 mM liposomes containing 0.5% of radiolabeled PI or PI(4)P. Extracted [^{32}P]PI(4)P or [^{3}H]PI in the supernatant was quantified and calculated against total radioactivity input to give percent extraction. An experiment with no protein added was used to correct for non- specific extraction. First, OSBP was incubated with liposomes containing 0.5% of [^{3}H]PI or [^{32}P]PI(4)P. OSBP extracted significantly more [^{32}P]PI(4)P compared to [^{3}H]PI (Figure 3.7A). Direct extraction of [^{32}P]PI(4)P was also assayed using different amounts of OSBP (0, 25, 50, 100, and 200 pmol; Figure 3.7B). It was evident that [^{32}P]PI(4)P extraction by OSBP was dose-dependent and became non-linear at high protein concentration (100 to 200 pmol). OSBP-RR/EE is PH domain mutant that does not bind PI(4)P [79]. Increasing amounts of OSBP-RR/EE showed a similar extraction curve compared with wildtype OSBP, indicating that the binding interaction between PI(4)P and PH domain did not facilitate the extraction process. The aforementioned histidine pair of the SBD is

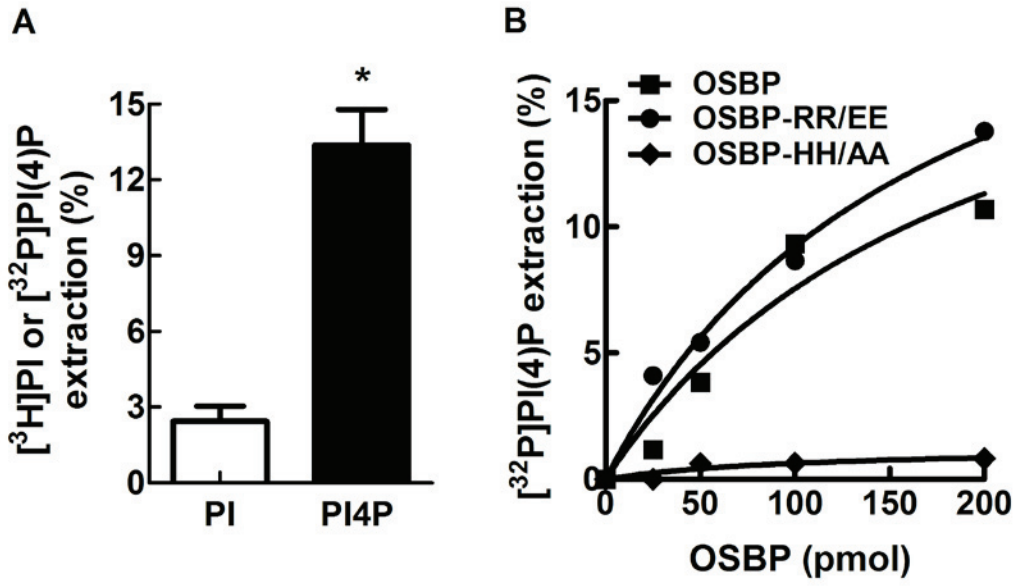

Figure 3.7. OSBP specifically extracts PI(4)P from membranes. (A) OSBP (50 pmol) was incubated with 0.1 mM liposomes containing 0.5% [^{3}H]PI or [^{32}P]PI(4)P at 25 °C. Percent extraction is calculated based on total radioactivity input in each assay as 100%. Results shown are the mean and standard errors from three experiments (*$p < 0.05$). (B) Different amounts of OSBP, OSBP-RR/EE, and OSBP-HH/AA (0 to 200 pmol) were incubated with liposomes containing 0.5% [^{32}P]PI(4)P. Results shown are mean from two experiments. Extraction curves are fit by one site binding model.

essential for Osh4p PI(4)P extraction [63]. To test whether this histidine pair in the SBD of OSBP is also essential for PI(4)P extraction, a OSBP-HH/AA mutant was expressed and purified from SF21 cells (Figure 3.1). This mutant showed constantly low PI(4)P extraction (less than 1%) regardless of protein input (Figure 3.7B). Therefore, this mutant did not extract PI(4)P from liposome. Collectively, OSBP could specifically extract PI(4)P from liposomes and the histidine pair in the SBD of OSBP is essential for PI(4)P extraction.

3.7 PI(4)P is also a ligand for ORP9L and ORP9S

Using competitive and direct extraction assays, we have shown that PI(4)P is also a ligand for OSBP, the founding member of the ORP family. ORP9 also has a conserved histidine pair and therefore could bind PI(4)P competitively with cholesterol. We attempted to determine whether PI(4)P was also a ligand for ORP9. Both ORP9L and ORP9S were purified from SF21 cells (Figure 3.1) and assayed in the direct [^{32}P]PI(4)P extraction assay. Indeed, both ORP9L and ORP9S extracted PI(4)P from liposomes (Figure 3.8A). PI(4)P extraction demonstrated a linear relationship with ORP9 protein input (0-100 pmol). ORP9S does not have the PH domain compared with ORP9L. Interestingly, the absence of the PH domain did not abolish the PI(4)P extraction function of ORP9S. This result strongly indicated that the PH domain of ORP9L is not required for PI(4)P extraction. Furthermore, at high protein concentration (100 to 200 pmol), ORP9S seemed to extract more PI(4)P compared with ORP9L, although the differences between those data points was not significant.

Mutation of the histidine pair in the SBD of OSBP inhibited PI(4)P extraction. We attempted to determine whether this histidine pair in ORP9 was also crucial for

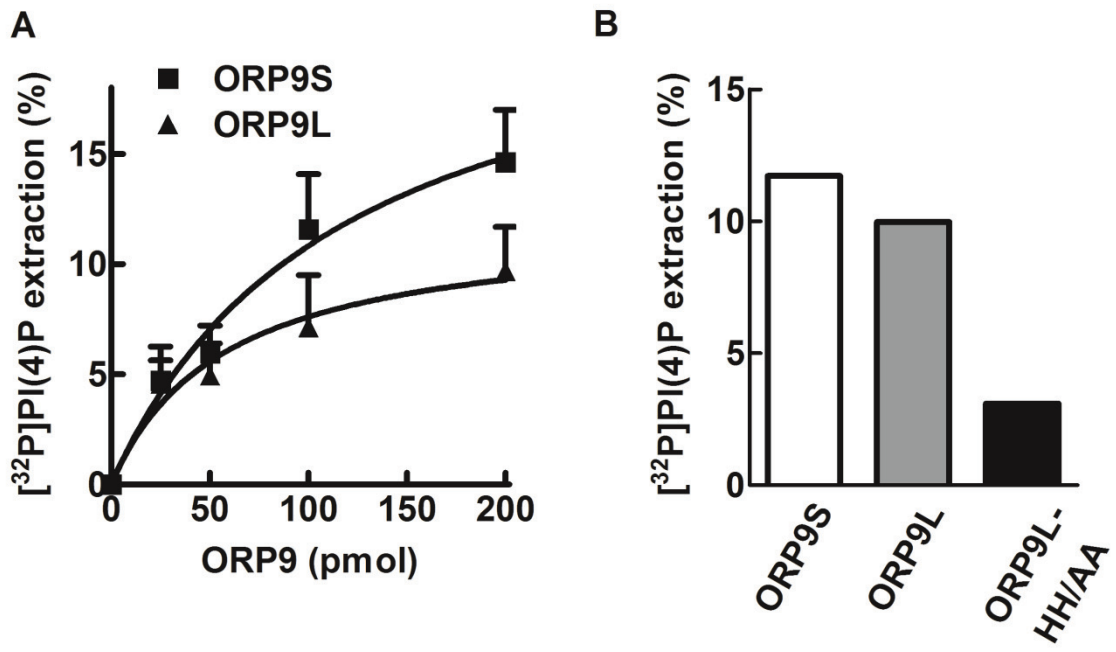

Figure 3.8. ORP9L and ORP9S extract PI(4)P from liposomes. ORP9 was incubated with 0.1 mM liposomes containing 0.5% [^{32}P]PI(4)P at 25 °C. Percent extraction is calculated by using total radioactivity input in each assay as 100%. (A) Increasing amounts of ORP9S or ORP9L (0, 25, 50, 100, and 200 pmol) were used to extract [^{32}P]PI(4)P. Results shown are mean and standard errors from three experiments. (B) 100 pmol of ORP9S, ORP9L or ORP9L-HH/AA (B) were used to extract [^{32}P]PI(4)P. Results shown are mean of two independent experiments.

PI(4)P extraction. To this end, ORP9L-HH/AA mutant was constructed by site-directed mutagenesis and expressed and purified from SF21 cells (Figure 3.1). In a direct [^{32}P]PI(4)P extraction assay, 100 pmol of ORP9S, ORP9L, and ORP9L-HH/AA were assayed for PI(4)P extraction. Indeed, ORP9L-HH/AA showed approximately 3% extraction compared with 12% and 10% extraction for ORP9S and ORP9L, respectively (Figure 3.8B). Thus, the histidine pair is also essential for ORP9 to extract PI(4)P from liposomes.

3.8 PI(4)P extraction defective mutant ORP9L-HH/AA extracts CTL

In previous sections, the double histidines in the SBD of OSBP and ORP9L were shown to be essential in PI(4)P extraction. The SBD of ORP9 also binds cholesterol and oxysterols. We then attempted to determine whether these two histidines were involved in cholesterol binding, using the FRET-based extraction assay (as described in Section 3.3). Wildtype ORP9L showed more than 30% extraction of CTL, similar to results shown in the previous section (Section 3.3). Interestingly, ORP9L-HH/AA caused FRET emission to decrease to approximately 50%, indicating that there was roughly one-half CTL extraction occurred (Figure 3.9). This result indicated that the histidine pair in the SBD of ORP9 is not required for CTL extraction.

Since ORP9L-HH/AA did not extract PI(4)P but could still extract CTL, we speculated that this mutant might transfer cholesterol better. ORP9L-HH/AA was tested in the FRET-based transfer assay but did not cause FRET emission to increase in the presence or absence of PI(4)P (Figure 3.5).

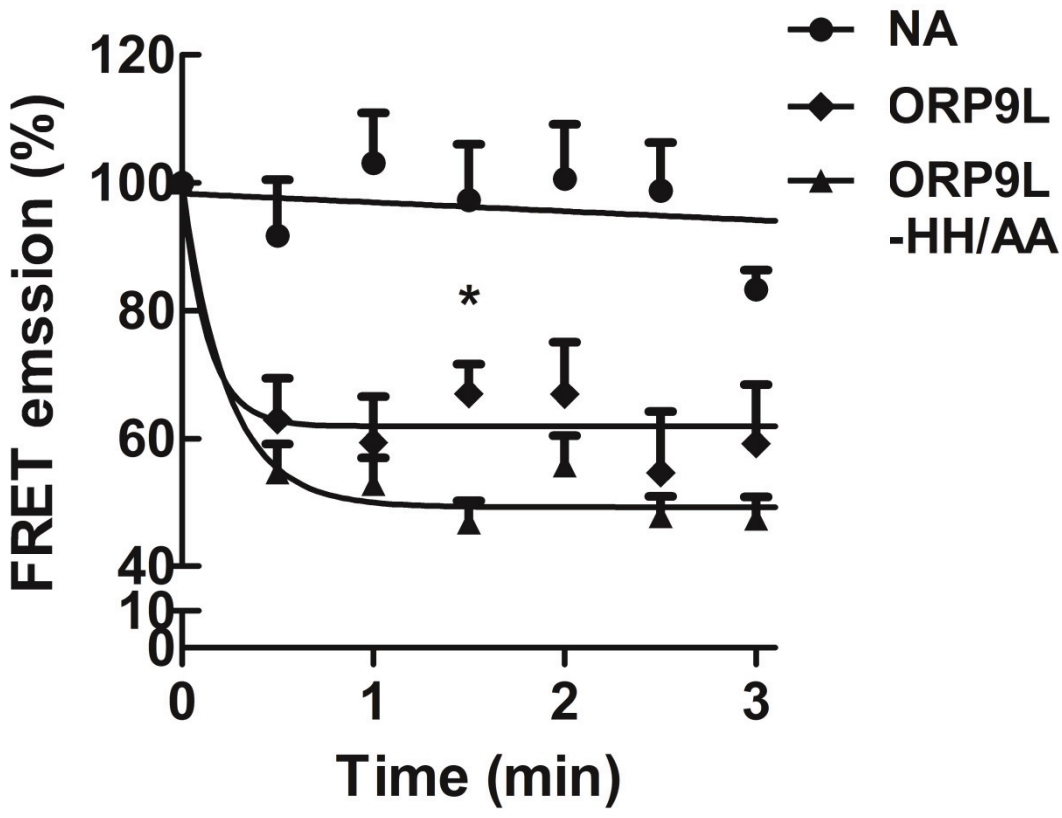

Figure 3.9. PI(4)P binding defective mutant ORP9L-HH/AA extracts CTL from liposomes. In each extraction assay, 0.05 mM liposome containing 2.5 mol% CTL and 2.5 mol% dansyl-PE was incubated with 150 pmol ORP9L and ORP9L-HH/AA at 30 °C. FRET emission measurement and calculation was conducted as described in the legend to Figure 3.3. Results shown are mean and standard errors from three experiments (*$p<0.05$). Each experiment has at least one repeat. No-addition results are fitted by using linear regression. ORP9L and ORP9L-HH/AA curves are fitted by using one-phase exponential decay model.

3.9 Effects of PI(4)P on CTL extraction

PI(4)P was shown to be a ligand for ORP9L and ORP9S. In Section 3.6, we showed that inclusion of PI(4)P in liposomes inhibited [^{3}H]cholesterol extraction by OSBP. We speculated that the competition between PI(4)P and cholesterol would be common in the ORP family. Instead of using a radioactive-based extraction assay, the FRET-based extraction was applied. A similar FRET-based extraction assay was conducted as described in Section 3.3, with PI(4)P incorporated into liposomes to test the effects on CTL extraction. Unfortunately, inclusion of 1 mol% PI(4)P in extraction liposome caused no significant changes on CTL extraction for both ORP9L and ORP9S, except for the data points at 1 min for ORP9L (Figure 3.10A&C)

Inclusion of 1 mol% PI(4)P might be low relative to 2.5 mol% CTL to cause changes in CTL extraction. Therefore, 2.5 mol% of PI(4)P was also incorporated into extraction liposomes to further investigate the effect of this ligand on CTL extraction. Again, inclusion of 2.5 mol% PI(4)P demonstrated no significant changes on CTL extraction for both ORP9L and ORP9S (Figure 3.10B&D).

3.10 Knockdown of ORP9L does not affect PI(4)P distribution in HeLa cells

As we showed in Section 3.7, PI(4)P is a ligand for ORP9L and ORP9S. It is reasonable to speculate that these proteins could regulate PI(4)P distribution or metabolism in cells. To this end, we knocked down ORP9L gene expression using siRNAs in HeLa cells to investigate the role of ORP9L on PI(4)P distribution. It was not necessary to knockdown the short form of ORP9, since ORP9S is not expressed in commonly used immortalized cell lines (unpublished results). HeLa cells were transfected with a combination of three siORP9L, incubated for 48 h, and examined by

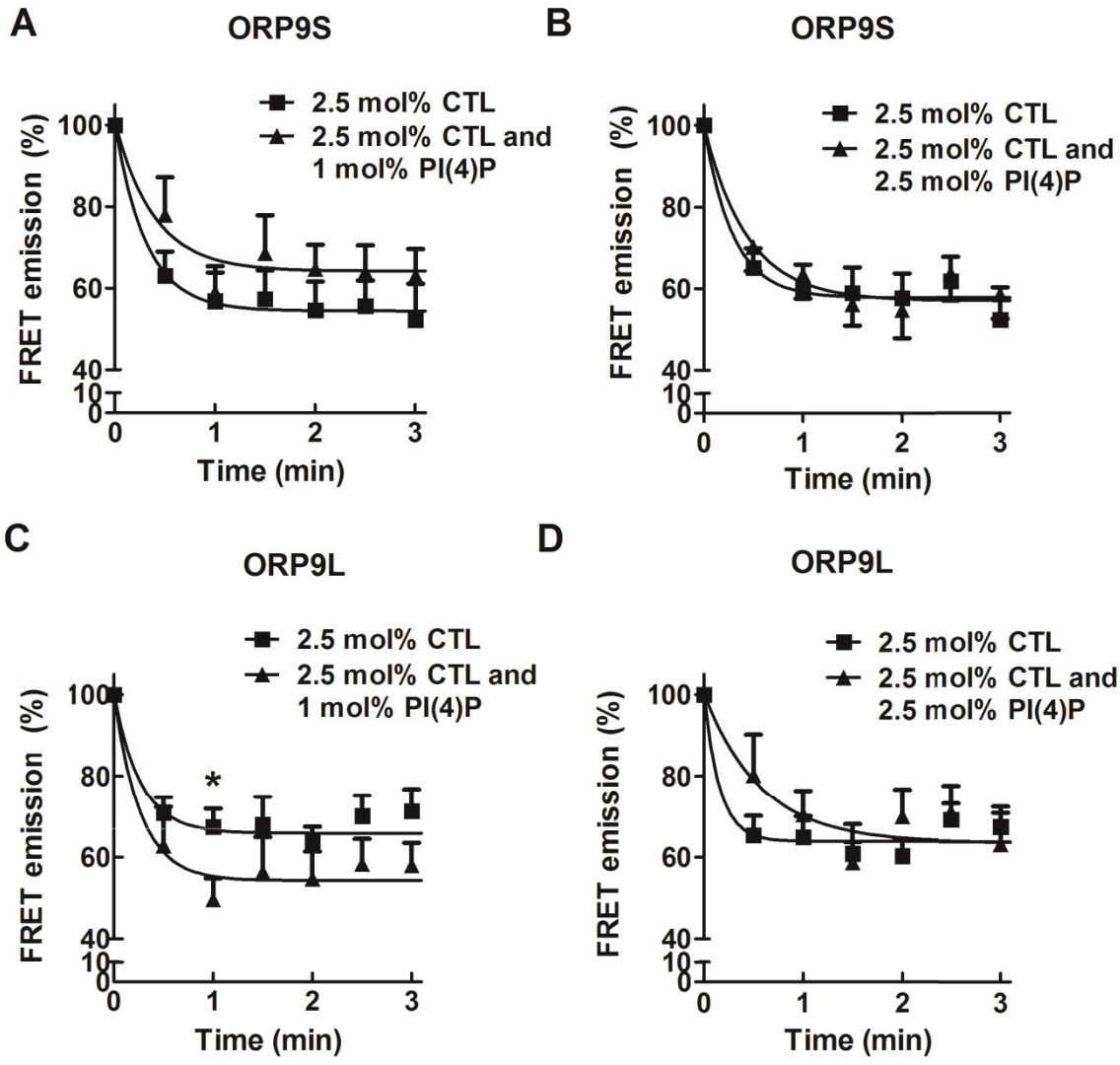

Figure 3.10. Effects of additional PI(4)P on CTL extraction. In each FRET-based extraction assay, 150 pmol of ORP9L or ORP9S were incubated with 0.05 mM of extraction liposomes containing 1 mol% or 2.5 mol% PI(4)P for 10 min at 30 °C. FRET emission measurement and calculation was conducted as described in the legend to Figure 3.3. (A) and (B) ORP9S were incubated with extraction liposomes and with additional 1 mol% or 2.5 mol% PI(4)P, respectively. (C) and (D) ORP9L were incubated with extraction liposomes and with additional 1 mol% or 2.5 mol% PI(4)P, respectively. Results are the mean and standard errors of three experiments (*$p<0.05$).

immunoblot for expression. As shown in Figure 3.11A, ORP9L was knocked down by approximately 70% compared with the non-targeting siRNA (ORP9L level normalized to actin).

ORP9L and PI(4)P in HeLa cells were visualized using an ORP9 polyclonal antibody and a goat anti-rabbit IgG-488 secondary antibody, and PI(4)P monoclonal antibody detected by goat anti-mouse IgM-594 antibody, respectively. The same exposure time was used for imaging both non-targeting and ORP9L knocked down cells to monitor ORP9L levels. ORP9L is previously reported to be localized to the trans-Golgi/TGN compartment [56]. Our experiment agreed with this observation. In cells transfected with non- targeting siRNA, ORP9L co-localized with PI(4)P in the TGN [56]. After transfection with siORP9L, it was evident that most cells had lower ORP9L expression level and lost their Golgi pattern staining (Figure 3.11B). PI(4)P is concentrated in the TGN [138] and therefore its localization overlapped with ORP9L. Interestingly, upon ORP9L knockdown, PI(4)P localization did not noticeably change compared with non-targeting counterparts. Furthermore, the overall PI(4)P signal level did not show a dramatic change. Collectively, lowering ORP9L protein level did not affect PI(4)P distribution and amount.

3.11 Overexpression of ORP9 in CHO cells attenuates PI(4)P immunofluorescence detection

OSBP has a similar localization pattern compared with ORP9 in cells and also binds PI(4)P *in vitro*. Therefore, OSBP and ORP9 may have functional overlap in cellular PI(4)P distribution. This putative functional overlap between OSBP and ORP9 may explain why depletion of ORP9L in HeLa cells did not show changes on PI(4)P

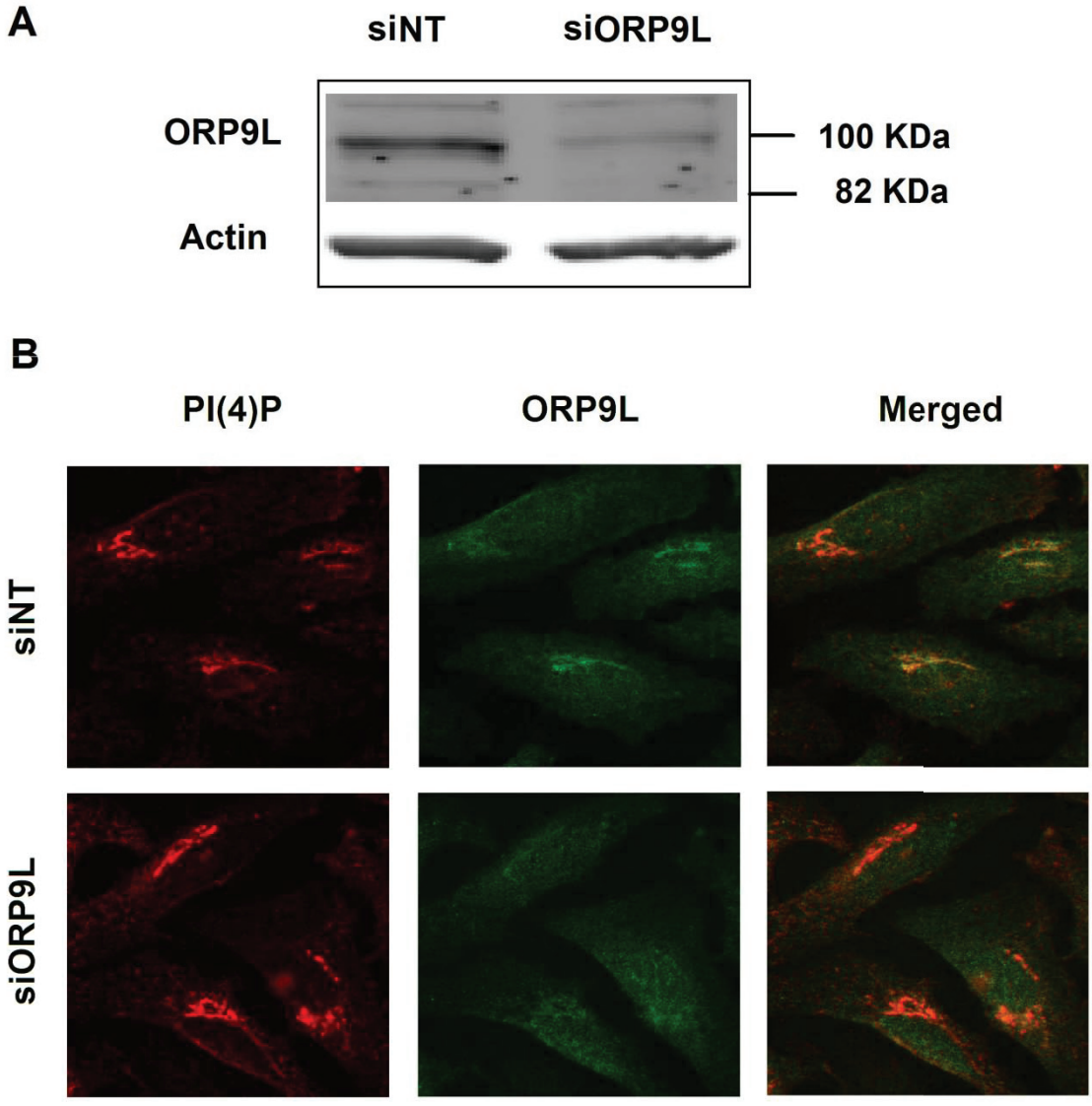

Figure 3.11. Knockdown of ORP9L in HeLa cells does not affect PI(4)P distribution. Hela cells at 70% confluency were transfected with siNT or siORP9L and incubated for 48 h. (A) HeLa cells grown directly on dishes were collected and immunoblotted for ORP9L and actin. Results shown are from a representative experiment. (B) HeLa cells grown on coverslips were probed with ORP9 and PI(4)P antibodies detected by goat anti-rabbit IgG 488 antibody and goat anti-mouse IgM594 antibody, respectively. Results shown are fluorescent images taken under same exposure time for both non-targeting and ORP9L knockdown experiments.

distribution and amount in our experiments. In yeast cells, overexpression of Osh4p causes the cellular PI(4)P level to decrease [139]. Thus, we speculated that overexpression of ORP9L and ORP9S would have similar effects on PI(4)P level in mammalian cells. CHO cells containing ORP9L and ORP9S cDNAs controlled by a doxycycline-inducible promoter (generated previously) were used to examine the effects of ORP9L or ORP9S expression on cellular PI(4)P. CHO cells were incubated with doxycycline and ORP9L, ORP9S and PI(4)P were probed as stated in the previous section. When induced, some CHO cells efficiently expressed ORP9L or ORP9S (Figure 3.12). Interestingly, low levels of PI(4)P were observed in these cells. In contrast, cells without overexpressed ORP9 proteins showed normal PI(4)P distribution in the TGN (Figure 3.12).

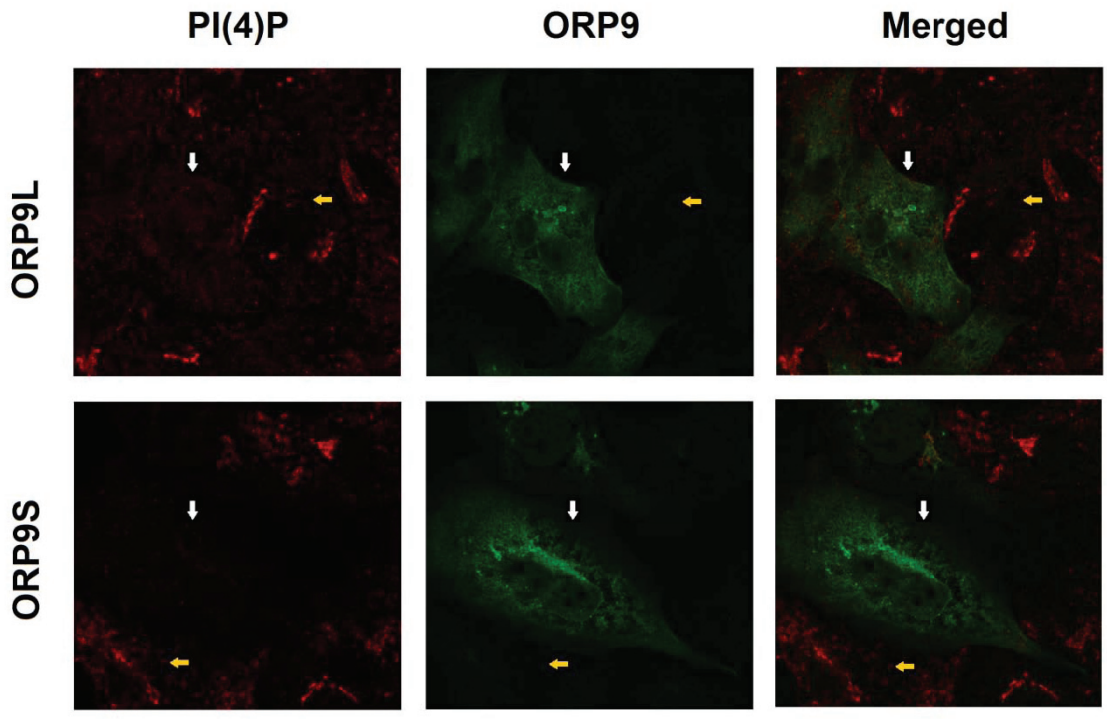

Figure 3.12 Overexpression of ORP9L or ORP9S in CHO cells attenuates PI(4)P immunofluorescence detection. CHO cells containing plasmids encoding for ORP9L or ORP9S were incubated on coverslips in medium B with 1 μg/ml doxycycline for 24 h. Detection of ORP9L, ORP9S and PI(4)P were conducted as described in the legend to Figure 3.11. Images are confocal scans of 0.8 μm sections. White and yellow arrows indicate cells with and without overexpressed ORP9 proteins, respectively.

CHAPTER 4 DISCUSSION

Cholesterol is an essential component of ER and Golgi membranes and is involved in various biological activities that occur at these sites, such as regulation of intracellular cholesterol homeostasis and cargo delivery [140-142]. The ER is the site where cholesterol is synthesized and serves as an important regulatory site for cholesterol homeostasis. Cholesterol content in the Golgi is higher than the ER and peaks at the TGN relative to the *cis* and *medial* compartments [143]. The cholesterol enriched environment of the TGN is for important in the formation of lipid rafts and secretory vesicles [144,145]. Despite the importance of cholesterol in these organelles, how cholesterol distribution is achieved between these two sites remains largely unknown.

The two cholesterol binding proteins, OSBP and ORP9L, have been implicated in transfer of cholesterol from the ER to the Golgi apparatus [56,113]. An *in vitro* assay demonstrated that OSBP and ORP9L can transfer cholesterol between liposomes [56]. This assay measures [^{3}H]cholesterol transfer from donor (1 mol% [^{3}H]cholesterol) to acceptor (10 mol% lactosyl-PE) liposomes [111,146]. Acceptor liposomes with transferred [^{3}H]cholesterol are sedimented after centrifugation by the addition of lectin, which binds to lactosyl-PE [56]. One problem with this assay is that OSBP and ORP9 seem to tether both donor and acceptor liposomes (unpublished data). Therefore, donor liposomes containing [^{3}H]cholesterol may be pulled down along with acceptor liposomes, making it difficult to determine a true cholesterol transfer. Also, it is unknown whether a cholesterol molecule is transferred to an acceptor liposome or ORPs bound with cholesterol associate with acceptor liposomes without transferring. Similar problems also occur in [^{3}H]cholesterol-based extraction assays (Figure 2.1). For instance, ORPs may

extract [^{3}H]cholesterol but remain associated with liposomes, resulting in a underestimation of extraction activity. Furthermore, [^{3}H]cholesterol-based assays fail to provide any kinetic information for the extraction and transfer processes. Energy transfer in FRET-based assays requires proximity (1-10 nm) of two chromophores. Therefore, FRET-based assays do not have these problems and even provide kinetic information, as emissions are measured in real time. We attempted to set up a FRET-based assay to more accurately study sterol extraction and transfer processes by OSBP and ORP9.

CTL was determined to be the best donor molecule in the FRET pair, since it competed with [^{3}H]cholesterol for binding to OSBP in aqueous solution but DHE did not (Figure 3.1). DHE is structurally similar to CTL, but has an extra double bond and methyl group on the hydrocarbon chain (Figure 1.1).The extra methyl group may cause some steric hindrance with the putative lid region of OSBP, making it unfavourable to bind to OSBP. ORP9 was not tested, since it does not bind cholesterol and 25-OH in aqueous solution [56]. We demonstrated that FRET emission occurred when liposomes containing both CTL and dansyl-PE were excited at 324 nm (Figure 3.2). The FRET emission was also sensitive to CTL extraction as verified by CD addition, suggesting this type of liposome is useful in a FRET-based extraction assay. Interestingly, background emissions were identified in the extraction liposomes, probably due to a overlap of the CTL and dansyl-PE excitation spectra. The background emission was corrected by using liposomes containing 0 mol% CTL (Figure 3.2B). Corrected FRET emissions demonstrated a linear relationship with the CTL content of liposomes, indicating that the FRET emission directly reflects the CTL content in extraction liposomes (Figure 3.2C).

Both OSBP and ORP9L extract [^{3}H]cholesterol from liposomes *in vitro* [56]. Using the FRET-based extraction assay, we showed that ORP9L rapidly extracted CTL from liposomes and the short form of OPR9L, ORP9S which contains only the SBD and FFAT motif, also rapidly extracted CTL (Figure 3.3). Extraction by ORP9 was further verified by the fact that inclusion of 2.5 mol% of cholesterol in the extraction liposomes suppressed the CTL extraction by both ORP9L and ORP9S (Figure 3.4).

It is well established that OSBP binds 25-OH and cholesterol dispersed in solution and extracts cholesterol from liposomes [56,69,91,93]. The fluorescent probe CTL has a similar structure to cholesterol (Figure 1.1) and competed with [^{3}H] cholesterol for binding to OSBP (Figure 3.1). Therefore, we expected that OSBP would extract CTL from liposomes. Surprisingly, OSBP did not extract CTL from liposomes, as its FRET emission curve overlapped with no-addition experiment (Figure 3.3). This may be because CTL is not a good ligand for OSBP, since CTL showed poor inhibition at high ligand concentration compared with unlabelled cholesterol in the competitive binding assays (Figure 3.1B and C).

The FRET-based extraction assay also provided us with some kinetic information about the extraction process. When ORP9L and ORP9S were used, the extraction processes was completed by 1 min (Figure 3.3). This time frame is comparable to that obtained from Osh4p DHE extraction experiments [63]. Also, comparison of extraction rates among different ORPs or under different experimental conditions is possible using this FRET-based extraction assay. However, in order to obtain a more accurate rate constant, more data points were required during the time when an extensive extraction occurred (0-1 min). Unfortunately, only three data pointes were obtained from 0 to 1 min

since we had to open the fluorometer and load the proteins after the first reading. A stop-flow injector can be introduced to overcome this problem. Overall, using FRET-based extraction assay, we showed that ORP9L and ORP9S rapidly extract CTL from liposomes. This extraction assay may be applied to study other ORPs.

FRET-based assays also provide a method to study sterol transfer between liposomes. In a FRET-based transfer assay, CTL can be transferred from a donor liposome to an acceptor liposome, which contains dansyl-PE (Figure 2.1B). FRET emission increase will occur when CTL is transferred to the acceptor liposomes. Unfortunately, both ORP9L and ORP9S failed to transfer CTL molecules between liposomes, even though they both extracted CTL (Figure 3.5A). PI(4)P incorporated into liposomes stimulated cholesterol transfer in a [^{3}H]cholesterol-based transfer assay [56]. Nevertheless, the inclusion of PI(4)P in donor, acceptor or both liposomes did not show any CTL transfer (Figure 3.5 B-D). Therefore, ORP9L or ORP9S did not transfer CTL between liposomes under our experimental conditions. Since these proteins extracted CTL liposomes under similar conditions, the negative results of transfer were probably because ORP9s did not release their bound CTL to acceptor liposomes. Co-factor proteins, such as VAP, are implicated in the putative cholesterol transfer process but were not introduced into our *in vitro* transfer assays. These co-factors may be required for proper cholesterol release. Based on [^{3}H]cholesterol-based transfer assay conducted in our lab, it was also noted that OSBP and ORP9 could simultaneously bind to donor and acceptor liposomes when anionic lipids, such as PI(4)P, was present. Close membrane contact is required for DHE transfer mediated by Osh4p [112]. Therefore, methods that enhance liposome association can be introduced into our FRET-based

transfer assay to promote CTL transfer by ORP9. It is also possible that a small fraction of the CTL transfer occurred, but under our experimental conditions, the FRET emission change was undetectable due to the low transfer level. Unfortunately, unlike the FRET-based extraction assay, we have not developed a positive control to show CTL transfer. Addition of CD extracted CTL from liposome (Figure 3.2B), but did not transfer CTL between liposomes in our FRET-based transfer assay (results not shown).

It is well-established that PI(4)P is enriched in the TGN and essential for its functions [147]. For instance, PI(4)P regulates sphingolipid biosynthesis by recruiting corresponding proteins. Through the interaction between its PH domain and PI(4)P, CERT transfers ceramide from ER to the TGN for SM production [118]. Moreover, PI(4)P is required for anterograde trafficking from the Golgi [147]. However, the distribution and metabolism of PI(4)P in cells is poorly understood. The yeast ORP, Osh4p was recently shown to specifically extract PI(4)P from liposomes using its SBD, indicating that this protein can regulate PI(4)P distribution and levels between cellular compartments coupled with the PI(4)P production and turnover processes [63]. For instance, Osh4p and other yeast ORPs interact with PI(4)P phosphatase Sac1 via the SBD to stimulate PI(4)P dephosphorylation [148]. We demonstrated that OSBP, ORP9L and ORP9S also extracted PI(4)P from liposomes (Figure 3.7 and 3.8). PI(4)P extraction depended on the ORP9 protein input and was roughly proportional to protein input from 0 to100 pmol. Moreover, PI(4)P binding by OSBP is specific, supported by the fact that OSBP specifically extracted PI(4)P rather than PI (Figure 3.7A) and inclusion of PI or $PI(4,5)P_2$ did not inhibit [^{3}H]cholesterol extraction (Figure 3.6A). The competition between sterol and PI(4)P also indicates that PI(4)P binds to the same region of OSBP,

the SBD. Furthermore, although the PH domain binds to PI(4)P and targets OSBP to the TGN [57], it was not required for the PI(4)P extraction, since the PH binding defective mutant OSBP-RR/EE had similar extraction curve compared with wildtype OSBP (Figure 3.7B).

The structure of Osh4p bound with PI(4)P, and disruption of PI(4)P extraction using mutated Osh4p proteins revealed important residues that are essential for PI(4)P binding [63]. The histidine pair in the ORP signature sequence is crucial for Osh4p PI(4)P binding. To test this histidine pair is also essential for mammalian ORPs, we constructed OSBP and ORP9L recombinant proteins with the histidine pair mutated to alanines. Indeed, OSBP-HH/AA and ORP9L-HH/AA mutants did not bind PI(4)P, agreeing with the results found using Osh4p (Figure 3.7B and 3.8B). Since the histidine pair is in the SBD, these results further indicate that the SBD is the PI(4)P binding region and its ability to bind to PI(4)P is a common function shared by other ORP members. Interestingly, various highly ordered interactions are identified between the polar head of PI(4)P and mouth of the sterol-binding pocket of the Osh4p [63]. However, the hydrocarbon chain of sterols did not form strong interaction at this region of Osh4p [89]. Thus, despite the fact that both sterols and PI(4)P occupy the same binding pocket, Osh4p utilizes a different mechanism to bind sterols or PI(4)P. Therefore, we speculated that the PI(4)P binding defective mutant would not affect the sterol binding. Indeed, ORP9L-HH/AA mutant still efficiently extracted CTL from liposomes (Figure 3.9).

Knowing that PI(4)P is also a ligand for ORP9, it is reasonable to speculate that inclusion of PI(4)P in liposomes would inhibit CTL extraction in the FRET-based extraction assay. However, the presence of PI(4)P (both 1 mol% and 2.5 mol%) in

extraction liposomes did not show significant difference on CTL extraction for ORP9L and ORP9S (Figure3.10). Other extraction liposomes containing different amounts of PI(4)P (such as 0.5 mol% and 5 mol%) can be tested in the future to determine whether the presence of PI(4)P in liposomes would affect CTL extraction.

The finding that ORP9 extracts PI(4)P *in vitro* indicates that ORP9 can transfer its bound PI(4)P between organelles and in turn regulate PI(4)P distribution. However, depletion of ORP9L in HeLa cells did not change PI(4)P distribution and content (Figure 3.11B). The effects caused by ORP9L depletion are probably not noticeable, because OSBP may have functional redundancy relative to ORP9L in PI(4)P distribution and content. Therefore, ORP9L or ORP9S were overexpressed in CHO cells to examine the effect of these proteins in PI(4)P distribution and content. Indeed, lower levels of PI(4)P were observed in CHO cells overexpressing ORP9L or ORP9S relative to those without expression (Figure 3.12). The difference observed in PI(4)P level suggests that overexpressed ORP9 proteins may attenuate PI(4)P levels in cells, possibly coupled with PI(4)P metabolism. It is also possible that those overexpressed ORP9 proteins extract PI(4)P, blocking PI(4)P molecules from detection by PI(4)P antibody. Therefore, quantification of cellular PI(4)P is required to determine whether PI(4)P mass is reduced due to ORP9 overexpression.

Cholesterol is a well-known ligand for the SBD of OSBP and ORP9 (reviewed in [6]). We also showed that PI(4)P is a ligand for OSBP and ORP9. These proteins probably use their SBD rather than the PH domain to bind PI(4)P, supported by the facts that presence of PI(4)P inhibits cholesterol extraction by OSBP; the histidine pair in the SBD of OSBP and ORP9 is essential for PI(4)P extraction; the PH domain is not

required for PI(4)P extraction since the PH mutant of OSBP and ORP9S showed PI(4)P extraction. Based on the structure of Osh4p, cholesterol binds to the protein with its 3-hydroxyl group forming ordered interactions at the bottom of the sterol-binding pocket, while the fused ring structure and carbon chain forms weak Van Der Waals interactions [89]. In contrast, PI(4)P accommodates the SBD with the two acyl chains inserted in the sterol-binding pocket and the polar head group forming highly ordered interactions with the mouth region of ORP [63]. Therefore, ORPs probably use different regions to recognize and bind the polar moieties of cholesterol and PI(4)P. The hydrophobic moieties are surrounded by the sterol-binding pocket with weak interactions. Moreover, the structure of the sterol-binding pocket may vary among ORPs, therefore, conferring specific ligand binding. CTL has a similar structure to cholesterol, with extra two double bonds within the fused ring structure. CTL can be extracted by ORP9L and ORP9S but not OSBP.

Evidence has accumulated in recent years, suggesting that OSBP and ORP9 transport cholesterol between the ER and Golgi apparatus [6]. More specifically, these two proteins may bind newly synthesized cholesterol at the ER and transfer it to the TGN in a PI(4)P-dependent manner. Our FRET-based extraction assay showed that OSBP and ORP9 extract CTL from liposomes, partially supporting the putative cholesterol transfer function. Another issue that is important for the cholesterol transport process is directionality. As we know cholesterol is more concentrated in the Golgi apparatus than it is in the ER, putative cholesterol transfer is against the concentration gradient. Therefore, regulation is required for a proper cholesterol transport. The transport process can be regulated by a phosphorylation cycle. For example, phosphorylation at Ser^{240} of

OSBP by PKD attenuates Golgi localization in the presence of 25-OH [96]; an OSBP mutant mimicking dephosphorylation at Ser^{381} and phosphorylation at Ser^{192}, Ser^{195} and Ser^{200} is mainly localized in the ER [105]. Competition between sterol and PI(4)P for the sterol-binding pocket of OSBP and ORP9 provides a new explanation of the directionality of cholesterol transport. Figure 4.1 outlines how these two ligands can be reversely transported between ER and Golgi apparatus. In brief, OSBP or ORP9 can extract cholesterol molecules from the ER membrane and transfer them to TGN, where PI(4)P is accessible to compete for binding with cholesterol for the SBD of ORPs. As a result, OSBP and ORP9 can extract PI(4)P rather than re-extract cholesterol, causing a net cholesterol transfer from ER to Golgi apparatus. PI(4)P bound with OSBP and ORP9 can be transferred to the ER, where the ER anchored Sac1 can dephosphorylate PI(4)P to PI.

A similar lipid transport function coupled with phosphoinositides has also been hypothesized for the hepatic α-tocopherol (vitamin E) transfer protein (α-TTP) [149]. This protein competitively binds α-tocopherol and $PI(4,5)P_2$ and counter-exchanges these two ligands between liposomes *in vitro*. The crystal structure of α-TTP revealed simultaneous binding of α-tocopherol and $PI(4,5)P_2$, implying an intermediate stage of ligand exchange. Moreover, the preference of α-TTP to bind $PI(4,5)P_2$ presumably targets the protein to PM, where $PI(4,5)P_2$ is concentrated. These results further indicate that lipid/phosphoinositide exchange is a conserved function for other lipid transfer proteins.

In conclusion, we have shown that PI(4)P is also a ligand for OSBP and ORP9. The highly conserved residues (histidine pair) essential for PI(4)P binding prompt us to

speculate that the PI(4)P binding function is shared by other mammalian ORPs. More studies are required on the function of ORPs in PI(4)P distribution, and whether they exchange cholesterol and PI(4)P between ER and Golgi. We also set up a FRET-based extraction assay and showed that ORP9 proteins rapidly extracted CTL from liposomes. The assay can be used to study other mammalian ORPs and under different conditions. The FRET-based transfer assay did not show CTL transfer using ORP9 proteins. More work can be done to further study the possible sterol transfer process using the FRET-based transfer assay. A positive control (such as Osh4p) is essential for the FRET-based transfer assay to demonstrate CTL transfer process. Sterol transfer by ORPs may require close membrane contact. Therefore, a method that generates liposome aggregation, such as adding Mg^{2+} to tether liposomes containing anionic lipids, can be introduced to the transfer assay.

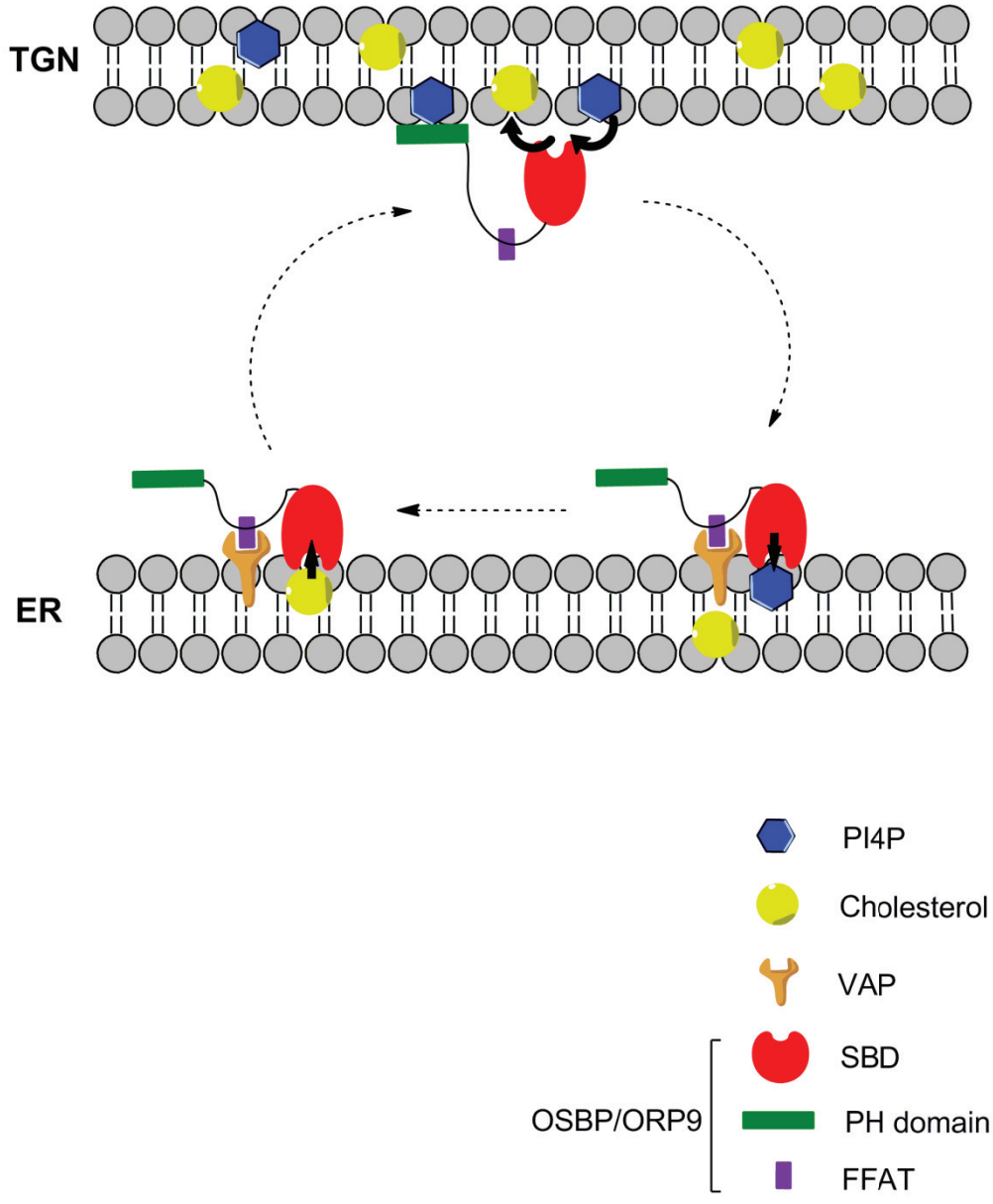

Figure 4.1. A proposed model for the transport of cholesterol and PI(4)P between the ER and TGN by OSBP or ORP9. The FFAT motif of OSBP/ORP9 interacts with VAP and mediates these proteins to localize to the ER, where OSBP/ORP9 extract cholesterol from the ER membrane. The PH domain binds to PI(4)P in the TGN and target OSBP/ORP9 to the TGN. The competition between cholesterol and PI(4)P to the SBD of ORPs occurs in the TGN, conferring a net cholesterol transfer. OSBP/ORP9 transfer bound PI(4)P back to the ER.

REFERENCES

1 Simons, K. and Vaz, W. L. (2004) Model systems, lipid rafts, and cell membranes. Annu. Rev. Biophys. Biomol. Struct. **33**, 269-295. doi:10.1146/annurev.biophys.32.110601.141803

2 Huang, J. and Feigenson, G. W. (1999) A microscopic interaction model of maximum solubility of cholesterol in lipid bilayers. Biophys. J. **76**, 2142-2157. doi:10.1016/S0006-3495(99)77369-8

3 McConnell, H. M. and Radhakrishnan, A. (2003) Condensed complexes of cholesterol and phospholipids. Biochim. Biophys. Acta. **1610**, 159-173.

4 Balasubramanian, N., Scott, D. W., Castle, J. D., Casanova, J. E. and Schwartz, M. A. (2007) Arf6 and microtubules in adhesion-dependent trafficking of lipid rafts. Nat. Cell Biol. **9**, 1381-1391. doi:10.1038/ncb1657

5 Viola, A. and Gupta, N. (2007) Tether and trap: Regulation of membrane-raft dynamics by actin-binding proteins. Nat. Rev. Immunol. **7**, 889-896. doi:10.1038/nri2193

6 Ngo, M. H., Colbourne, T. R. and Ridgway, N. D. (2010) Functional implications of sterol transport by the oxysterol-binding protein gene family. Biochem. J. **429**, 13-24. doi:10.1042/BJ20100263; 10.1042/BJ20100263

7 Pentchev, P.G., Vanier, M.T., Suzuki, K., and Patterson, M.C. (1995) Niemann-pick disease type C: A cellular cholesterol lipidosis. In The Metabolic and Molecular Basis of Inherited Disease (Scriver C.R., Beaudet A.L., Sly W.S., Valle D., Childs B., Kinzler K.W., Vogelstein B., ed.), pp. 2625–2639, McGraw-Hill Inc., New York.

8 McIntosh, A. L., Atshaves, B. P., Huang, H., Gallegos, A. M., Kier, A. B. and Schroeder, F. (2008) Fluorescence techniques using dehydroergosterol to study cholesterol trafficking. Lipids. **43**, 1185-1208. doi:10.1007/s11745-008-3194-1; 10.1007/s11745-008-3194-1

9 Ohvo-Rekila, H., Akerlund, B. and Slotte, J. P. (2000) Cyclodextrin-catalyzed extraction of fluorescent sterols from monolayer membranes and small unilamellar vesicles. Chem. Phys. Lipids. **105**, 167-178.

10 Halling, K. K. and Slotte, J. P. (2004) Membrane properties of plant sterols in phospholipid bilayers as determined by differential scanning calorimetry, resonance energy transfer and detergent-induced solubilization. Biochim. Biophys. Acta. **1664**, 161-171. doi:10.1016/j.bbamem.2004.05.006

11 Du, X., Kumar, J., Ferguson, C., Schulz, T. A., Ong, Y. S., Hong, W., Prinz, W. A., Parton, R. G., Brown, A. J. and Yang, H. (2011) A role for oxysterol-binding protein-related protein 5 in endosomal cholesterol trafficking. J. Cell Biol. **192**, 121-135. doi:10.1083/jcb.201004142; 10.1083/jcb.201004142

12 Fischer, R. T., Stephenson, F. A., Shafiee, A. and Schroeder, F. (1984) Delta 5,7,9(11)-cholestatrien-3 beta-ol: A fluorescent cholesterol analogue. Chem. Phys. Lipids. **36**, 1-14.

13 Scheidt, H. A., Muller, P., Herrmann, A. and Huster, D. (2003) The potential of fluorescent and spin-labeled steroid analogs to mimic natural cholesterol. J. Biol. Chem. **278**, 45563-45569. doi:10.1074/jbc.M303567200

14 Xu, Z., Farver, W., Kodukula, S. and Storch, J. (2008) Regulation of sterol transport between membranes and NPC2. Biochemistry. **47**, 11134-11143. doi:10.1021/bi801328u; 10.1021/bi801328u

15 Grundy, S. M. (1983) Absorption and metabolism of dietary cholesterol. Annu. Rev. Nutr. **3**, 71-96. doi:10.1146/annurev.nu.03.070183.000443

16 Volpe, J. J. and Hennessy, S. W. (1977) Cholesterol biosynthesis and 3-hydroxy-3-methyl-glutaryl coenzyme A reductase in cultured glial and neuronal cells. regulation by lipoprotein and by certain free sterols. Biochim. Biophys. Acta. **486**, 408-420

17 Radhakrishnan, A., Ikeda, Y., Kwon, H. J., Brown, M. S. and Goldstein, J. L. (2007) Sterol-regulated transport of SREBPs from endoplasmic reticulum to golgi: Oxysterols block transport by binding to insig. Proc. Natl. Acad. Sci. U. S. A. **104**, 6511-6518. doi:10.1073/pnas.0700899104

18 Sun, L. P., Seemann, J., Goldstein, J. L. and Brown, M. S. (2007) Sterol-regulated transport of SREBPs from endoplasmic reticulum to golgi: Insig renders sorting signal in scap inaccessible to COPII proteins. Proc. Natl. Acad. Sci. U. S. A. **104**, 6519-6526. doi:10.1073/pnas.0700907104

19 Goldstein, J. L. and Brown, M. S. (1990) Regulation of the mevalonate pathway. Nature. **343**, 425-430. doi:10.1038/343425a0

20 Sever, N., Song, B. L., Yabe, D., Goldstein, J. L., Brown, M. S. and DeBose-Boyd, R. A. (2003) Insig-dependent ubiquitination and degradation of mammalian 3-hydroxy-3-methylglutaryl-CoA reductase stimulated by sterols and geranylgeraniol. J. Biol. Chem. **278**, 52479-52490. doi:10.1074/jbc.M310053200

21 Rader, D. J., Alexander, E. T., Weibel, G. L., Billheimer, J. and Rothblat, G. H. (2009) The role of reverse cholesterol transport in animals and humans and relationship to atherosclerosis. J. Lipid Res. **50 Suppl**, S189-94. doi:10.1194/jlr.R800088-JLR200; 10.1194/jlr.R800088-JLR200

22 Oram, J. F. and Vaughan, A. M. (2006) ATP-binding cassette cholesterol transporters and cardiovascular disease. Circ. Res. **99**, 1031-1043. doi:10.1161/01.RES.0000250171.54048.5c

23 Baldan, A., Tarr, P., Lee, R. and Edwards, P. A. (2006) ATP-binding cassette transporter G1 and lipid homeostasis. Curr. Opin. Lipidol. **17**, 227-232. doi:10.1097/01.mol.0000226113.89812.bb

24 Tontonoz, P. and Mangelsdorf, D. J. (2003) Liver X receptor signaling pathways in cardiovascular disease. Mol. Endocrinol. **17**, 985-993. doi:10.1210/me.2003-0061

25 Chang, T. Y., Chang, C. C., Lin, S., Yu, C., Li, B. L. and Miyazaki, A. (2001) Roles of acyl-coenzyme A:Cholesterol acyltransferase-1 and -2. Curr. Opin. Lipidol. **12**, 289-296

26 Maxfield, F. R. and Wustner, D. (2002) Intracellular cholesterol transport. J. Clin. Invest. **110**, 891-898. doi:10.1172/JCI16500

27 Prinz, W. (2002) Cholesterol trafficking in the secretory and endocytic systems. Semin. Cell Dev. Biol. **13**, 197-203

28 Liscum, L. and Munn, N. J. (1999) Intracellular cholesterol transport. Biochim. Biophys. Acta. **1438**, 19-37

29 Cai, H., Reinisch, K. and Ferro-Novick, S. (2007) Coats, tethers, rabs, and SNAREs work together to mediate the intracellular destination of a transport vesicle. Dev. Cell. **12**, 671-682. doi:10.1016/j.devcel.2007.04.005

30 Springer, S., Spang, A. and Schekman, R. (1999) A primer on vesicle budding. Cell. **97**, 145-148

31 Hammer, J. A.,3rd and Wu, X. S. (2002) Rabs grab motors: Defining the connections between rab GTPases and motor proteins. Curr. Opin. Cell Biol. **14**, 69-75

32 Matanis, T., Akhmanova, A., Wulf, P., Del Nery, E., Weide, T., Stepanova, T., Galjart, N., Grosveld, F., Goud, B., De Zeeuw, C. I., Barnekow, A. and Hoogenraad, C. C. (2002) Bicaudal-D regulates COPI-independent golgi-ER transport by recruiting the dynein-dynactin motor complex. Nat. Cell Biol. **4**, 986-992. doi:10.1038/ncb891

33 Shorter, J., Beard, M. B., Seemann, J., Dirac-Svejstrup, A. B. and Warren, G. (2002) Sequential tethering of golgins and catalysis of SNAREpin assembly by the vesicle-tethering protein p115. J. Cell Biol. **157**, 45-62. doi:10.1083/jcb.200112127

34 Sollner, T., Whiteheart, S. W., Brunner, M., Erdjument-Bromage, H., Geromanos, S., Tempst, P. and Rothman, J. E. (1993) SNAP receptors implicated in vesicle targeting and fusion. Nature. **362**, 318-324. doi:10.1038/362318a0

35 Soccio, R. E. and Breslow, J. L. (2004) Intracellular cholesterol transport. Arterioscler. Thromb. Vasc. Biol. **24**, 1150-1160. doi:10.1161/01.ATV.0000131264.66417.d5

36 Hornick, C. A., Hui, D. Y. and DeLamatre, J. G. (1997) A role for retrosomes in intracellular cholesterol transport from endosomes to the plasma membrane. Am. J. Physiol. **273**, C1075-81

37 Gagescu, R., Demaurex, N., Parton, R. G., Hunziker, W., Huber, L. A. and Gruenberg, J. (2000) The recycling endosome of madin-darby canine kidney cells is a mildly acidic compartment rich in raft components. Mol. Biol. Cell. **11**, 2775-2791

38 Sugii, S., Reid, P. C., Ohgami, N., Du, H. and Chang, T. Y. (2003) Distinct endosomal compartments in early trafficking of low density lipoprotein-derived cholesterol. J. Biol. Chem. **278**, 27180-27189. doi:10.1074/jbc.M300542200

39 Hao, M., Lin, S. X., Karylowski, O. J., Wustner, D., McGraw, T. E. and Maxfield, F. R. (2002) Vesicular and non-vesicular sterol transport in living cells. the endocytic recycling compartment is a major sterol storage organelle. J. Biol. Chem. **277**, 609-617. doi:10.1074/jbc.M108861200

40 Holtta-Vuori, M., Tanhuanpaa, K., Mobius, W., Somerharju, P. and Ikonen, E. (2002) Modulation of cellular cholesterol transport and homeostasis by Rab11. Mol. Biol. Cell. **13**, 3107-3122. doi:10.1091/mbc.E02-01-0025

41 Infante, R. E., Wang, M. L., Radhakrishnan, A., Kwon, H. J., Brown, M. S. and Goldstein, J. L. (2008) NPC2 facilitates bidirectional transfer of cholesterol between NPC1 and lipid bilayers, a step in cholesterol egress from lysosomes. Proc. Natl. Acad. Sci. U. S. A. **105**, 15287-15292. doi:10.1073/pnas.0807328105; 10.1073/pnas.0807328105

42 DeGrella, R. F. and Simoni, R. D. (1982) Intracellular transport of cholesterol to the plasma membrane. J. Biol. Chem. **257**, 14256-14262

43 Urbani, L. and Simoni, R. D. (1990) Cholesterol and vesicular stomatitis virus G protein take separate routes from the endoplasmic reticulum to the plasma membrane. J. Biol. Chem. **265**, 1919-1923

44 Prinz, W. A. (2007) Non-vesicular sterol transport in cells. Prog. Lipid Res. **46**, 297-314. doi:10.1016/j.plipres.2007.06.002

45 Heino, S., Lusa, S., Somerharju, P., Ehnholm, C., Olkkonen, V. M. and Ikonen, E. (2000) Dissecting the role of the golgi complex and lipid rafts in biosynthetic transport of cholesterol to the cell surface. Proc. Natl. Acad. Sci. U. S. A. **97**, 8375-8380. doi:10.1073/pnas.140218797

46 Baumann, N. A., Sullivan, D. P., Ohvo-Rekila, H., Simonot, C., Pottekat, A., Klaassen, Z., Beh, C. T. and Menon, A. K. (2005) Transport of newly synthesized sterol to the sterol-enriched plasma membrane occurs via nonvesicular equilibration. Biochemistry. **44**, 5816-5826. doi:10.1021/bi048296z

47 Murphy, D. J. and Vance, J. (1999) Mechanisms of lipid-body formation. Trends Biochem. Sci. **24**, 109-115

48 Pol, A., Luetterforst, R., Lindsay, M., Heino, S., Ikonen, E. and Parton, R. G. (2001) A caveolin dominant negative mutant associates with lipid bodies and induces intracellular cholesterol imbalance. J. Cell Biol. **152**, 1057-1070

49 Alpy, F. and Tomasetto, C. (2005) Give lipids a START: The StAR-related lipid transfer (START) domain in mammals. J. Cell. Sci. **118**, 2791-2801. doi:10.1242/jcs.02485

50 Charman, M., Kennedy, B. E., Osborne, N. and Karten, B. (2010) MLN64 mediates egress of cholesterol from endosomes to mitochondria in the absence of functional niemann-pick type C1 protein. J. Lipid Res. **51**, 1023-1034. doi:10.1194/jlr.M002345; 10.1194/jlr.M002345

51 Di Paolo, G. and De Camilli, P. (2006) Phosphoinositides in cell regulation and membrane dynamics. Nature. **443**, 651-657. doi:10.1038/nature05185

52 Berridge, M. J. and Irvine, R. F. (1989) Inositol phosphates and cell signalling. Nature. **341**, 197-205. doi:10.1038/341197a0

53 Kutateladze, T. G. (2010) Translation of the phosphoinositide code by PI effectors. Nat. Chem. Biol. **6**, 507-513. doi:10.1038/nchembio.390; 10.1038/nchembio.390

54 Lemmon, M. A. (2008) Membrane recognition by phospholipid-binding domains. Nat. Rev. Mol. Cell Biol. **9**, 99-111. doi:10.1038/nrm2328; 10.1038/nrm2328

55 Hama, H., Schnieders, E. A., Thorner, J., Takemoto, J. Y. and DeWald, D. B. (1999) Direct involvement of phosphatidylinositol 4-phosphate in secretion in the yeast saccharomyces cerevisiae. J. Biol. Chem. **274**, 34294-34300

56 Ngo, M. and Ridgway, N. D. (2009) Oxysterol binding protein-related protein 9 (ORP9) is a cholesterol transfer protein that regulates golgi structure and function. Mol. Biol. Cell. **20**, 1388-1399. doi:10.1091/mbc.E08-09-0905; 10.1091/mbc.E08-09-0905

57 Levine, T. P. and Munro, S. (1998) The pleckstrin homology domain of oxysterol-binding protein recognises a determinant specific to golgi membranes. Curr. Biol. **8**, 729-739

58 Wenk, M. R. and De Camilli, P. (2004) Protein-lipid interactions and phosphoinositide metabolism in membrane traffic: Insights from vesicle recycling in nerve terminals. Proc. Natl. Acad. Sci. U. S. A. **101**, 8262-8269. doi:10.1073/pnas.0401874101

59 Gaidarov, I. and Keen, J. H. (1999) Phosphoinositide-AP-2 interactions required for targeting to plasma membrane clathrin-coated pits. J. Cell Biol. **146**, 755-764

60 Wang, Y. J., Wang, J., Sun, H. Q., Martinez, M., Sun, Y. X., Macia, E., Kirchhausen, T., Albanesi, J. P., Roth, M. G. and Yin, H. L. (2003) Phosphatidylinositol 4 phosphate regulates targeting of clathrin adaptor AP-1 complexes to the golgi. Cell. **114**, 299-310

61 Honing, S., Ricotta, D., Krauss, M., Spate, K., Spolaore, B., Motley, A., Robinson, M., Robinson, C., Haucke, V. and Owen, D. J. (2005) Phosphatidylinositol-(4,5)-bisphosphate regulates sorting signal recognition by the clathrin-associated adaptor complex AP2. Mol. Cell. **18**, 519-531. doi:10.1016/j.molcel.2005.04.019

62 Owen, D. J., Collins, B. M. and Evans, P. R. (2004) Adaptors for clathrin coats: Structure and function. Annu. Rev. Cell Dev. Biol. **20**, 153-191. doi:10.1146/annurev.cellbio.20.010403.104543

63 de Saint-Jean, M., Delfosse, V., Douguet, D., Chicanne, G., Payrastre, B., Bourguet, W., Antonny, B. and Drin, G. (2011) Osh4p exchanges sterols for phosphatidylinositol 4-phosphate between lipid bilayers. J. Cell Biol. **195**, 965-978. doi:10.1083/jcb.201104062; 10.1083/jcb.201104062

64 D'Angelo, G., Vicinanza, M., Di Campli, A. and De Matteis, M. A. (2008) The multiple roles of PtdIns(4)P -- not just the precursor of PtdIns(4,5)P2. J. Cell. Sci. **121**, 1955-1963. doi:10.1242/jcs.023630; 10.1242/jcs.023630

65 Guo, S., Stolz, L. E., Lemrow, S. M. and York, J. D. (1999) SAC1-like domains of yeast SAC1, INP52, and INP53 and of human synaptojanin encode polyphosphoinositide phosphatases. J. Biol. Chem. **274**, 12990-12995

66 Hsu, N. Y., Ilnytska, O., Belov, G., Santiana, M., Chen, Y. H., Takvorian, P. M., Pau, C., van der Schaar, H., Kaushik-Basu, N., Balla, T., Cameron, C. E., Ehrenfeld, E., van Kuppeveld, F. J. and Altan-Bonnet, N. (2010) Viral reorganization of the secretory pathway generates distinct organelles for RNA replication. Cell. **141**, 799-811. doi:10.1016/j.cell.2010.03.050; 10.1016/j.cell.2010.03.050

67 Taylor, F. R., Saucier, S. E., Shown, E. P., Parish, E. J. and Kandutsch, A. A. (1984) Correlation between oxysterol binding to a cytosolic binding protein and potency in the repression of hydroxymethylglutaryl coenzyme A reductase. J. Biol. Chem. **259**, 12382-12387

68 Dawson, P. A., Van der Westhuyzen, D. R., Goldstein, J. L. and Brown, M. S. (1989) Purification of oxysterol binding protein from hamster liver cytosol. J. Biol. Chem. **264**, 9046-9052

69 Dawson, P. A., Ridgway, N. D., Slaughter, C. A., Brown, M. S. and Goldstein, J. L. (1989) cDNA cloning and expression of oxysterol-binding protein, an oligomer with a potential leucine zipper. J. Biol. Chem. **264**, 16798-16803

70 Levanon, D., Hsieh, C. L., Francke, U., Dawson, P. A., Ridgway, N. D., Brown, M. S. and Goldstein, J. L. (1990) cDNA cloning of human oxysterol-binding protein and localization of the gene to human chromosome 11 and mouse chromosome 19. Genomics. **7**, 65-74

71 Lehto, M., Laitinen, S., Chinetti, G., Johansson, M., Ehnholm, C., Staels, B., Ikonen, E. and Olkkonen, V. M. (2001) The OSBP-related protein family in humans. J. Lipid Res. **42**, 1203-1213

72 Beh, C. T., Cool, L., Phillips, J. and Rine, J. (2001) Overlapping functions of the yeast oxysterol-binding protein homologues. Genetics. **157**, 1117-1140

73 Alphey, L., Jimenez, J. and Glover, D. (1998) A drosophila homologue of oxysterol binding protein (OSBP)--implications for the role of OSBP. Biochim. Biophys. Acta. **1395**, 159-164

74 Avrova, A. O., Taleb, N., Rokka, V. M., Heilbronn, J., Campbell, E., Hein, I., Gilroy, E. M., Cardle, L., Bradshaw, J. E., Stewart, H. E., Fakim, Y. J., Loake, G. and Birch, P. R. (2004) Potato oxysterol binding protein and cathepsin B are rapidly up-regulated in independent defence pathways that distinguish R gene-mediated and field resistances to phytophthora infestans. Mol. Plant. Pathol. **5**, 45-56. doi:10.1111/j.1364-3703.2004.00205.x; 10.1111/j.1364-3703.2004.00205.x

75 Skirpan, A. L., Dowd, P. E., Sijacic, P., Jaworski, C. J., Gilroy, S. and Kao, T. H. (2006) Identification and characterization of PiORP1, a petunia oxysterol-binding-protein related protein involved in receptor-kinase mediated signaling in pollen, and analysis of the ORP gene family in arabidopsis. Plant Mol. Biol. **61**, 553-565. doi:10.1007/s11103-006-0030-y

76 Sugawara, K., Morita, K., Ueno, N. and Shibuya, H. (2001) BIP, a BRAM-interacting protein involved in TGF-beta signalling, regulates body length in caenorhabditis elegans. Genes Cells. **6**, 599-606

77 Fukuzawa, M. and Williams, J. G. (2002) OSBPa, a predicted oxysterol binding protein of dictyostelium, is required for regulated entry into culmination. FEBS Lett. **527**, 37-42

78 Zeng, B. and Zhu, G. (2006) Two distinct oxysterol binding protein-related proteins in the parasitic protist cryptosporidium parvum (apicomplexa). Biochem. Biophys. Res. Commun. **346**, 591-599. doi:10.1016/j.bbrc.2006.05.165

79 Levine, T. P. and Munro, S. (2002) Targeting of golgi-specific pleckstrin homology domains involves both PtdIns 4-kinase-dependent and -independent components. Curr. Biol. **12**, 695-704

80 Levine, T. P. and Munro, S. (2001) Dual targeting of Osh1p, a yeast homologue of oxysterol-binding protein, to both the golgi and the nucleus-vacuole junction. Mol. Biol. Cell. **12**, 1633-1644

81 Li, X., Rivas, M. P., Fang, M., Marchena, J., Mehrotra, B., Chaudhary, A., Feng, L., Prestwich, G. D. and Bankaitis, V. A. (2002) Analysis of oxysterol binding protein homologue Kes1p function in regulation of Sec14p-dependent protein transport from the yeast golgi complex. J. Cell Biol. **157**, 63-77. doi:10.1083/jcb.200201037

82 Wang, C., JeBailey, L. and Ridgway, N. D. (2002) Oxysterol-binding-protein (OSBP)-related protein 4 binds 25-hydroxycholesterol and interacts with vimentin intermediate filaments. Biochem. J. **361**, 461-472

83 Johansson, M., Bocher, V., Lehto, M., Chinetti, G., Kuismanen, E., Ehnholm, C., Staels, B. and Olkkonen, V. M. (2003) The two variants of oxysterol binding protein-related protein-1 display different tissue expression patterns, have different intracellular localization, and are functionally distinct. Mol. Biol. Cell. **14**, 903-915. doi:10.1091/mbc.E02-08-0459

84 Wyles, J. P. and Ridgway, N. D. (2004) VAMP-associated protein-A regulates partitioning of oxysterol-binding protein-related protein-9 between the endoplasmic reticulum and golgi apparatus. Exp. Cell Res. **297**, 533-547. doi:10.1016/j.yexcr.2004.03.052

85 Jaworski, C. J., Moreira, E., Li, A., Lee, R. and Rodriguez, I. R. (2001) A family of 12 human genes containing oxysterol-binding domains. Genomics. **78**, 185-196. doi:10.1006/geno.2001.6663

86 Laitinen, S., Olkkonen, V. M., Ehnholm, C. and Ikonen, E. (1999) Family of human oxysterol binding protein (OSBP) homologues. A novel member implicated in brain sterol metabolism. J. Lipid Res. **40**, 2204-2211

87 Anniss, A. M., Apostolopoulos, J., Dworkin, S., Purton, L. E. and Sparrow, R. L. (2002) An oxysterol-binding protein family identified in the mouse. DNA Cell Biol. **21**, 571-580. doi:10.1089/104454902320308942

88 Lehto, M., Tienari, J., Lehtonen, S., Lehtonen, E. and Olkkonen, V. M. (2004) Subfamily III of mammalian oxysterol-binding protein (OSBP) homologues: The expression and intracellular localization of ORP3, ORP6, and ORP7. Cell Tissue Res. **315**, 39-57. doi:10.1007/s00441-003-0817-y

89 Im, Y. J., Raychaudhuri, S., Prinz, W. A. and Hurley, J. H. (2005) Structural mechanism for sterol sensing and transport by OSBP-related proteins. Nature. **437**, 154-158. doi:10.1038/nature03923

90 Suchanek, M., Hynynen, R., Wohlfahrt, G., Lehto, M., Johansson, M., Saarinen, H., Radzikowska, A., Thiele, C. and Olkkonen, V. M. (2007) The mammalian oxysterol-binding protein-related proteins (ORPs) bind 25-hydroxycholesterol in an evolutionarily conserved pocket. Biochem. J. **405**, 473-480. doi:10.1042/BJ20070176

91 Ridgway, N. D., Dawson, P. A., Ho, Y. K., Brown, M. S. and Goldstein, J. L. (1992) Translocation of oxysterol binding protein to golgi apparatus triggered by ligand binding. J. Cell Biol. **116**, 307-319

92 Wyles, J. P., Perry, R. J. and Ridgway, N. D. (2007) Characterization of the sterol-binding domain of oxysterol-binding protein (OSBP)-related protein 4 reveals a novel role in vimentin organization. Exp. Cell Res. **313**, 1426-1437. doi:10.1016/j.yexcr.2007.01.018

93 Wang, P. Y., Weng, J., Lee, S. and Anderson, R. G. (2008) The N terminus controls sterol binding while the C terminus regulates the scaffolding function of OSBP. J. Biol. Chem. **283**, 8034-8045. doi:10.1074/jbc.M707631200; 10.1074/jbc.M707631200

94 Thiele, C., Hannah, M. J., Fahrenholz, F. and Huttner, W. B. (2000) Cholesterol binds to synaptophysin and is required for biogenesis of synaptic vesicles. Nat. Cell Biol. **2**, 42-49. doi:10.1038/71366

95 Lemmon, M. A. (2007) Pleckstrin homology (PH) domains and phosphoinositides. Biochem. Soc. Symp. **(74)**, 81-93. doi:10.1042/BSS0740081

96 Nhek, S., Ngo, M., Yang, X., Ng, M. M., Field, S. J., Asara, J. M., Ridgway, N. D. and Toker, A. (2010) Regulation of oxysterol-binding protein golgi localization through protein kinase D-mediated phosphorylation. Mol. Biol. Cell. **21**, 2327-2337. doi:10.1091/mbc.E10-02-0090; 10.1091/mbc.E10-02-0090

97 Godi, A., Di Campli, A., Konstantakopoulos, A., Di Tullio, G., Alessi, D. R., Kular, G. S., Daniele, T., Marra, P., Lucocq, J. M. and De Matteis, M. A. (2004) FAPPs control golgi-to-cell-surface membrane traffic by binding to ARF and PtdIns(4)P. Nat. Cell Biol. **6**, 393-404. doi:10.1038/ncb1119

98 Wang, P., Duan, W., Munn, A. L. and Yang, H. (2005) Molecular characterization of Osh6p, an oxysterol binding protein homolog in the yeast saccharomyces cerevisiae. FEBS J. **272**, 4703-4715. doi:10.1111/j.1742-4658.2005.04886.x

99 Wyles, J. P., McMaster, C. R. and Ridgway, N. D. (2002) Vesicle-associated membrane protein-associated protein-A (VAP-A) interacts with the oxysterol-binding protein to modify export from the endoplasmic reticulum. J. Biol. Chem. **277**, 29908-29918. doi:10.1074/jbc.M201191200

100 Manford, A. G., Stefan, C. J., Yuan, H. L., Macgurn, J. A. and Emr, S. D. (2012) ER-to-plasma membrane tethering proteins regulate cell signaling and ER morphology. Dev. Cell. **23**, 1129-1140. doi:10.1016/j.devcel.2012.11.004; 10.1016/j.devcel.2012.11.004

101 Hamamoto, I., Nishimura, Y., Okamoto, T., Aizaki, H., Liu, M., Mori, Y., Abe, T., Suzuki, T., Lai, M. M., Miyamura, T., Moriishi, K. and Matsuura, Y. (2005) Human VAP-B is involved in hepatitis C virus replication through interaction with NS5A and NS5B. J. Virol. **79**, 13473-13482. doi:10.1128/JVI.79.21.13473-13482.2005

102 Kaiser, S. E., Brickner, J. H., Reilein, A. R., Fenn, T. D., Walter, P. and Brunger, A. T. (2005) Structural basis of FFAT motif-mediated ER targeting. Structure. **13**, 1035-1045. doi:10.1016/j.str.2005.04.010

103 Loewen, C. J., Roy, A. and Levine, T. P. (2003) A conserved ER targeting motif in three families of lipid binding proteins and in Opi1p binds VAP. EMBO J. **22**, 2025-2035. doi:10.1093/emboj/cdg201

104 Loewen, C. J. and Levine, T. P. (2005) A highly conserved binding site in vesicle-associated membrane protein-associated protein (VAP) for the FFAT motif of lipid-binding proteins. J. Biol. Chem. **280**, 14097-14104. doi:10.1074/jbc.M500147200

105 Goto, A., Liu, X., Robinson, C. A. and Ridgway, N. D. (2012) Multisite phosphorylation of oxysterol-binding protein regulates sterol binding and activation of sphingomyelin synthesis. Mol. Biol. Cell. **23**, 3624-3635. doi:10.1091/mbc.E12-04-0283; 10.1091/mbc.E12-04-0283

106 Rocha, N., Kuijl, C., van der Kant, R., Janssen, L., Houben, D., Janssen, H., Zwart, W. and Neefjes, J. (2009) Cholesterol sensor ORP1L contacts the ER protein VAP to control Rab7-RILP-p150 glued and late endosome positioning. J. Cell Biol. **185**, 1209-1225. doi:10.1083/jcb.200811005; 10.1083/jcb.200811005

107 Mosavi, L. K., Cammett, T. J., Desrosiers, D. C. and Peng, Z. Y. (2004) The ankyrin repeat as molecular architecture for protein recognition. Protein Sci. **13**, 1435-1448. doi:10.1110/ps.03554604

108 Kvam, E. and Goldfarb, D. S. (2004) Nvj1p is the outer-nuclear-membrane receptor for oxysterol-binding protein homolog Osh1p in saccharomyces cerevisiae. J. Cell. Sci. **117**, 4959-4968. doi:10.1242/jcs.01372

109 Johansson, M., Lehto, M., Tanhuanpaa, K., Cover, T. L. and Olkkonen, V. M. (2005) The oxysterol-binding protein homologue ORP1L interacts with Rab7 and alters functional properties of late endocytic compartments. Mol. Biol. Cell. **16**, 5480-5492. doi:10.1091/mbc.E05-03-0189

110 Johansson, M., Rocha, N., Zwart, W., Jordens, I., Janssen, L., Kuijl, C., Olkkonen, V. M. and Neefjes, J. (2007) Activation of endosomal dynein motors by stepwise assembly of Rab7-RILP-p150Glued, ORP1L, and the receptor betalll spectrin. J. Cell Biol. **176**, 459-471. doi:10.1083/jcb.200606077

111 Raychaudhuri, S., Im, Y. J., Hurley, J. H. and Prinz, W. A. (2006) Nonvesicular sterol movement from plasma membrane to ER requires oxysterol-binding protein-related proteins and phosphoinositides. J. Cell Biol. **173**, 107-119. doi:10.1083/jcb.200510084

112 Schulz, T. A., Choi, M. G., Raychaudhuri, S., Mears, J. A., Ghirlando, R., Hinshaw, J. E. and Prinz, W. A. (2009) Lipid-regulated sterol transfer between closely apposed membranes by oxysterol-binding protein homologues. J. Cell Biol. **187**, 889-903. doi:10.1083/jcb.200905007; 10.1083/jcb.200905007

113 Banerji, S., Ngo, M., Lane, C. F., Robinson, C. A., Minogue, S. and Ridgway, N. D. (2010) Oxysterol binding protein-dependent activation of sphingomyelin synthesis in the golgi apparatus requires phosphatidylinositol 4-kinase IIalpha. Mol. Biol. Cell. **21**, 4141-4150. doi:10.1091/mbc.E10-05-0424; 10.1091/mbc.E10-05-0424

114 Lagace, T. A., Byers, D. M., Cook, H. W. and Ridgway, N. D. (1997) Altered regulation of cholesterol and cholesteryl ester synthesis in chinese-hamster ovary cells overexpressing the oxysterol-binding protein is dependent on the pleckstrin homology domain. Biochem. J. **326 (Pt 1)**, 205-213

115 Perry, R. J. and Ridgway, N. D. (2006) Oxysterol-binding protein and vesicle-associated membrane protein-associated protein are required for sterol-dependent activation of the ceramide transport protein. Mol. Biol. Cell. **17**, 2604-2616. doi:10.1091/mbc.E06-01-0060

116 Lagace, T. A., Byers, D. M., Cook, H. W. and Ridgway, N. D. (1999) Chinese hamster ovary cells overexpressing the oxysterol binding protein (OSBP) display enhanced synthesis of sphingomyelin in response to 25-hydroxycholesterol. J. Lipid Res. **40**, 109-116

117 Bowden, K. and Ridgway, N. D. (2008) OSBP negatively regulates ABCA1 protein stability. J. Biol. Chem. **283**, 18210-18217. doi:10.1074/jbc.M800918200; 10.1074/jbc.M800918200

118 Hanada, K., Kumagai, K., Tomishige, N. and Yamaji, T. (2009) CERT-mediated trafficking of ceramide. Biochim. Biophys. Acta. **1791**, 684-691. doi:10.1016/j.bbalip.2009.01.006; 10.1016/j.bbalip.2009.01.006

119 Fugmann, T., Hausser, A., Schoffler, P., Schmid, S., Pfizenmaier, K. and Olayioye, M. A. (2007) Regulation of secretory transport by protein kinase D-mediated phosphorylation of the ceramide transfer protein. J. Cell Biol. **178**, 15-22. doi:10.1083/jcb.200612017

120 Tomishige, N., Kumagai, K., Kusuda, J., Nishijima, M. and Hanada, K. (2009) Casein kinase I{gamma}2 down-regulates trafficking of ceramide in the synthesis of sphingomyelin. Mol. Biol. Cell. **20**, 348-357. doi:10.1091/mbc.E08-07-0669; 10.1091/mbc.E08-07-0669

121 Saito, S., Matsui, H., Kawano, M., Kumagai, K., Tomishige, N., Hanada, K., Echigo, S., Tamura, S. and Kobayashi, T. (2008) Protein phosphatase 2Cepsilon is an endoplasmic reticulum integral membrane protein that dephosphorylates the ceramide transport protein CERT to enhance its association with organelle membranes. J. Biol. Chem. **283**, 6584-6593. doi:10.1074/jbc.M707691200; 10.1074/jbc.M707691200

122 Wang, P. Y., Weng, J. and Anderson, R. G. (2005) OSBP is a cholesterol-regulated scaffolding protein in control of ERK 1/2 activation. Science. **307**, 1472-1476. doi:10.1126/science.1107710

123 Yao, Z. and Seger, R. (2009) The ERK signaling cascade--views from different subcellular compartments. Biofactors. **35**, 407-416. doi:10.1002/biof.52; 10.1002/biof.52

124 Yan, D., Lehto, M., Rasilainen, L., Metso, J., Ehnholm, C., Yla-Herttuala, S., Jauhiainen, M. and Olkkonen, V. M. (2007) Oxysterol binding protein induces upregulation of SREBP-1c and enhances hepatic lipogenesis. Arterioscler. Thromb. Vasc. Biol. **27**, 1108-1114. doi:10.1161/ATVBAHA.106.138545

125 Romeo, G. R. and Kazlauskas, A. (2008) Oxysterol and diabetes activate STAT3 and control endothelial expression of profilin-1 via OSBP1. J. Biol. Chem. **283**, 9595-9605. doi:10.1074/jbc.M710092200; 10.1074/jbc.M710092200

126 Hanada, M., Feng, J. and Hemmings, B. A. (2004) Structure, regulation and function of PKB/AKT--a major therapeutic target. Biochim. Biophys. Acta. **1697**, 3-16. doi:10.1016/j.bbapap.2003.11.009

127 Lessmann, E., Ngo, M., Leitges, M., Minguet, S., Ridgway, N. D. and Huber, M. (2007) Oxysterol-binding protein-related protein (ORP) 9 is a PDK-2 substrate and regulates akt phosphorylation. Cell. Signal. **19**, 384-392. doi:10.1016/j.cellsig.2006.07.009

128 Perttila, J., Merikanto, K., Naukkarinen, J., Surakka, I., Martin, N. W., Tanhuanpaa, K., Grimard, V., Taskinen, M. R., Thiele, C., Salomaa, V., Jula, A., Perola, M., Virtanen, I., Peltonen, L. and Olkkonen, V. M. (2009) OSBPL10, a novel candidate gene for high triglyceride trait in dyslipidemic finnish subjects, regulates cellular lipid metabolism. J. Mol. Med. (Berl). **87**, 825-835. doi:10.1007/s00109-009-0490-z; 10.1007/s00109-009-0490-z

129 Evans, R. M. (1994) Intermediate filaments and lipoprotein cholesterol. Trends Cell Biol. **4**, 149-151

130 Maier, O., Oberle, V. and Hoekstra, D. (2002) Fluorescent lipid probes: Some properties and applications (a review). Chem. Phys. Lipids. **116**, 3-18

131 Rogers, J., Lee, A. G. and Wilton, D. C. (1979) The organisation of cholesterol and ergosterol in lipid bilayers based on studies using non-perturbing fluorescent sterol probes. Biochim. Biophys. Acta. **552**, 23-37

132 Schroeder, F., Nemecz, G., Gratton, E., Barenholz, Y. and Thompson, T. E. (1988) Fluorescence properties of cholestatrienol in phosphatidylcholine bilayer vesicles. Biophys. Chem. **32**, 57-72

133 Hyslop, P. A., Morel, B. and Sauerheber, R. D. (1990) Organization and interaction of cholesterol and phosphatidylcholine in model bilayer membranes. Biochemistry. **29**, 1025-1038

134 Peterson, G. L. (1977) A simplification of the protein assay method of lowry et al. which is more generally applicable. Anal. Biochem. **83**, 346-356

135 Kilsdonk, E. P., Yancey, P. G., Stoudt, G. W., Bangerter, F. W., Johnson, W. J., Phillips, M. C. and Rothblat, G. H. (1995) Cellular cholesterol efflux mediated by cyclodextrins. J. Biol. Chem. **270**, 17250-17256

136 Klein, U., Gimpl, G. and Fahrenholz, F. (1995) Alteration of the myometrial plasma membrane cholesterol content with beta-cyclodextrin modulates the binding affinity of the oxytocin receptor. Biochemistry. **34**, 13784-13793

137 John, K., Kubelt, J., Muller, P., Wustner, D. and Herrmann, A. (2002) Rapid transbilayer movement of the fluorescent sterol dehydroergosterol in lipid membranes. Biophys. J. **83**, 1525-1534. doi:10.1016/S0006-3495(02)73922-2

138 Mayinger, P. (2009) Regulation of golgi function via phosphoinositide lipids. Semin. Cell Dev. Biol. **20**, 793-800. doi:10.1016/j.semcdb.2009.03.016; 10.1016/j.semcdb.2009.03.016

139 Fairn, G. D., Curwin, A. J., Stefan, C. J. and McMaster, C. R. (2007) The oxysterol binding protein Kes1p regulates golgi apparatus phosphatidylinositol-4-phosphate function. Proc. Natl. Acad. Sci. U. S. A. **104**, 15352-15357. doi:10.1073/pnas.0705571104

140 Ikonen, E. (2008) Cellular cholesterol trafficking and compartmentalization. Nat. Rev. Mol. Cell Biol. **9**, 125-138. doi:10.1038/nrm2336; 10.1038/nrm2336

141 Ridsdale, A., Denis, M., Gougeon, P. Y., Ngsee, J. K., Presley, J. F. and Zha, X. (2006) Cholesterol is required for efficient endoplasmic reticulum-to-golgi transport of secretory membrane proteins. Mol. Biol. Cell. **17**, 1593-1605. doi:10.1091/mbc.E05-02-0100

142 Runz, H., Miura, K., Weiss, M. and Pepperkok, R. (2006) Sterols regulate ER-export dynamics of secretory cargo protein ts-O45-G. EMBO J. **25**, 2953-2965. doi:10.1038/sj.emboj.7601205

143 Orci, L., Montesano, R., Meda, P., Malaisse-Lagae, F., Brown, D., Perrelet, A. and Vassalli, P. (1981) Heterogeneous distribution of filipin--cholesterol complexes across the cisternae of the golgi apparatus. Proc. Natl. Acad. Sci. U. S. A. **78**, 293-297

144 Wang, Y., Thiele, C. and Huttner, W. B. (2000) Cholesterol is required for the formation of regulated and constitutive secretory vesicles from the trans-golgi network. Traffic. **1**, 952-962

145 Ying, M., Grimmer, S., Iversen, T. G., Van Deurs, B. and Sandvig, K. (2003) Cholesterol loading induces a block in the exit of VSVG from the TGN. Traffic. **4**, 772-784

146 Kasper, A. M. and Helmkamp, G. M.,Jr. (1981) Intermembrane phospholipid fluxes catalyzed by bovine brain phospholipid exchange protein. Biochim. Biophys. Acta. **664**, 22-32

147 Graham, T. R. and Burd, C. G. (2011) Coordination of golgi functions by phosphatidylinositol 4-kinases. Trends Cell Biol. **21**, 113-121. doi:10.1016/j.tcb.2010.10.002; 10.1016/j.tcb.2010.10.002

148 Stefan, C. J., Manford, A. G., Baird, D., Yamada-Hanff, J., Mao, Y. and Emr, S. D. (2011) Osh proteins regulate phosphoinositide metabolism at ER-plasma membrane contact sites. Cell. **144**, 389-401. doi:10.1016/j.cell.2010.12.034; 10.1016/j.cell.2010.12.034

149 Kono, N., Ohto, U., Hiramatsu, T., Urabe, M., Uchida, Y., Satow, Y. and Arai, H. (2013) Impaired alpha-TTP-PIPs interaction underlies familial vitamin E deficiency. Science. **340**, 1106-1110. doi:10.1126/science.1233508; 10.1126/science.1233508